SCUOLA DI DOTTORATO
UNIVERSITÀ DEGLI STUDI DI MILANO-BICOCCA

Dipartimento di / Department of

Biotechnology and Biosciences

Dottorato di Ricerca in / PhD program Chemical, Geological and Environmental Science
Ciclo / Cycle XXXI

Curriculum in (se presente / if it is) Chemical Science

Design and Synthesis of Nanostructured Biomaterials for regenerative medicine

Cognome / Surname **Guizzardi** Nome / Name **Roberto**

Matricola / Registration number **784899**

Tutore / Tutor: **Prof. Laura Francesca Cipolla**

Cotutore / Co-tutor: **Prof. Francesco Nicotra**
(se presente / if there is one)

Supervisor:
(se presente / if there is one)

Coordinatore / Coordinator: **Prof. Maria Luce Frezzotti**

ANNO ACCADEMICO / ACADEMIC YEAR 2017-2018

Introduction

The evolution of biomaterials publications. From 1990 to 2017

In the last three decades biomaterials have gained more interest in the field of life sciences and biomedical research, supporting several area such as drug delivery, molecular imaging or molecular/cellular biology. As consequence, new sphere around clinical treatments are emerging as possible solution to resolve many pathological or injured states. In particular way, has been studied biomaterials in tissue engineering and medicinal chemistry as route to restore injured tissues through regenerative medicine applications. However, to do this, it's necessary know and control the deepest physiological mechanisms responsible to cell fate, cell-cell interactions and last but not least cell-environment interactions. All of this in order to improve the knowledge behind cellular behaviour.

Looking for the publications containing "biomaterials" as keyword, is possible observe the number of them increase, starting from 1990, a little less than 0.2k articles/year, reaching 2k articles into 2017; highlighting numerous efforts in this field[1]. (**Figure 1**, data from Scopus, adapted from Materials Today 16.11, 2013).

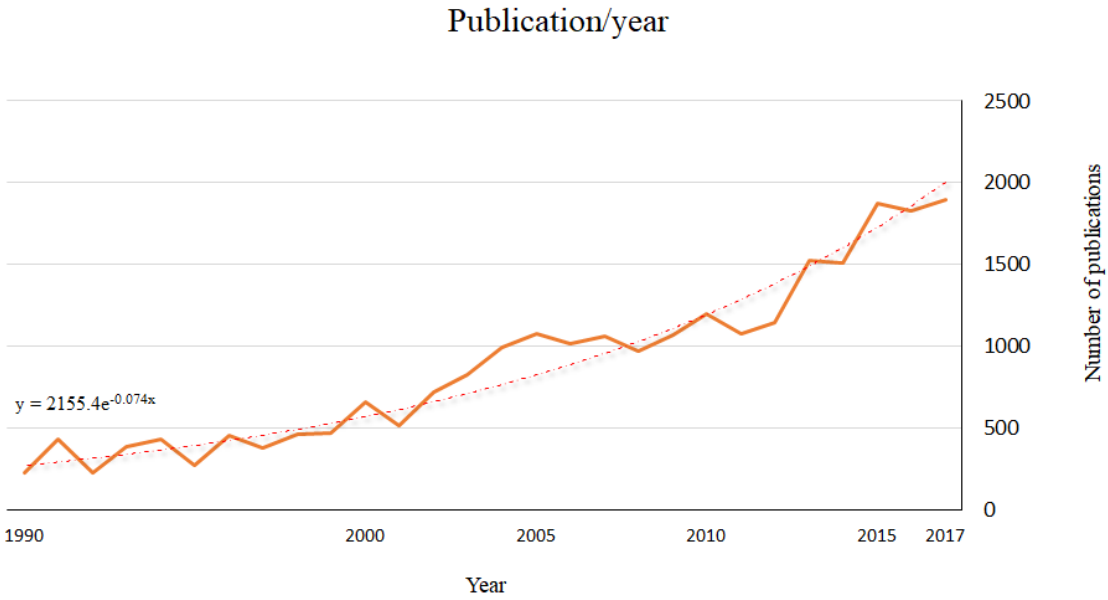

Figure 1 Number of publication increase from 1990 to 2017; Scopus research with Biomaterials as keyword

Up to now the major areas of interest, regarding biomaterials publications, include Materials Science (28 %); Material Engineering (23 %); Chemical Engineering (11 %); Biochemistry, Genetics and Molecular Biology (11%); Physics and Astronomy (8%); Chemistry (8%) and Medicine (4%). The remaining percentage regards other fields such as Computer Science, Environmental Science and Veterinary (**Figure 2**). These data suggest an increase of interest on biomaterials in several technological areas which are focalised on materials science and consequently on their applications. The major fields of applications of biomaterials regard regenerative medicine in which biomaterials are applied to restore injured tissue and failed organs[2]. Subsequently, this suggests the importance of biotechnologies in the modern age to improve the quality of life (from life sciences to engineering fields).

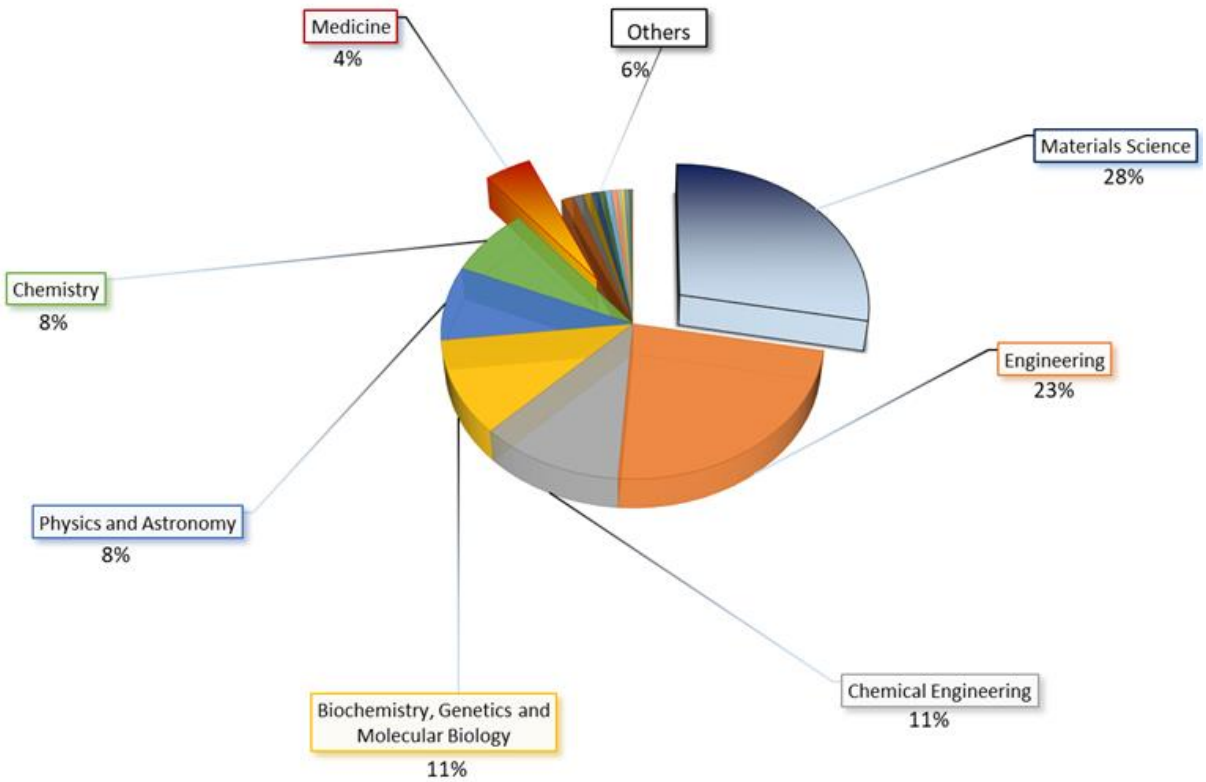

Figure 2 Distribution of Biomaterials concept in several interesting areas

Furthermore, other curious informations may be the number of publications produced from each state in these last three decades. In this context, the results, suggest bigger interest derived from country (or territory) such as U.S.A., China and Japan. In this view Italy domains just eighth position, late than South Korea, France and Germany; despite the fewer laboratories and less financing policies (**Figure 3**).

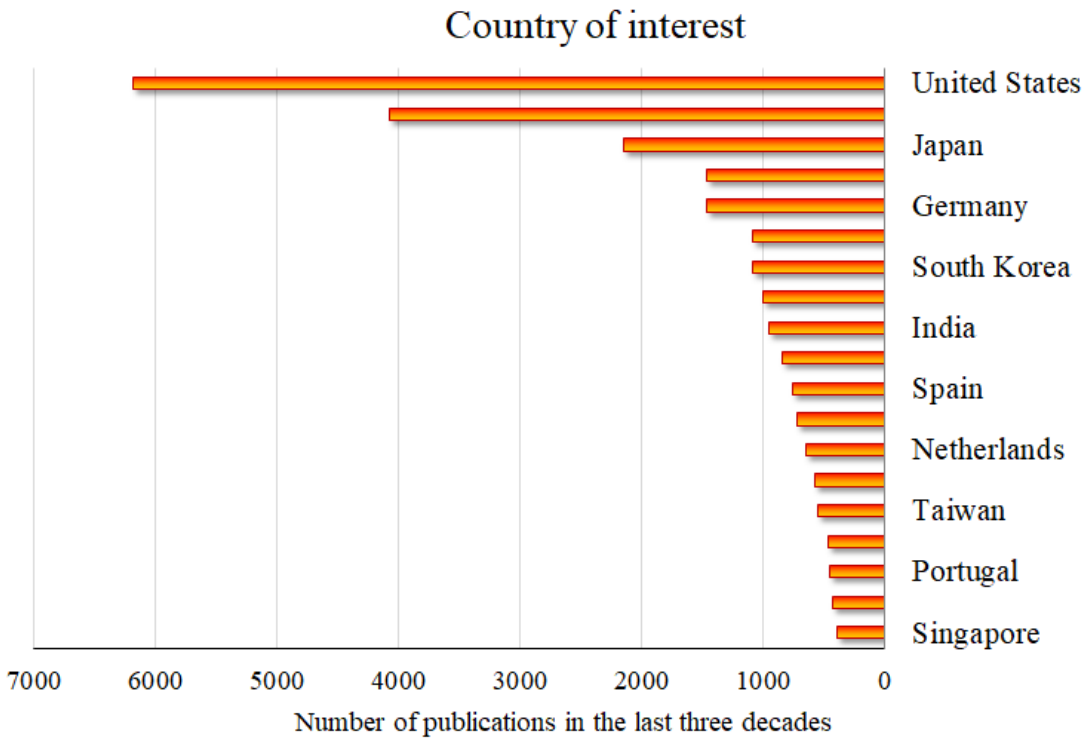

Figure. 3 Mains countries of interest

Chapter 1 – Basics of regenerative medicine

Regenerative medicine has the goal to heal or replace tissues and organs damaged by age, diseases, trauma, or eventually to restore congenital defects.[3] Different key elements can be involved into regenerative approaches; among them, bio-scaffolds may be crucial components, developed to afford mechanical support and ECM-mimicking cues, contributing to cells behaviour control.

Over the years, innovative bio-materials have been developed, showing that physical and biochemical signals are able to drive cell fate toward specific biological responses. The advancements in the understanding of cell biology,[4,5] including signal mechano-transduction,[6,7] together with the technological improvements in material science, fabrication techniques and engineering[8] are greatly fostering the regenerative medicine field. Natural or artificial scaffolds can be efficiently projected in order to fine-tune mechanical properties resembling natural tissues (i.e., hardness for bone, elasticity for blood vessels, or cartilage), or to mimic the native cell microenvironment, i.e. the extra-cellular matrix (ECM),[9,10,11] including complex biochemical signals. ECM is composed by an array of molecules secreted by the cells, specific for each tissue and organ, in which the main components are proteins (such as collagen, elastin, laminin, ...); proteoglycans and glycosaminoglycans, which undergoing self-assembly as well as cell-directed assembly to form complex organized meshworks.

The composition of ECM plays important roles in development and regulation of eukaryotic cell homeostasis, directing cellular fate and promoting cell-cell communication and/or cell-environment interactions (**figure 1.1**). In addition, it contributes to the establishment and maintenance of differentiated tissues and organs, setting the concentration of soluble molecules (such as growth factors), receptors expression and the physico-chemical stimuli.

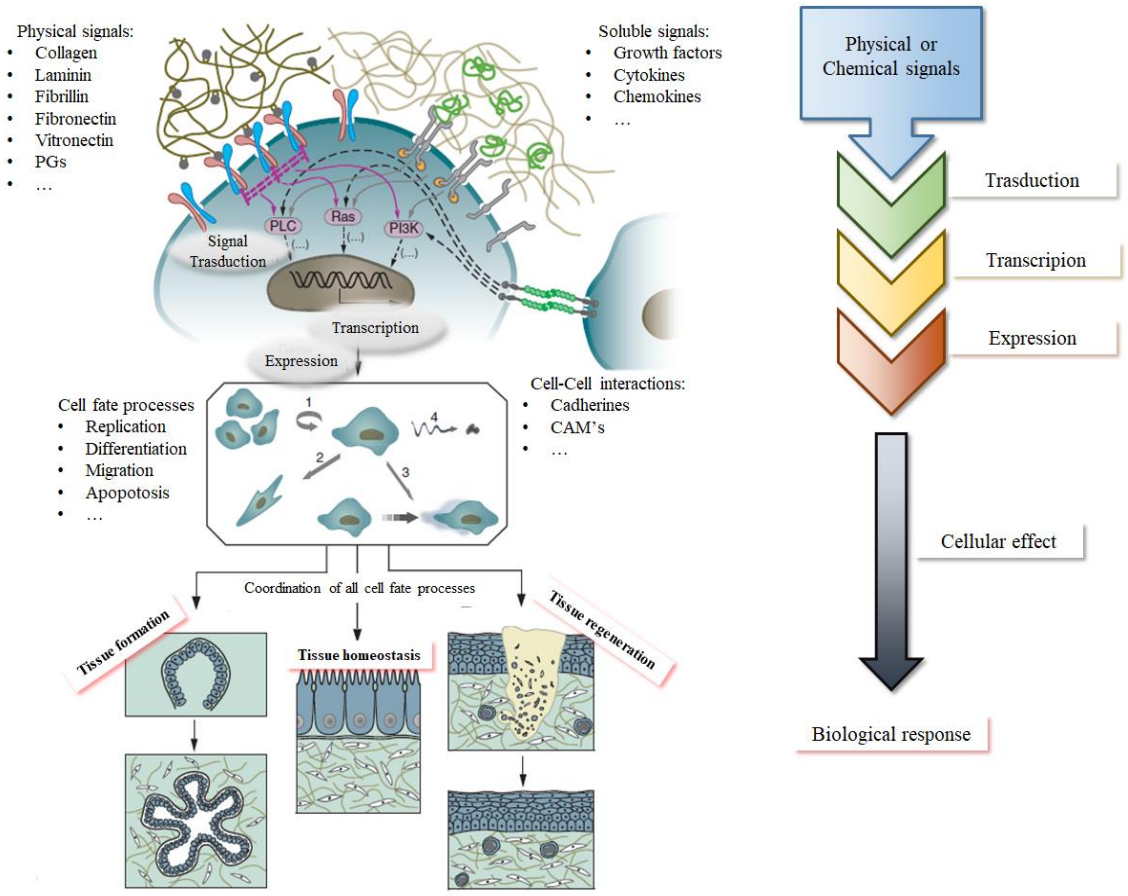

Figure 1.1 Representative scheme about goals of regenerative medicine and processes underlying cellular effect and biological response (adapted from: *Nat. biotechnol.* **2005,** *23.1*, 47.)

In this respect, the generation of bioactive microenvironments, through scaffolds design and bioactivation, with the aim to create extracellular matrix like environment, is of utmost interest.

1.1. Extra-Cellular Matrix (**ECM**)

In more detail, all biological tissues contain a mixture of cells and non-cellular components, which form well-organized network, previously called ECM. Different ECMs appear like meshworks able to support mechanically cells providing not only physical stimuli, in which cells are embedded, but also regulating many cellular processes included growth, migration, differentiation, survival, homeostasis and morphogenesis, all of this through a plethora of biochemical signals.[12,13]

Currently, detailed ECM composition, for each tissue, is not fully understood, nevertheless, the knowledge underlying this issue suggests high levels of complexity and variability from tissue to tissue. Nowadays, it is well known the major constituents of ECMs are fibrous-forming proteins, (previously reported as collagen, elastin, fibronectin and laminin) which can be modified and, in particular way, can be glycosylated generating glycoproteins, proteoglycans (PGs) and glycosaminoglycans. In most ECM architectures, it was mainly found collagen type I as predominant protein, in association to other isoforms as well as collagen type II or III, which cowork together to generate so called “meshwork”. In addition various PGs are interconnected generating multi-molecular structures, building the complex three-dimensional matrix (**figure 1.2**).[14]

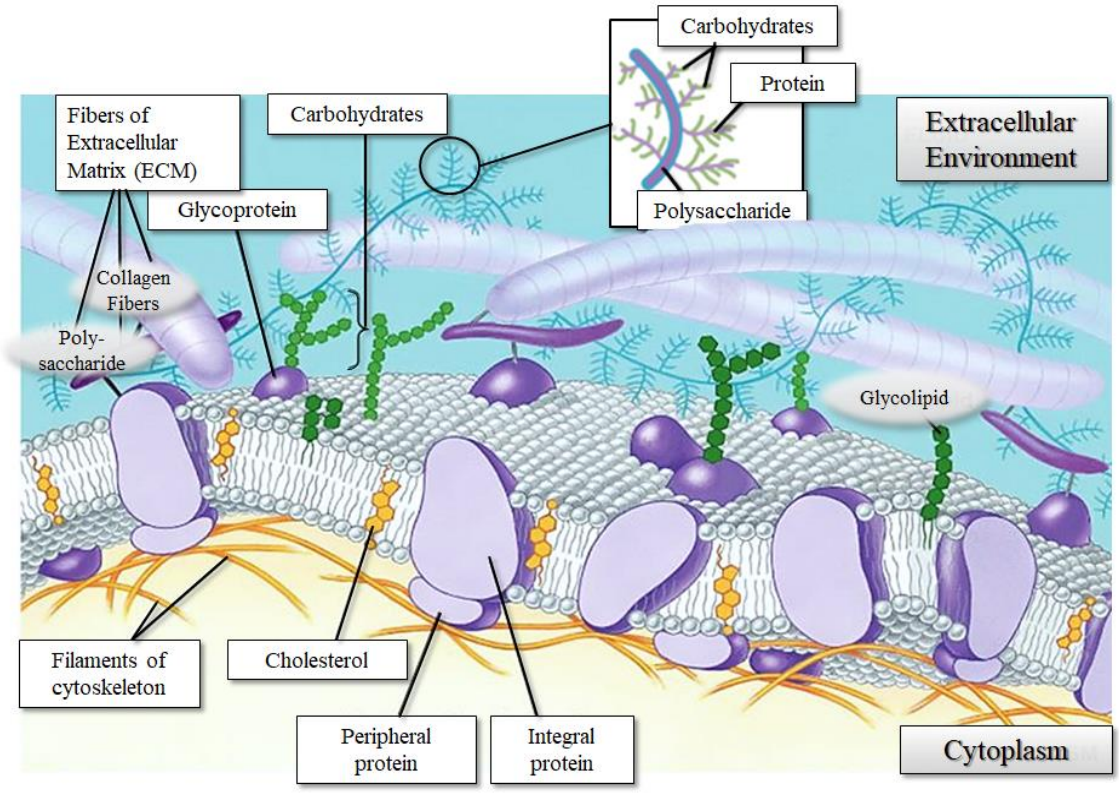

Figure 1.2, Representative scheme about ECM structure (adapted from: Encyclopedia of Biomedical Polymers and Polymeric Biomaterials, **2015**, Taylor and Francis, Munmaya Mishra)

On the base of macromolecular composition and structure, ECMs can be classified in two principal types: "interstitial and pericellular". On one hand, the interstitial ECMs surround cell, providing mechanical support; whereas, on the other hand pericellular matrices are in close contact with cells, in this context basement membrane is a type of pericellular matrix and provides anchoring sheet-like layers, preventing cells from ripping apart. In these case, basement membrane is composed principally from collagen type IV, laminin and various PGs such as perlecan and agrin. Here laminin, provides epithelial cell adhesion sites while collagen stabilizes the overall structure.[15] In these cases, whereas bio-signalling functions of each component are not completely understood, structural relevance of tight connections between collagen and laminin network is well known, featuring biomechanical properties of basement membrane.[16]

As previously described, innovative biomaterials, in regenerative medicine field, are quickly growing; among them, decellularized ECMs are emerging as components for biomaterials scaffolds, which can be bio-activated with signalling molecules able to influence cell fate, driving cell responses and tissue regeneration. Recently, data highlight how collagen or laminin based biomaterials can be promising tools for tissue engineering and regenerative medicine applications. These proteins, in form of 2D matrices, or in their hydrolysed forms can be activated with different biomolecules, from monosaccharides to specific short peptide sequences. Alternatively, collagen amino-acidic sequence offers many starting point to bound organic molecules, giving new opportunities to organic chemistry offering new challenges on bioconjugations matter.[17,18]

At the same time hydrogels, as biomaterials, has also been taken into account. Hydrogels are three-dimensional hydrophilic polymeric networks, obtained from synthetic and/or natural polymers. They are able to swell and absorb a large portion of water when placed in an aqueous solution. Hydrogels are become increasingly studied as matrices for tissue engineering, as a matter of fact, this kind of material is able to guarantee a 3D ECM-like environment for cell culture.

1.2. The “biomimetic” approach in tissue engineering.

As widely seen, tissues development and cellular homeostasis maintenance are coordinated by a plethora of regulatory factors, interacting at multiple levels, in time and space; including physics stimuli and chemical signals. For these reasons, who works on the field of regenerative medicine, necessary needs to a model able to offer a complete control over the local environment, with real-time insight on molecular events characterizing each analysed condition.

Cells cultures allow a good control of biomolecular events specific to cell responses, however, in this case, there is an oversimplified experimental model that make *in vivo* experimentation a fundamental step to reach clinical applications. In this field, our aim is represented by an improvement of knowledge on basic mechanisms, which drive cellular responses toward cellular growth, differentiation, and finally injured tissues recovery. However, to do this, is necessary work with an environment able to give the same factors responsible of cellular processes *in vivo*, this environment is so called matrix like environment (ECM-like).[19] Many of ECM proteins previously described (for example collagen or elastin), are being studied for a lot of applications in the field of regenerative medicine, this because natural proteins provide chemical, physical structures and biochemical properties, able to mimic cellular microenvironment (for example RGD sequences, see later). Extracellular matrix, mechanically, supports interactions between cells, like a scaffold that provides the framework for a high-rise building. Moreover, unlike high-rise building, ECM supports signalling functions in order to ensure a correct preservation of physiological functions.[20]

Up to now, it is well established that ECM possesses significant biochemical role in angiogenesis, wound healing and immune cell migration; as previously mentioned, RGD (Arginine-Glycine-Aspartic acid) and IKVAV (Isoleucine-Lysine-Valine-Alanine-Valine) sequences, found in fibronectin and laminin respectively, are able to mimic some cellular microenvironmental signals, promoting cell adhesion triggering integrins interaction. Further, glycosaminoglycans and proteoglycans are able to entrap growth factors and other biomolecules, inducing specific cell responses, sometimes also thank to last glyco-epitope, which is able to interact with lectin (C-Types lectins), coordinating cell-events such as adhesion between leukocytes and endothelial cells during immune-response.[21] From here, one of the most common properties of biomaterials should be cell adhesion. Initially, the strategy adopted was coating scaffolds with proteins, such as laminin or fibronectin, that are able to induce cell adhesion and spreading, subsequently, cell-binding-peptides (e. g., RGD, IKVAV) were used to covalently functionalize biomaterials surface; modulating their concentration and spacing, scientists, were able to direct cell spreading in both 2D and 3D culture

systems.[22] Another example is represented by natural anionic proteoglycans (GAGs) which appear able to interact with growth factors (GF) and cytokines. Their negatively charges stimulate hydrogen interaction, increasing GF local concentration. At the same time, local growth factors concentration may be controlled combining heparan sulfate with natural or synthetic materials modulating in this way negative charge density[23]. Finally, carbohydrates play a key role in cell communication, as a matter of fact, they decorate the outer membrane of cells, promoting receptors interaction driving interactions with adjacent cells, extracellular matrix, and secreted biomolecules.

Summarizing, a widely defined and specialized cell microenvironment is a key element for correct tissue development and maintenance. Different tissues and different stages of development show diversity in ECMs composition due to different isoforms, ratios and geometrical disposition of proteins like collagen, elastin, fibronectin, laminin and also proteoglycans[24]. This creates an environment full of biological signals and mechanism which modulate cues dissemination[25].

1.3. Scaffolds design: From ECM to materials chemistry

Nowadays several kinds of materials are extensively explored in regenerative medicine and tissue engineering[26]. Generally, the chemistry used to develop new biomaterials highlights a sort of classification; on one side, we find natural polymers (proteins or carbohydrates, more rarely nucleic acids), while on other side synthetic polymers such as ε-polycaprolactone (PCL) or polylactic-acid (PLA) appear as good alternative.[27] Polymers from natural source present some advantages, among them are well known an higher biocompatibility, in terms of cell viability, higher cell-proliferation and in some case the native presentation of receptor-binding ligand, such as previously reported RGD peptides. However, natural-based scaffold may have also some problems

regarding immunogenicity, deriving purifications strategies from corresponding natural source. Moreover, in some cases, they can be associated to pathogen transmission. Although some of these drawbacks can be overcome through heterologous proteins expression, synthetic materials offer greater control of structural and chemical properties.[28]

Natural materials used in regenerative medicine include several ECM proteins, as yet reported, (i.e. collagen, elastin)[29] or polysaccharides both from mammalian ECM or non-mammalian sources (i.e. hyaluronic acid, alginates, chitosan).[30] Among polymeric materials studied, appear PCL,[31] PLA, poly(glycolic acid, PGA), polylactic-coglycolic acid (PLGA), having biodegradability properties *in vivo*.[32,33]

In addition, also minerals or inorganic compounds find a wide application in tissue engineering. They are sometimes used for the preparation of inorganic scaffolds, such as hydroxyapatite, ceramics, bio-glasses and metal alloys, which confer specific mechanical properties, thus to simulate stiffness of specific tissue (i.e. hydroxyapatite composed by calcium minerals for bone tissue engineering).[34,35] However, despite their well-known osteoconductivity properties, inorganic materials are not able to "cross-talk" with cells; for this reason is necessary further functionalization to improve their biological activity.[36,37,38,39] Furthermore, bio-glasses and ceramics, could be upgraded into hybrid materials where inorganic and organic chemistry merge to improve fine scale interactions and chemical properties. These new features allow the inorganic and organic species to interact at the molecular level through new emerging properties.[40,41,42,43,44]

Over the past decades, several strategies have been proposed in order to improve both biocompatibility and bioactivity of scaffolds, introducing bioactive molecules which are able to stimulate specific cellular responses.

To achieve these aims, strategies such as physical adsorption, entrapment or ionic interaction were developed in order to generate bioresponsive matrix or drug release systems. Otherwise, chemical functionalization can give more stable matrix. In this

context, bioorthogonal click chemistry has contributed to substantial improvements in diversity and complexity of material functionalizations, due to its extremely high chemoselectivity, versatility in mild reaction conditions, often in physiologically-friendly environment, with high yields.[45,46] Currently, several biomaterials are in clinical trials as tissue replacement devices or already approved in therapies for regenerative medicine.[47]

Reasonably, each application requires biomaterials with a specific set of features and mechanical properties, for these reasons, and as previously mentioned, materials functionalization could be lead with different methods, including physical, chemical techniques (**Scheme 1.1**). In more detail the strategies behind functionalizations are based on:

a) physical immobilization (van der Waals, electrostatic, affinity, adsorbed cross-linked), based on physical strategies;

b) Chemical immobilization, taking advantage of different natural or unnatural functional groups present both on the biomolecules and on the material surfaces (chemo-selective ligation, via amino functionalities, heterobifunctional linkers, etc.). [48]

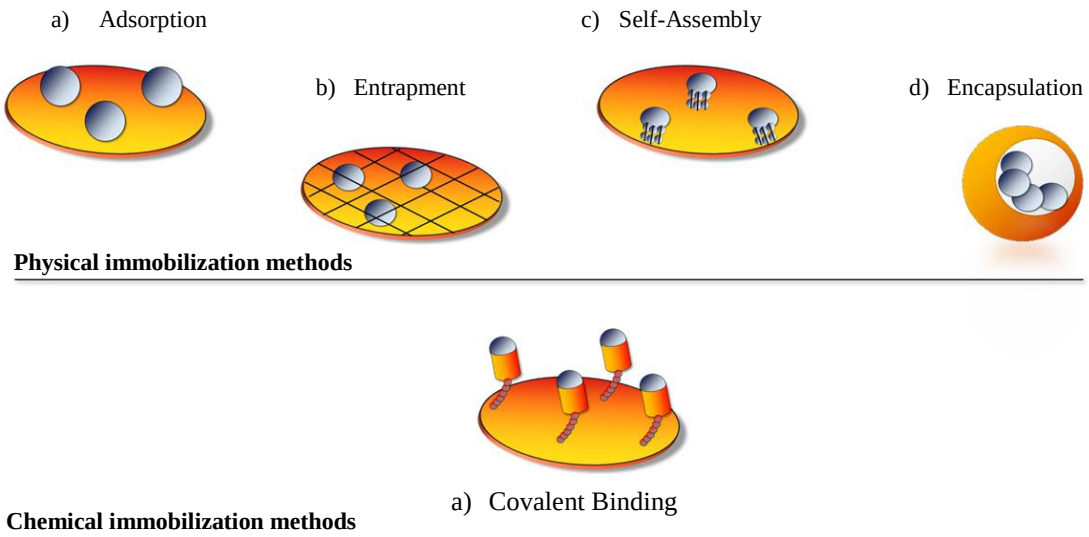

Scheme 1.1 Representative scheme about functionalization strategies.

Physical methods. Through physical modifications, functional molecules or active chemical groups can be introduced on the surfaces of materials, leading to the functionalization and activation. Behind strategies, such as molecular coating (or adsorption), surface entrapment, and physical treating with plasma, ozone, or UV; there are different advantages such as the simplicity in handling and mild conditions operating; all of this in order to avoid biomolecules damaging, decreasing, eventually, their bioactivities. These methods, however, also show certain limitations, among which there are physical linkages, often formed between the substrates and coatings. These physical linkages and interactions are considered to be weak, if compared to chemical bonds, therefore, functional molecules and entities may detach from the surfaces of modified materials. Particularly when certain serum components compete for active binding sites in physiological conditions. Non-covalent adsorption is sometimes desirable, as in some drug delivery applications.[49]

Covalent linkage. Covalent conjugation of biomolecules produces stable bonds with a controlled exposition and orientation on material surface, often limiting cellular metabolic degradation and biomolecules washing from material 2D scaffolds, finally, extending them half-life.[50] However many factors (such as GF) require to be free in

solution to influence cell life ensuring some biological responses; for these reasons, sometimes covalent linkage need to be reversible or degradable to ensure a correct release of these factors. Among them, has been described so called "Cell-responsive" scaffolds in which some cell behaviours (such as growth or migration) result in matrix enzymatic degradation, which can be catalysed by specific factors release. In these cases, factors release can be "on demand", also, opening new way toward drug delivery. For example, peptides immobilization through a sensible linker toward metalloproteases (MMP) activity can be released by dermal fibroblasts growth. In stress conditions, fibroblasts secrete MMPs catalysing peptides release.[51] Furthermore, these factors can overcross cell membrane, interacting with different intracellular targets stimulating opportune signalling pathways. However, factors internalization, often can lead to cytotoxic effects, for these reason the choice of drug represents a crucial element. A covalent and stable bound over the time, doesn't would allow this process and stop biological response.

1.4. Covalent Functionalization strategies

As described above, polymers used in biomaterials to develop new medical devices, often need to further functionalization in order enhance specific biological responses. Through the modification is possible control their properties, conferring new biological functionalities and structural features to better allow their integration with biological systems. These modified materials can lead to new emerging properties toward a variety of biomedical applications, ranging from implant engineering and regulated drug delivery, to clinical biosensors and diagnostics.[52]

As well known, immobilized molecules can interact with cellular receptors presenting on membrane surface. For example, neuronal outgrowth need to NGF, as key factor that

induces cells stimuli, by signalling at the plasma membrane, promoting neuron survival when internalized.[53] Often, surface conjugation has been successfully used to attach several factors to a variety of natural and synthetic biomaterials. Signalling by these immobilized bioactive ligands, may be more potent than signalling by soluble versions, that are free added directly to culture media. Different studies, also show that the immobilization strategy should considers protein structure and active region topology.[54] Anyway, is very important keeping mind that any interaction through covalent linkage on biomaterial surface doesn't replicate correctly physiological interaction, due to covalent linkage. Finally, some factors may be better delivered in a continuous manner, while others take advantage from direct attachment to the biomaterial surface.[55] Generally, covalent functionalization, first requires reactive groups (such as -OH, NH_2, COOH, SH, etc...) and secondly, synthetic strategies to afford functionalization steps, possibly in mild and biocompatible conditions in order to avoid biomaterial degradation. When the material doesn't contain reactive groups, they can be introduced by chemical and physical modification, on the polymer surfaces in order to allow covalent attachment of biomolecules. In this context, a wide number of surface modification strategies have been developed, from physical techniques, including plasma, ionic radiation graft polymerization, photochemical grafting, to chemical modification and derivatization.[56] In addition, matrices that bring carboxylic acid groups can be reacted with N-terminus functionalities, after activation with 1-ethyl-3-(3-dimethylaminopropyl)-carbodiimide (EDC, also referred to as water soluble carbodiimide, WSC) or dicyclohexyl-carbodiimide (DCC). This is the case of peptides functionalization or generic NH_2-equipped biomolecules (**scheme 1.2**).

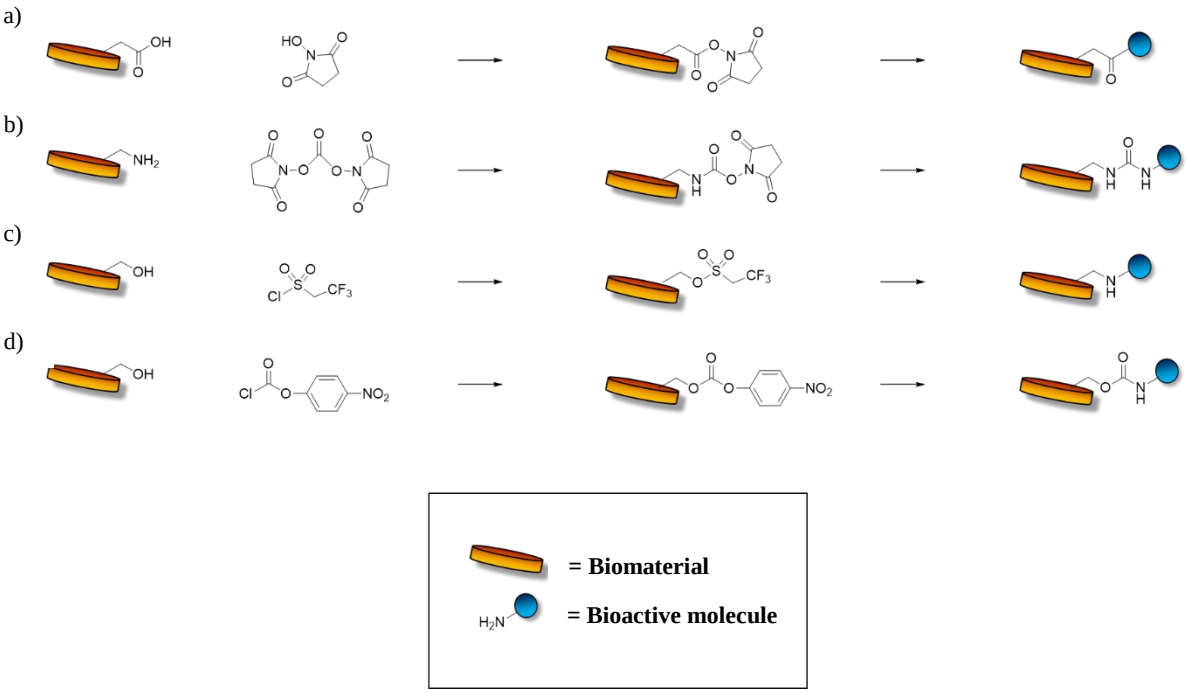

Scheme 1.2 Coupling methods to different groups on materials

At the same time, ligation strategies need to be chemoselective and stereoselective in order to ensure a correct exposition of our molecules. Chemoselective ligation is referred as a strategy able to form stable bond without the necessity of an activating agent and without interfering with other functional groups which are usually encountered in biomolecules. In biomaterials environment, chemoselective reactions proceed usually under mild conditions and result in good yields. Specially on natural based scaffold. [57]

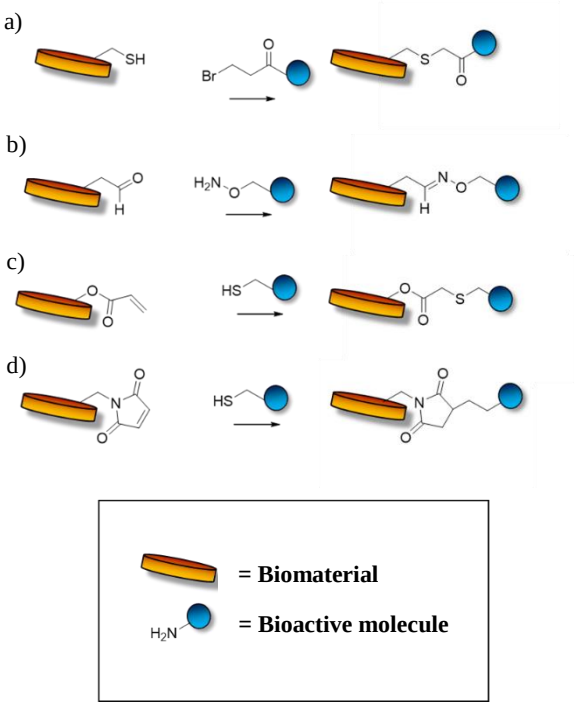

Scheme 1.3 Examples of chemoselective strategies.

Furthermore, many molecules, to interact with appropriate targets, often need to have conformational freedom and spacers, all of this to ensure an adequate distance from membrane anchoring point, ensuring, at the same time, biomolecular interactions with target receptors on cell membrane. For these reasons, using covalent spacer arm between biomaterial and molecule could result in a better access to the specific target receptor. One useful and biocompatible spacer is polyethylene glycol (PEG) that can be differently functionalized at the two extremities.[58] Metal or ceramic surfaces may also be silanised, exploiting functionalized triethoxysilanes.[59]

1.5. 2D/3D biomaterials and nanotechnology development

Cell cultures in vitro are frequently used to advance understanding the mechanisms that undergoes cell behaviour *in vivo*. These behaviours include cell differentiation, migration, growth, and self-interactions, which are impacted by their biochemical and biomechanical microenvironment. Deciphering mechanisms behind these behaviours is vital to understanding in *vivo* processes that result in formation and function of tissues and organs. Ideally, experiments should be performed with a three-dimensional (3D) models that closely mimic cellular microenvironments; creating models which include construction of tissue-tissue interface, controlling the spatio-temporal distributions of oxygen and carbon dioxide, nutrients, and waste.[60] Nevertheless, 2D cell cultures represents intermediate and fundamental step, used to follow a specific biological response arising from 2D matrix like environments, opportunely bio-activated. However, although experimental evidences suggest, under some circumstances, the 2D models can result in a reasonable cell bio-activation, deviations could be observed; obviously these approach cannot fully replicate 3D environment. Especially, in the case of cancer cells, some important characteristics cannot be appropriately modelled in 2D cultures.[61]

To better mimic *vivo* conditions, novel 3D systems need to be developed, most promising 3D biomaterials are presented by peptide-amphiphile (PA) nanofibers which are produced by molecular self-assembly technologies with an high water content, [62,63] or hydroxyapatite porous scaffolds for bone tissue engineering. In this case scaffolds for osteogenesis should mimic bone morphology, structure and function in order to optimize integration into surrounding tissue. Bone is a structure composed of hydroxyapatite ($Ca_{10}(PO_4)_6(OH)_2$) crystals deposited within an organic matrix (95% is type I collagen).[64] One of most famous 3D systems is represented gelatine-based hydrogel able to “encapsulate” cell. In the last years these systems have showed that, increasing the dimensionality of extracellular matrix (ECM) around cells, from 2D to 3D, can significantly improve cell proliferation, stimulating also several processes such

as differentiation or mechano-responses. Overall, 3D systems offer an attractive alternative for 2D cell culture.[65,66,67] As shown in **figure 1.3**, several features between 2D and 3D biomaterials are reported, among which cell polarity, adhesion in all three dimension and the presence of nutrients gradient, make 3D cell culture a complete model to replicate certain *vivo* conditions.

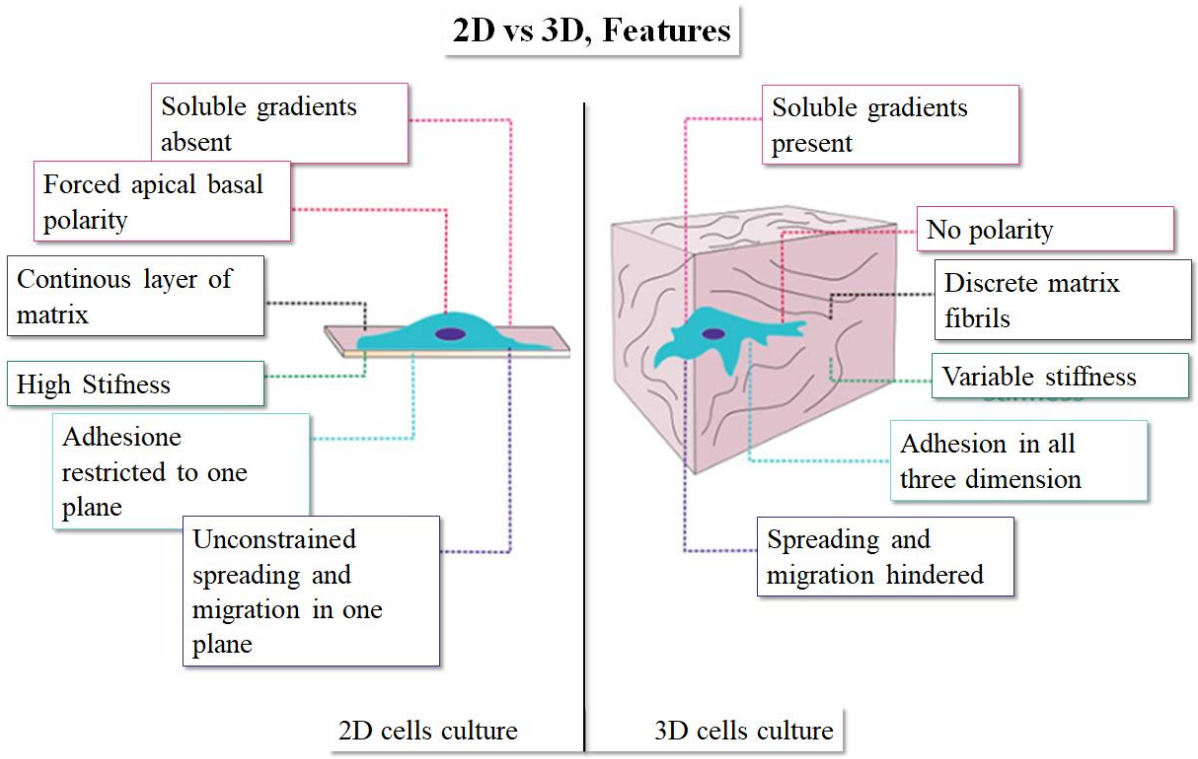

Figure 1.3, representative figure about the differences between 2D culture and 3D culture (adapted from: *Physiology* **2017**; *32*(4), 266-277)

In addition to creating ECM-like structures with appropriate majesties, nanomaterials can be useful, as mentioned, to drive specific cellular response; always focused on regenerative medicine. One of the most rationale purpose behind incorporating nanostructures is to compensate for other scaffold limitations, such as electrical conductivity or other mechanical properties. For example, carbon nanotubes show

viscoelastic properties similar to that observed in soft-tissue membranes[68], so they have been used to increase tensile strength of the hybrid biomaterial and certain viscoelastic properties.

Carbon nanotubes were also used for neurons cultures, and in recent years, several studies have shown that conjugation of these nanotubes to different substrates, with proposed strategies, can effect on cell fate and promote cell spreading, growth, differentiation and long-term survival of neurons.[69;70;71] One of the main obstacles in neural regeneration is represented by the loss of anisotropic conduction, within the cell-seeded support owing to lack conductivity ability of the biomaterial. In these cases, approaches to addressing this problem regard the incorporate conducting nanostructures into the cell culture, showing neurons more efficient signal transmission.[72] Moreover, carbon nanotubes have also been used to create 3D conductive structures like a "sponges", resulting in composites with high electrical conductivity. The potential of these hybrid scaffolds to support the cultivation of neurons or cardiomyocytes should be further explored. Furthermore, nanostructures can also be used to increase the viability and adhesiveness of cells to pre-formed microporous scaffolds.[73;74]

In recent years, nanoparticles have also been used to manipulate biomaterials and cells in order to create desired tissue structures. Several works shown as magnetic beads can be manipulated to create an initial 2D hexagonal array that served as nucleation sites for the growth of fibril fibres that assembled into an ordered scaffold.

Endothelial cells seeded on these scaffolds shown high adhesion and vitality and their actin filaments aligns together in according to the scaffold fibres.[75] In other cases, cells were conjugated to magnetic nanoparticles and seeded on culture plates, in this case cells move on forming multi-layered tissue that can be detached by removing the magnet. With these strategies scientist as Souza and co-workers report new approaches to control the assembly of 3D tissue providing an alternative to biodegradable scaffolds and protein matrices[76].

In these cases, technology is based on cellular uptake and subsequent magnetic levitation of a hydrogel composed of phage, magnetic iron oxide and gold nanoparticles. By spatially controlling the magnetic field while cells divide and grow, the researchers were able to manipulate the geometry of the cell mass and engineer 3D structures. This approach can be used to engineer complex tissues composed of several cell types, organized in specialized niches by transferring cells to their specific locations. But to do this but to do all this it is necessary to know and deepen the conjugation tenets of biomaterials and cell culture[77].

Concluding, it's our opinion that, each event regarding cell-cell and cell-environment interaction is interconnected to chemical and mechanical properties of cell membrane and extracellular matrix. The focus of this thesis is show what are some basis of a specific cellular behaviour (i.e. angiogenesis or cell proliferation) and how some chemical strategies can help us to achieve these results, developing new bio-inspired 2D and 3D matrices. Every year several strategies are developed in order to find the correct way to stimulate these specific cell responses, however, often this are not enough and new nano-systems are necessary to find which are the molecular events trigger certain states. Also at the level of cellular membrane and cellular components if necessary.

In this respects, dendrimers and collagen offer great potentiality to achieve these purposes; for these reasons finding new promising chemical strategies and new tools is necessary to boost this field toward new applicable medical devices. For example, as we will see later (in the chapter 5), lectins represent one of the main protagonists in cell communication and here glycondendrons offers many opportunities to improve the knowledge behind these interactors. This is the reason why developing new dendrimers with glycoepitopes can give the basis of a correct interaction on a hypothetic 2D matrices, because also spatial configuration in the carbohydrate chemistry can alter the results.

Once we find which are the molecules responsible for a specific cell behaviour, also mechanical properties of supposed 3D matrices are important to ensure a correct clinic therapy. As a matter of fact, cells not only responds to molecular events as signals, but,

as well seen, also mechanical features could drive cells fate. At the end the awaited biological event most probably will be a response resulting from all these stimuli. In this case chemical and physical components will interplay to give a response arising from new emerging properties.

For described assumptions, in this PhD course have been applied several strategies of organic chemistry for the syntesis of new 2D/3D scaffolds and glyco-functionalized dendrimers, giving new interesting biomaterials for tissue engineering applications (in the first case) and tools for the study of lectins carbohydrate interactions (in the second case). In this thesis there are the collected results by my work, with a special attention on hydrogels synthesis, as a 3D scaffold, to mimic extra-cellular matrix and studying the deepest cell behaviours.

In **Chapter 2,** peptide bioactivation of collagen based biomaterial is presented. It is well known how short peptide with a specific sequence could mimic some functional epitopes of native proteins and then, stimulate in the same way the functional role of native proteins, ideally promoting fundamental biological processes. Among them **β**-**T**hymosin **P**eptide (Tβ4) and **H**uman **V**asonectin **P**eptide (HVP) exert a pro-angiogenic activity or adhesion activity through interaction with actin binding site,[78] promoting **V**ascular **E**ndothelial **G**rowth **F**actor (VEGF) expression. Here, is presented collagen bio-conjugation with these peptides and outcomes.

In **Chapter 3** another 2D collagen based biomaterial is shown. In the field of regenerative medicine also oxygen level is a crucial parameter for the tissue development both *in vitro* and *in vivo* because in the absence of tissue perfusion, or any adequate solution, starts to experience metabolic suffering. Perfluorocarbons (PFC), in the last decades, have been gained more interest due to their ability in oxygen storage or oxygen carriers.[79] With these premises **5-(2,3,4,5,6-Pentafluorophenyl)-3-undecyl-1,2,4-oxadiazole** was used to functionalize collagen based biomaterials.

In Chapter 4, after a global view of complex world of hydrogels, the chapter is splitted in two parts, where in each ones new strategic way has been proposed developing

hydrogels for regenerative medicine purposes. In the first part, triazoledione chemistry has been proposed as a click-reaction for the chemoselective bioconjugation to tyrosine residues, meanwhile, in the second part, 3,4-Diethoxy-cyclobutene-1,2-dione (SQ) has been used for lysines chemoselective cross-linking.

In Chapter 5, new glycol-functionalized dendrimers structures are described exploring carbohydrate chemistry. Here, we propose the synthesis of novel oxime-armed dendrimers structures which allow multivalent conjugation of carbohydrates through oxime coupling.

Chapter 2 - Protein, peptides and material bio-activation

2.1. Introduction

Signalling peptides identification within ECM adhesion or structural proteins,[80] has opened an important gate to creation of ligand-bioactivated materials. Up to now different cell-adhesive peptides have been grafted to material,[81,82,] in which, both concentration and spatial orientation can be modulated, and consequently, may help in deciphering the complexity of signalling events in cell-ECM interactions. To design new bio-inspired materials, wide studies on ligand density and quantitative informations, for a particular cellular response,[83] need to be discovered, all of this to study the biochemical relevance of target peptides and improve the biochemical systems efficiency. For these reasons, peptides, have become increasingly important in the design and fabrication of bioactive materials for medical applications.[84,85,86,87] Moreover, highly refined structure, and gram-scale methodology synthesis of peptides containing up to 50 amino acids (SPPS), making them good candidates for medical devices. In addition, degradability in physiological conditions brings to amino acids which can readily reabsorbed or excreted. Another relevant feature is the intriguing diversity in functional properties, as result of a subset of 20 amino acid building blocks. From the several motif of ECM proteins numerous peptides have been identified with specific bio-functions, for example, RGD peptides have been found in fibronectin, which is known to bind integrins on cell surface and enhance cell adhesion.[88] Furthermore certain peptides are known to readily self-assemble to form secondary structure, such as helix or sheet, also here, making them useful to fabricate hierarchical structures with thermal stability or pH sensitivity or pH tuning. In addition the use of native proteins as drugs to enhance the healing process, is often hindered by several

disadvantages, such as low tertiary structure stability and high cost.[89] Summarizing, each peptide provides particular bioactive properties such as receptor-binding ability or self-assembly behaviour, which originate from the sequence. The concept is: combining these sequences to "transfer" their properties generating, where possible, new emerging properties.

For these purpose, it is reasonable thinking how each peptide can be designed and synthesized for a specific application. In the world of biomaterials, several peptides has been used to functionalize biomaterials for *in vitro* studies of cell behaviour in order to find many application in therapeutic and diagnostics medicine, drug delivery, tissue engineering and finally, it is fundamental for the study of cell behaviours.[90,91] For these reasons, it is necessary apply technologies with high chemical specificity and reaction efficiency to obtain high yield with low cost. With this focus, ''Click'' reactions have emerged as ideal candidates, fulfilling prerequisites such as: (1) high yield, nearly quantitative conversion; (2) biologically benign conditions (aqueous solution, room temperature, and near physiological pH); (3) limited or no residual by-products. In this case we preferred using maleimido-Thiol coupling to develop new bio-inspired material able to stimulate angiogenesis and vascularization processes.

2.2. biomaterials peptide bioactivation

As described, it is well known short peptides, with a specific sequence, could mimic some functional epitopes of native proteins and then stimulate in the same way their functional role. Among them **β-T**hymosin **P**eptide (Tβ4) and **H**uman **V**asonectin **P**eptide (HVP) exert a pro-angiogenic activity or adhesive through interaction with actin binding site[92], promoting VEGF (**V**ascular **E**ndothelial **G**rowth **F**actor) factor expression of endothelial cells or, in the case of HVP osteoblast adhesion and spreading

on matrix components. VEGF induces endothelial cell proliferation, promotes cell migration and inhibits apoptosis. *In vivo* VEGF induces angiogenesis as well as permeabilization of blood vessels; for these reasons VEGF plays a central role in the regulation of vasculogenesis and tissue regenerations. [93]

β-Thymosin Peptide (Tβ4) Thymosins are a family of three polypeptides, α-, β-, and γ-thymosins; in mammalian cells only β-thymosins are expressed, and just thymosin β4 (Tβ4) represents 70-80% of the β-thymosins global content.[94,95] In particular, Tβ4 is highly conserved, water-soluble and composed by 43-amino acid with an overall acidic feature; is localized in both cytoplasm and nucleus, where probably acts as transcription factor inhibiting G-actin by 1:1 dimerization process,[96] by electrostatic interactions with residues 13-23. Whereas, residues 1-7 seems to be involved in the inhibition of G-actin polymerization.[97,98] 20 years ago, it was also demonstrated the ability of Tβ4 to induce angiogenesis[99] and, although this is clearly established as consequence of endothelial cell migration;[100,101,102] the molecular mechanisms behind this process, are not completely understood and need to be still explain. The major evidences suggest an angiogenic response involving the binding of Tβ4 to an unknown cell surface receptors, internalization of the peptide and rearrangement of the actin cytoskeleton; suggesting the possibility of a central role in tissues regeneration.[103] However, the precise and direct mechanism, by which Tβ4 directs, internalizes and drive cellular migration is only sketched and the role of these unknown receptor is still a matter of debate. Nevertheless, the several holes underlying biological mechanism, Tβ4 has reached initial phase 1 clinical trial showing safety, tolerability. Dose-escalation and pharmacokinetic studies are in due course in healthy volunteers who receives Tβ4 topically each day for 28 consecutive days. First results show Tβ4 being well tolerated, exhibiting no signs of toxicity at any given dose. Based on these results and on several nonclinical toxicology and dermal-sensitization studies, it has been suggested that the clinical introduction of Tβ4 is tolerated in patients with chronic cutaneous wounds.[104,105]

As seen in introduction section, collagen and other extra cellular matrix components possess key role in bio-signalling and cellular fate control, however, often the bio-

entities responsible of these role are not well known. For these reasons, developing new functionalized collagen based biomaterials, with these peptides, may help, first to understand responsibles molecular basis of vascularization processes and then, secondary, might add to the potency and useful applications of this molecule generating new biomaterials for tissue engineering and regenerative medicine application.

Human Vitronectin Protein (HVP) Another focus of regenerative medicine, represented by adhesion and spreading processes of specific cells type; for example, human osteoblasts.

Nowadays, it is clear how osteoblasts adhesion occur through interaction mechanisms with RGD motifs via cell membrane integrin receptors or through interaction between cell membrane heparin sulphate proteoglycans and heparin binding sites on extracellular matrix proteins.[106] Regarding first mechanism, as widely described above, RGD sequences are ubiquitous adhesive motifs, found in many extracellular proteins, especially in bone tissues, such as fibronectin, thrombospondin, osteopontin, type I collagen, osteonectin and bone sialoprotein.[107] Specialized cell surface proteins recognize RGD sequences and trigger cell attachment by non-specific mechanisms. His feature is a consequence of redundancy in the affinity of integrins for adhesive proteins and because a variety of cells possess the same integrins, the attachment of cells to RGD need to be nonspecific.[108]Among extracellular proteins, human vitronectin (hVN), is one of the major cell adhesion proteins found in the extracellular matrix.[109,110] HVN works principally as monomeric polypeptide (75 kDa) or as two different polypeptides (65 and 10 kDa) linked by a disulphide bond,[111] providing link between a wide range of biological activities, including tissue repair, angiogenesis, haemostasis and metastasis.[112] HVN interacts by specific conserved region with several proteins;[113,114,115] meanwhile, carboxyl-terminal region, contains an arginine-rich domain, which binds heparin.

Generally, In the field of regenerative medicine, adhesive and angiogenic proteins find a wide range of applications; however, are usually dificult to obtain in large quantity and with high purity; for these reasons, biomimetic peptides synthesis is considered one of

the most popular strategies to produce RGD sequences cheap, available in large quantity and with high purity. Moreover, they result being relatively more stable during conjugation processes. Among the several adhesion sequences in hVN proteins, the most used for regenerative medicine applications is, yet mentioned, tripeptide RGD, reproducing the signalling domain derived from vitronectin. Furthermore, also other sequences such as YIGSR, REDV, and IKVAV have been used, and often immobilized on different model substrates[116,117] such as glass[118,119] quartz[120], metal oxide[121] and natural or synthetic polymers.[122]

The choice of substrate for the conjugation of these biomolecules is based on parameters such as biocompatibility, cytotoxicity and mechanical properties. Collagen has been found in all connective tissues, in each of them possesses unique mechanical and signalling properties, making it one the most studied substrate for scaffold applications in regenerative medicine. Collagen molecules are composed by of three α chains that assemble together due to their molecular structure; every α chain is composed of more than a thousand amino acids based on the sequence -Gly-X-Y-. The presence of glycine is essential at every third amino acid position in order to allow for a tight packaging of the three α chains in the tropocollagen molecule, the X and Y positions are mostly occupied by proline and 4-hydroxy-proline. Cell-matrix interactions consist mainly in the interaction of cells with collagen, directly or indirectly. Direct cell-collagen interactions consist of cell receptors recognition of specific peptide sequences within collagen molecule;[123] in indirect-collagen interactions; on fibronectin the integrin recognized sequence RGD (Arg-Gly-Asp) was identified, [124] moreover, other proteins show this RGD or other motifs, binding to collagen, thus allowing indirect cell-collagen interactions. These are the reasons why collagen based scaffolds represent a great promise in regenerative medicine fields and it is selected as substrate for peptide bioconjugation. In addition, hVN, and its derivatives, have been used to promote osseointegration of implantable devices by improving surface cell interactions and increasing implant connectivity with surrounding bone.[125,126] These are reasons why collagen based biomaterials, RGD functionalized, need to be studied, improved and then applied to restore injured states.

2.3. Aim of the work

In this paragraph has been developed new biomaterials (in this case 2D collagen based biomaterials) which present functional motifs of these proteins, obtaining in this way new tools able to promote specific cellular behaviours inherent to vasculogenesis or adhesion processes. As a matter of fact, since collagen based biomaterials are well known to be biocompatible and approved for clinical use, it is here proposed a study of collagen bioactivation with an angiogenic motif of Thymosin β4 and an adhesion sequence of Human Vasonectin (called HVP). Then, these new bio-inspired scaffolds were tested to study their properties by several cellular lines culture as Human Dermal Lymphatic endothelial cell (HDLE) and human osteoblast (HO). All this in order to evaluate proliferation and adhesion capacity.

2.4. Results and discussion

One of the most popular click reactions in proteins conjugation, reported above, is Thiol-Michael addition.[127] In this reaction, the focal point is the thiol group acting as nucleophile toward an alkene linked to electron with drowing groups, in our case, given by the maleimido group; the reaction give a new stable thioether as final bond.

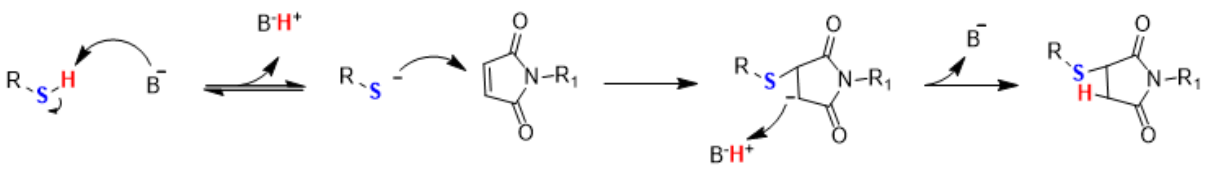

Scheme 2.1. Proposed mechanism for Thiol-Michael type addition in aqueous base catalysed conditions.

In this paragraph, Thiol-Michael type reaction represents a focal point of the collected results, which describe and reinforce all that is known in literature about extracellular matrix providing, at the same time, a new bio-inspired materials useful to enhance focalized cellular response. With this reaction is possible introduce thiol group on amino-acidic sequence, just adding cysteine residue to N-terminus. Moreover, classical click reactions sometimes, involve use of metal/copper catalyst (i.e. Huisgen cycloaddition to give azide-alkyne cycloaddition) or UV irradiations that can damage eventually tertiary protein or polypeptide structure (especially in the case of UV or x-ray). In presence of biological building blocks, as collagen, these conditions can cause alteration or damage to materials, making them less suitable to use for biological studies. Thiol-Michael type reaction, instead, allow to have an aqueous solvent able to give desired product with higher yields, optimal conditions to give fast reaction kinetics and quantitative conversion are: 1)weakly basic aqueous solution, 2) room temperature.[128] Therefore, (as shown **Scheme 2.2**), maleic groups have been previously functionalized on collagen scaffold surface, and subsequently, have been used as substrate for Michael reaction in order to functionalize collagen based matrix with the two peptides already described.

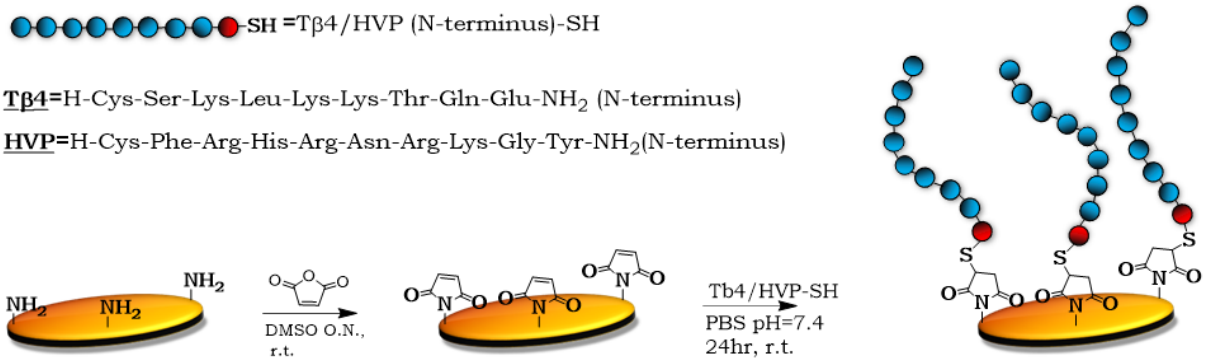

Scheme 2.2, upward, it is shown the sequences of used peptides. At the carboxyl end, a residue of cysteine was added to provide thiol group, necessary for the reaction. On the lower side it has been presented synthetic strategy to collagen scaffold bioactivation.

Many parameters can influence the reactivity of this reaction,[129] among them, adjacent amino acids to cysteine (in peptide sequence) represent the most evident variation which can alter kinetic and rate conversion. Generally, positive charged amino acids, like arginine, decrease the pKa of the neighbouring thiol and accelerate the reaction, while, negatively charged amino acids, like aspartic acids, show the opposite effect.[130] Reasonably, pH of aqueous solution and peptides isoelectric point may influence the reactions, but generally it has been study that basic conditions prompt higher reaction rates, the common pH used is 7–8.5.[131] Further, others parameters can alter reaction kinetics, for example it is known that the nature of structure of electron deficient vinyl groups can allow to higher or lower conversions rate. By chemical point of view, it has been reported the order of reactivity among types of C=C bond in Thiol-Michael addition as follows: maleimide > vinyl sulfone > acrylates/acrylamides > acrylonitrile > methacrylates/methacrylamides. Maleimide groups conversions are considered almost quantitative reaction.[132]

After 24 hour of reaction (390 μg, 0.30 μmol, 0.4 ml) FT-IR analysis confirm the success of the reaction. As a matter of fact, at 866 cm^{-1} it is possible see a new peak arising by first functionalization (**figure 2.1**; **a.** and **b.**; coated-mal., red line). In more detail the new absorption peak was assigned to alkene double bond stretching absorbance, confirming maleimido grafting. In the second step, cysteine thiol group reacts with this C double bond to give a new stable thioether (**scheme 2.2**), as consequence, the peak at 866 cm^{-1} disappears as result of peptide conjugation. (**figure 2.1**; **a.** and **b.**; coated-Tβ4 and HVP; respectively blue and green lines).

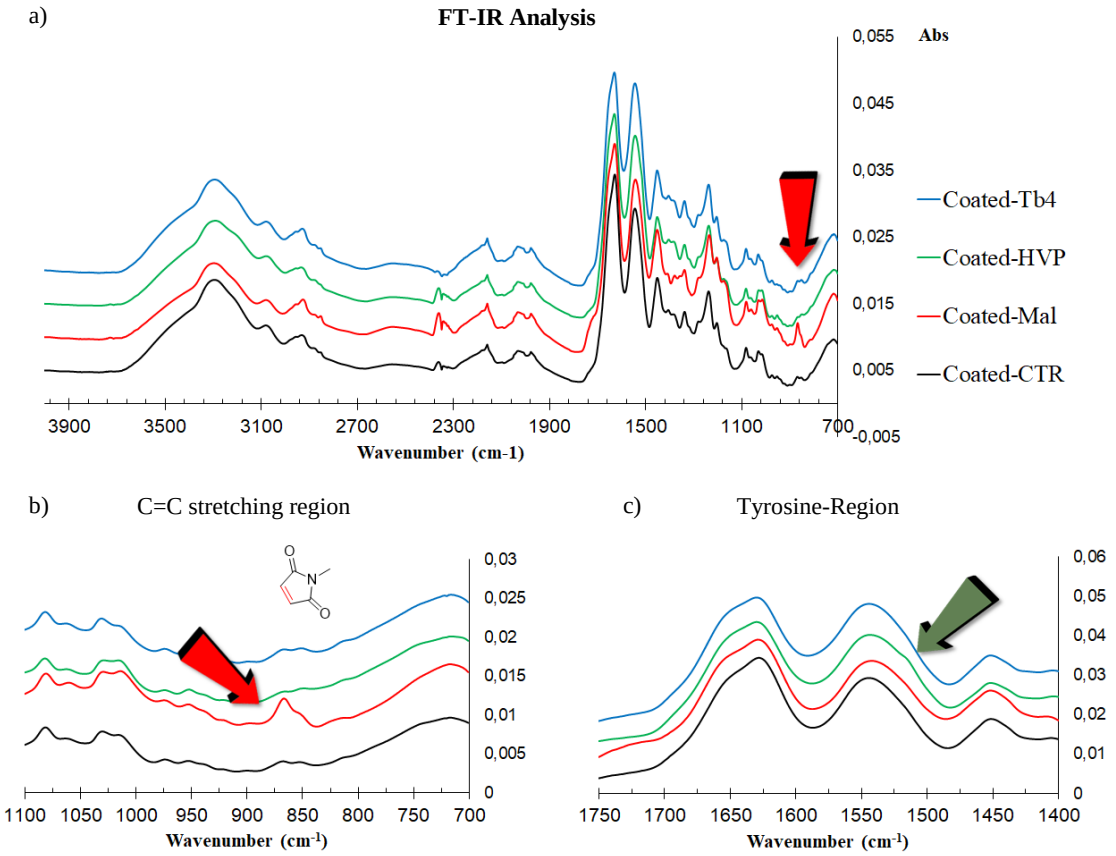

Figure 2.1 Analysed FT-IR spectra. a. global view of stacked FT-IR spectra (Coated-Tβ4 represent collagen coating Tβ4 functionalized; Coated-HVP, collagen coating HVP functionalized, Coated-Mal, collagen coating maleic grafted; Coated-CTR, collagen coating without functionalization) . b. region between 1100-700 cm^{-1} has been reported; in this case characteristic C=C stretching results after maleimido functionalization (Coated-Mal, red arrow/line) which disappears after peptide conjugation (Tβ4-coated and HVP-coated, respectively green and blue lines). c. represents a zoom between 1750-1400 cm^{-1} around Tyrosine region. In the coated-HVP sample (HVP-functionalized collagen, green line) a weak signal (see green arrow) is appreciable at the right of amide II stretching signal.

In addition, a further result emerges. Observing the region near to amide II absorption signal is possible note a slight deviation in coated-HVP sample (**figure 2.1**; **c.**; green line) It's our opinion that since collagen is really poor of tyrosines (less than 0.75%) and since HVP peptides conjugation involves tyrosine insertion, this results in FT-IR spectra modification in this region. Moreover, as reported in literature,[133] at 1516 cm^{-1}, a band, referred to tyrosine signals, can be found. This is the case of HVP in which the presence of new tyrosines has been noted after peptide conjugation (**Figure 2.1**; **a.** and **c.**). These

results were confirmed by second derivatives analysis. Furthermore, through the ratios between the intensity of a selected bands (in this case C=C) and an internal control bands is possible quantify relatively the intensity of the bands and estimate if the differences are verified by statistical t-student analysis. (**figure 2.2**; **b**. and **d**.).

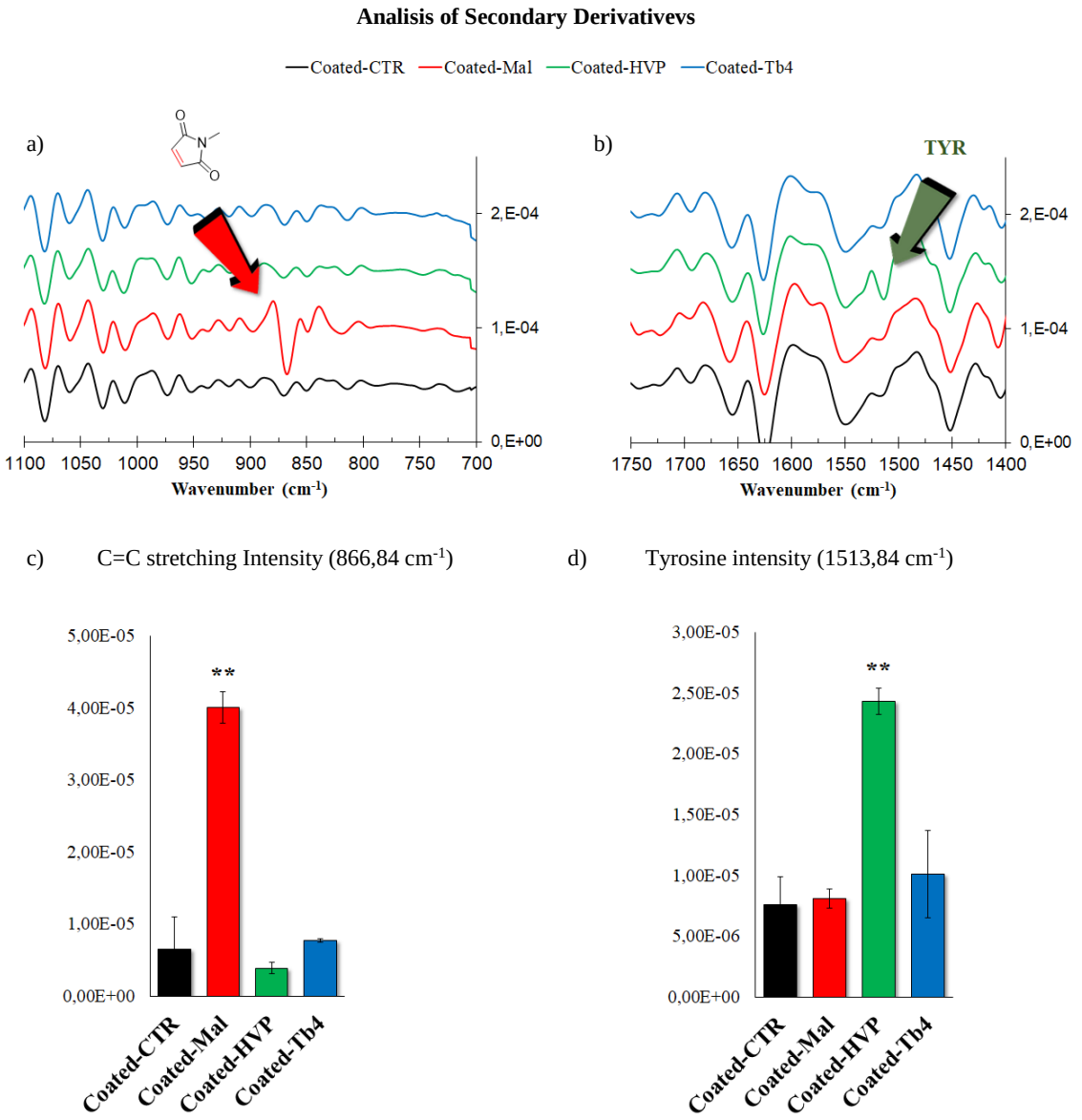

Figure 2.2 FT-IR second derivatives spectra were reported (CTR=pristine collagen, Coated-Mal=first functionalization with maleic groups, Coated-HVP=HVP grafted scaffold, Coated-Tβ4=Tβ4 grafted scaffold) a. in the range 1100-700 cm^{-1} is possible follow the peak arising from maleimido groups during each steps of functionalization. b. second derivatives of region between 1750-1400 cm^{-1} in which a new

peak confirms the presence of new tyrosines on collagen matrix. On down side, c e d show relative quantification of intensity peaks respectively of C=C and tyrosine (bars indicate standard deviation, t-student test for **p<0.01, *p<0.05).

Subsequently, these bio-inspired biomaterials, were tested for the study of biological properties, growing two cellular lines. In particular: Human Osteoblast, (HO) and Human Dermal Lymphatic Endothelial cell, (HDLE). In these fields HO and HDLE are used as model in order to evaluate proliferation and adhesion capacity, as a matter of fact and, as described subsequently, these cellular lines represent a good tool for these studies due to their key roles in angiogenesis processes. The capacity of adhesive peptides to promote cell adhesion and vitality was compared, following 2h culture on HVP functionalized collagen scaffold, osteoblasts adhesion significantly enhances, if compared with pristine collagen (HO_coated HVP Vs CTR, green and black, **figure 2.3**, **c.**). After 24 hr, adhesion is 5 time higher than control and then, over 3 days of growth, the cells reach confluence (**figure 2.3**, **c.**). On the other side, Tβ4 peptide weakly improve adhesion capacity of HDLE cells if compared with control (HDLEC_coated Tβ4 *vs* CTR, blue and black bars, **figure 2.3**, **d.**). In the same manner no exciting evidences have been seen between pristine collagen and Tβ4 coated collagen following HDLEC vitality (**figure 2.3**, **b.**).

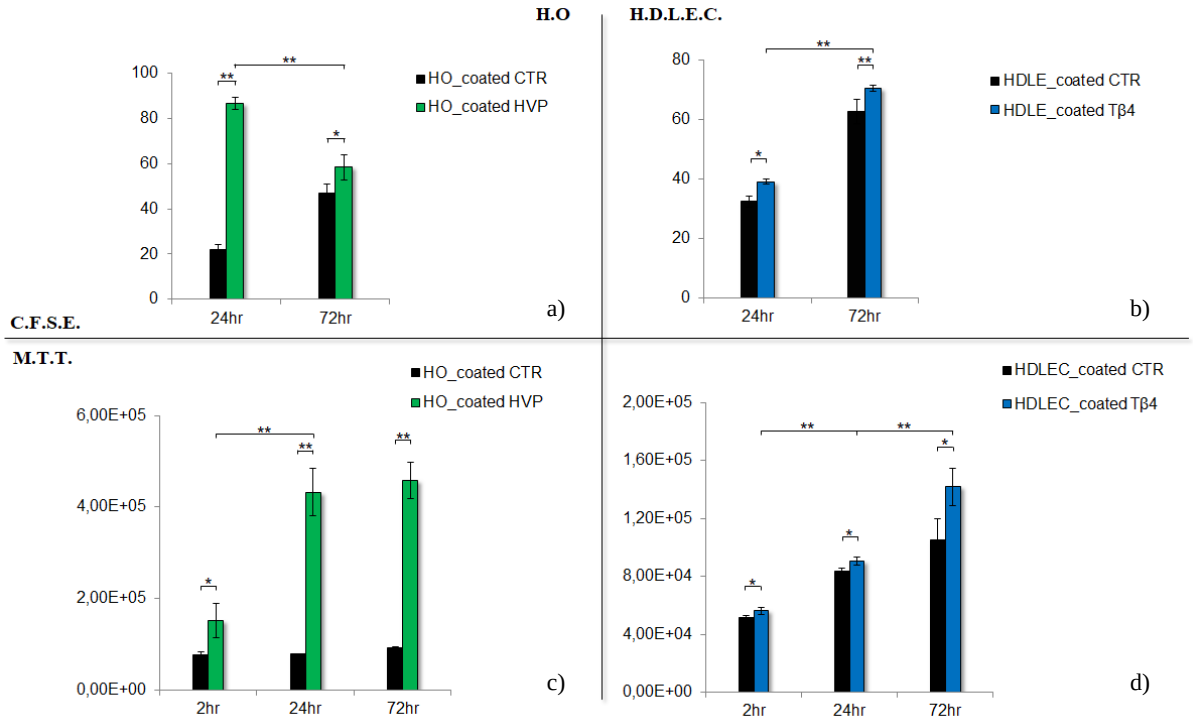

Figure 2.3. a. and b. respectively cell vitality of HO and HDLE. c MTT assay of HO (c. graph) and HDLE (d. graph). Significantly higher values observe for both Tβ4 and HVP (bars indicate standard deviation, t-student test for **p<0.01, *p<0.05) referred to CFSE assay.

After cellular culture, VEGF expression in HDLE was tested by quantitative relative PCR (**figure 2.4**). Here, cellular growth on Tβ4 grafted biomaterial results into significative increase of **V**ascular **E**ndothelial **G**rowth **F**actor (VEGF) if compared with control or HVP grafted material; suggesting a role in vasculogenesis processes. Furthermore, interesting is also the value of VEGF when cells are followed on HVP functionalized collagen, in this case VEGF expression are lower than pristine collagen, suggesting a regulatory role of HVP. All that verifies our hypothesis and suggesting the importance of these peptides in bio-inspired biomaterials developing.

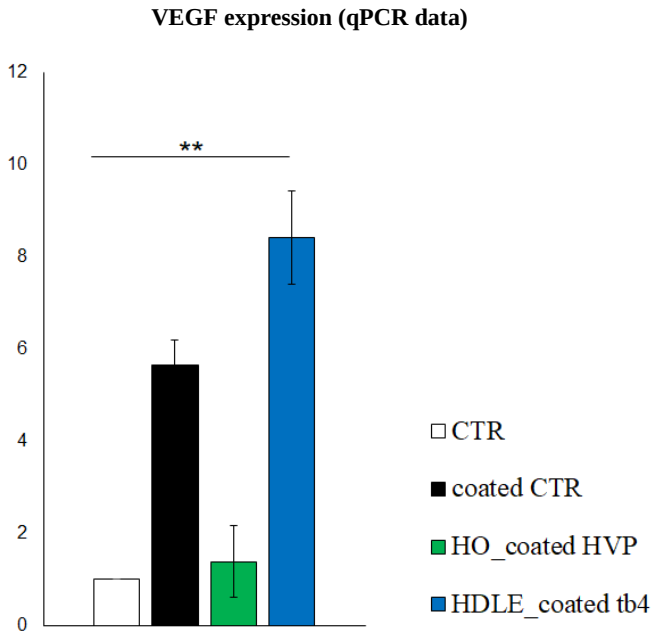

Figure 2.4. VEGF expression has been reported as results of qPCR. CTR indicates qPCR control, Coated-CTR=pristine collagen; HO_Coated HVP= osteoblast grown up on HVP grafted scaffolds, HDLE_Coated Tβ4= HDLE cells grown up Tβ4 grafted scaffolds, (bars indicate standard deviation, t-student test for **p<0.05).

2.5. Materials and Methods.

All reagents and solvents were purchased from Sigma-Aldrich and used without any further purification. The two peptides were provided by Prof. Monica Dettin in collaboration with Prof. Paola Brun (University of Padova, respectively: Department of Chemical Process Engineering and Department of Histology, Microbiology and Medical Biotechnology). The sequence of peptides are:

HVP = H-Cys-Phe-Arg-His-Arg-Asn-Arg-Lys-Gly-Tyr-NH2(N-terminus) (99% purity)

Tβ4=H-Cys-Ser-Lys-Leu-Lys-Lys-Thr-Gln-Glu-NH2 (N-terminus) (98% purity)

Collagen Preparation (coated-CTR).

Type I collagen coating from bovine Achilles tendon (Sigma-Aldrich, catalog no. C9879, CAS no 9007-34-5) were produced by solvent-casting method. Briefly, the collagen was dissolved in acetic acid 0.5 M (2g/L) for 4 h at 40 °C. The suspension was homogenized with a mixer for 10 min at maximum speed. The collagen solution was poured into a 24 culture multi-well (0.5 mL per well) and the solvent evaporated under the fume hood for 2 days. After complete solvent evaporation, thin transparent coatings (1 mg per well) were washed two times with deionized water (1 mL for 15 minutes on shaker with three-dimensional tumbling motion) and one time with ethanol (1 mL for 10 minutes).[134]

Collagen maleimido functionalization (Coated-Mal.).

In order to have maleimido grafting on collagen coating surface and coupling all amino groups of lysine side chains (expected 0.045mg per mg of collagen), a solution 2M of maleic anhydride in DMSO was prepared, then 1 mL was added to each well (containing collagen coating). Subsequently it was reacted over night, after this time, supernatant (containing an excess of maleic anhydride) was eliminated and collagen coating extensivel washed. one time with DMSO (1 mL for 10 minutes), then two times with deionized water (1mL for 15 minutes on shaker with three-dimensional tumbling motion) and one time with ethanol (1mL for 10 minutes).

Collagen Tβ4-functionalization. (coated-Tβ4).

A solution of Tβ4-Cys peptide was prepared dissolving 3 mg of peptide (MW=1300 g/mol) in 1 mL of PBS buffer solution (pH= 7.4). Then, 0.120 mL of this solution (390 µg, 0.30 µmol) was added to each well presenting scaffold (containing 1 mg of collagen), the final volume was adjusted around 0.4mL by addition furthers 0.280 mL of PBS. The solution was reacted for 24 hr. After this time, collagens coating was washed

two times with deionized water (1mL for 15 minutes on shaker with three-dimensional tumbling motion) and one time with ethanol (1mL for 10 minutes).

Collagen HVP-functionalization (coated-Tβ4).

solution of HVP-Cys peptide was prepared dissolving 11 mg of peptide (MW=1335 g/mol) in 2 mL of PBS buffer solution (pH= 7.4). Then, 0.074 mL of this solution (400 µg, 0.30µmol) was added to each well presenting scaffold (containing 1 mg of maleimide functionalized collagen), the final volume was adjusted around 0.4mL by addition furthers 0.326 mL of PBS. The solution was reacted to react for 24 hr. After this time, collagens coating were washed two times with deionized water (1mL for 15 minutes on shaker with three-dimensional tumbling motion) and one time with ethanol (1mL for 10 minutes).

FT-IR Characterization.

ATR-FTIR spectra of collagen coatings specimens were collected with the Varian 670-IR spectrometer equipped with the Quest (Specac) ATR device. Functionalized collagen scaffolds were analysed by FTIR measurements in attenuated total reflection (ATR). The ATR-FTIR absorption spectra of the different collagen coating samples display the typical spectral features of polypeptides and are characterized by the Amide I and Amide II bands. Small spectral changes were observed after maleimide functionalization and peptide coupling (see above).

2.6. Conclusion

In this section has been presented new bioinspired collagen based biomaterials which were functionalized with two different peptides giving two new biomaterials with different biological properties. The chemical structure has been analysed by FT-IR which highlights peptides conjugation. With same strategy has been shown how, modifying tyrosines content, its signal emerges reinforcing our result, with further confirm regarding biomaterial peptide grafting.

Biological responses were tested following growth of two cell lines considered as a model for these kinds of study. In the first case, it has been used human osteoblast to distinguish which, among two peptides, possesses adhesion capacity. Human osteoblast are implicated in bone tissue regeneration and this is the reason why these cells kind grow up necessary in the presence of adhesive motif. On the other hand, human dermal lymphatic epidermal cells, as widely described, are implicated in vasculogenesis process. In this chapter has been analysed the role of Thymosin Tβ4 motif in VEGF expression as fundamental key to drive cell fate, of injured tissues, toward regeneration and vasculogenesis.

Chapter 3 - Perfluoro Compounds (PFCs) as oxygen storage systems

3.1. Introduction

One of the main challenges in tissue repair is vascularization for new tissues and organs; currently, the application of new bio-inspired scaffolds for regenerative medicine are based on the ability to stimulate angiogenesis and blood vessel systems development. As a matter of fact, only in a few tissues like skin, cartilage or cornea, cells can be supplied with nutrients and oxygen via diffusion mechanisms,[135] instead, in almost all other tissues, cells are supplied by branched blood vessel systems which allow gas and nutrient perfusion; for example bone tissue. [136,137,138,139] During fracture bone healing, first step is represented by a well-organized response to injury and just subsequently, remodelling of newly formed bone which results in a repair that is indistinguishable from adjacent bones. During this last phase, it is well known that an interrupted angiogenic response may inhibit bone regeneration, leading several pathophysiology such as osteomyelitis, and osteonecrosis.[140,141,142].

In more detail, recent studies have shown that in osteoblast cells type, there is an active participation to angiogenesis processes during fracture repair by promoting, angiogenic factors in response to a variety of growth factors (as well known) and other extracellular stimuli (i.e. oxygen perfusion). Interesting, it was also demonstrated that osteoblasts elaborate most specific factors for endothelial cells, triggering consequently VEGF expressions and/or upregulations. At the same time, several factors are regulated by same processes such as insulin-like growth factor (IGF), TGF-b1, FGF-2,

prostaglandins E1 and E2, and 1,25-dihydroxyvitamin D3 [143], [144], [145],[146],[147]. Furthermore, and as seen before (**in chapter 1**) VEGF expression can be supposed controlled not only classical signalling peptides; but also mechanism such as hypoxia and gas perfusion; suggesting the key role of oxygen diffusion in bone wound healing. [148]

At the same time cardiovascular diseases are the most frequent cause of death in the western world, [149] in these situation therapeutic angiogenesis through biomaterials engineering proposes to restore original blood flow in ischemic tissues by controlling blood flux. Although, often the obstruction (in the case of ischemic situations) is located in the large arteries, expansion of the microvascular capillary tissue controlled by angiogenic factors, has been shown to induce the enlargement of upstream collateral arteries producing a biological bypass and restoring downstream perfusion. [150]

Summarizing these processes have the goal to supply tissues with sufficient nutrients and oxygen. As mentioned, angiogenesis is regulated mainly by oxygen levels within tissues. Hypoxic conditions result in growth factors and chemokines tissues secretion which, in certain conditions, promote vascular growth and remodelling of vascular network already present. [151] In these situation several study suggest how endothelial cells are stimulated to activate themselves to coordinate branching, and new lumenized network formation. [152] Increasing oxygen perfusion cell quiescence can be re-established resulting in a stable vascular network.[153]

Studying these arguments involves the knowledge of hypoxia regulating mechanisms and, to do this, it is necessary developing new oxygen delivery/storage systems to control gas perfusion in cells culture. Here it has been proposed a preliminary study about the strategies possible to achieve this focus.

3.2. Fluorinated compounds and oxygen perfusion

For the reasons described, and also as well known, the lack of oxygen perfusion leads cells to apoptosis with related tissues necrosis and therefore, is a critical limiting factor for developing functional tissues.[154,155]

In order to find potential solutions to overcome vasculogenesis problems, several strategies have been developed, studied and improved. Starting from the use of VEGF as simple additive in cell cultures, or the use of signalling peptide to conjugate scaffolds for cell cultures (**see chapter 2**); to pre-engineered tissues placed adjacent to a heavily vascularized tissue. *In vivo* conditions, these strategies help to achieve adequate vascularization.[156,157] However, not always this operation is feasible because the target implantation site may not be in close proximity to a heavily vascularized tissue. Alternatively several studies have presented the use of oxygen generating biomaterials[158] or synthetic oxygen carriers, such as perfluorocarbons or covalent bounded of four covalently stabilized hemoglobin tetramers, resulting in a polymeric hemoglobin molecule[159],[160,161]suggesting so called "oxygenated biomaterials".[162,163]

Oxygen generating biomaterials Among these systems, the most extensively studied are those employing peroxides (such as CaO_2,[164] MgO_2,[165] etc.) and enzymes coupled with H_2O_2 as oxygen generating systems.[166] Nevertheless, both systems involve the production, without an accurate kinetic control, of reactive oxygenated species (ROS), whose levels could harm cells and tissues.[167]

perfluorocarbons (PFCs): are class of molecule in which fluorine atoms replace hydrogen ones, are inert and stable (related to strong C-F bonds and to the dense, protective and repellent electron sheath that coats fluorines chains); designed and synthesized as amphiphilic molecules. The presence of fluorine allow them to dissolve large amounts of physiologically gases, among them oxygen and carbon dioxide, finding a plethora of application in biological fields, such as synthetic hemoglobin[168] and/or oxygen storage systems. Functional studies have shown that O_2 solubility in PFCs enriched medium is approximately 50 times higher than traditional BSA culture

medium.[169] Several studies explain how the bases of this phenomena are similar to the interaction between oxygen and hemoglobin heme groups, certainly with some differences. In detail, the interaction between O_2 and PFCs result to higher oxygen solubilization, this occurs by intermolecular interaction between oxygen and PFCs. In detail, while haemoglobin-oxygen interaction involves new strong localized chemical bond between O_2 and iron atom mediated by histidine residue (**figure 3.1 a.**), In the case of PFCs, fluorines low polarizability involve many non-directional Van der Waals forces, between molecules, allowing a greater interaction (**figure 3.1 b.**).

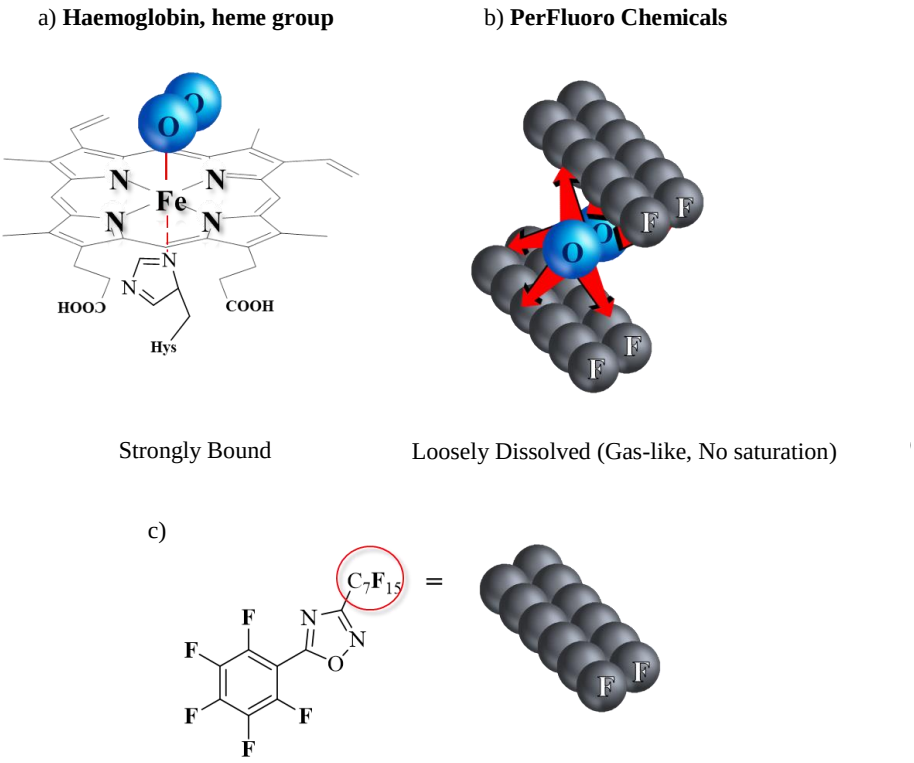

Figure 3.1: a. Oxygen interaction with haemoglobin and perfluorochemicals: in the case of Hb, O_2 is bound to the iron atom of a heme through a strong localized chemical bond (mediated by histidine residue). b. In PFCs, there exist only lose, non-directional van der waals interactions; PFCs and gases are alike, both present very low cohesive energy densities, which facilitates mutual solubilization. In c. is presented a classical PFC, in our case oxadiazole derivatives.

Furthermore, at this level, PFCs and non-polar gases (such as oxygen) both have very low cohesive energy densities, as expressed by very close Hildebrandt coefficients, the difference in the interaction mechanisms is reflected by the difference in O_2 uptake profiles as function of pO_2, i.e. sigmoidal for Hb vs. linear for PFC formulations. With PFCs, since there are not possibilities of chemical bonds, there is no saturation and interference with NO, CO or other reagents.[170]As consequence, PFC-dissolved O_2 is immediately available to tissues; it is also characterized by high extraction ratios.[171]

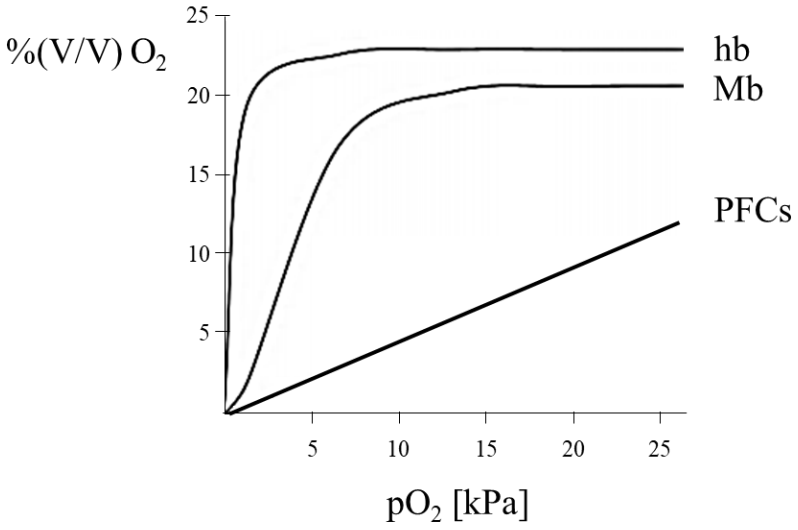

Figure 3.2: Comparison of oxygen capacity of hemoglobin, myoglobin and a generic PFC. (Pilarek, M. *Chem Process Eng* **2004**; *35(4)*, 463-487.).

However, since PFCs have only a limited capacity to supply oxygen and do not become reoxygenated, they can increase oxygenation by enhancing dissolved oxygen effective diffusivity through the matrix and not by serving as an oxygen reservoir. For these reasons, PFC solutions possess linear correlation between oxygen partial pressure and oxygen concentration, and could rapidly increase oxygenation of tissues under hypoxic condition (**figure 3.2**).

Nowadays, PFCs have been widely studied and, in some cases, used as pharmacological tools with several focus, including artificial blood substitution, organ preservation, ultrasound imaging and fluorine magnetic imaging.[172,173] More importantly, due to their high oxygen solubility, PFCs have been extensively explored as oxygen suppliers to increase the therapeutic outcome of radiotherapy or photodynamic therapy. In the first case, for example nano-PFCs were studied using an oxygen meter to measure dissolved oxygen concentrations in aqueous solutions e oxygen release profile, especially under certain circumstance. In more low-power/low frequency US treatment were applied onto solution nano-PFCs enriched; showing higher value of oxygen release in this solution, resulting into rapid increase of dissolved oxygen concentration Those results demonstrate that the oxygen release from PFC is sensitive to the applied external ultrasound waves finding many applications in innovative to realize highly efficient oxygen delivery into tissues[174].

Furthermore, PFCs are advantageous thanks to their commercial availability, chemical and biological inertness (as previously mentioned), and easy sterilization.[175] In this chapter is illustrated the use of 5-(2,3,4,5-Pentafluorophenyl)-3-perfluoroheptyl-1,2,4-oxadiazole as fluorinated substrate to functionalize collagen 2D scaffold in order to develop new bioinspired scaffold with gasses perfusion abilities.

3.3. Aim of the work

In the field of 2D bio-inspired materials, oxygen perfusion remains an important limiting step because the micro-inhomogeneity prevents a correct oxygen (and nutrients) perfusion, bringing cells to a metabolic suffering experience. At this point our approach is based on developing new oxygen higher content materials through the tethering of a fluorinated oxadiazole moiety to collagen based surface, thus obtaining

novel 2D collagen matrix, possessing collagen biocompatibility and the ability of PFCs to increase diffusivity of gases. This strategy will allow to obtain new biomaterials able to favour oxygen exchange.

For described reasons, the focus of this section is the project and design new potential matrix with a molecular system able to release and guarantee oxygen perfusion. To make this, already mentioned, 1,2,4-oxadiazole fluorinated derivative were used to functionalize collagen based biomaterials. In order to obtain PFC functionalization nucleophilic aromatic substitutions of fluorine atom in para position with lysine amino group were performed, exploring different conditions.

3.4. Results and discussion

In order to covalently functionalize **5-(2,3,4,5-Pentafluorophenyl)-3-perfluoroheptyl-1,2,4-oxadiazole (Compound 3.1)** on collagen scaffold, a nucleophilic substitution was proposed as chemical strategy. In this case, nucleophilic attack is performed by amino groups of side chains lysine toward fluorine atom in para position, in these conditions, SNAr reaction is favoured at the ortho position (**scheme 3.1**).[176,177] On the other side, fluorine atom leaves molecular site as F^-; and here, to avoid HF formation; an organic base are added restoring neutral conditions. Several conditions were tested to study the reaction and the different products were analysed by several spectroscopic techniques.

5-(2,3,4,5-Pentafluorophenyl)-3-perfluoroheptyl-1,2,4-oxadiazole (compound **3.1**)

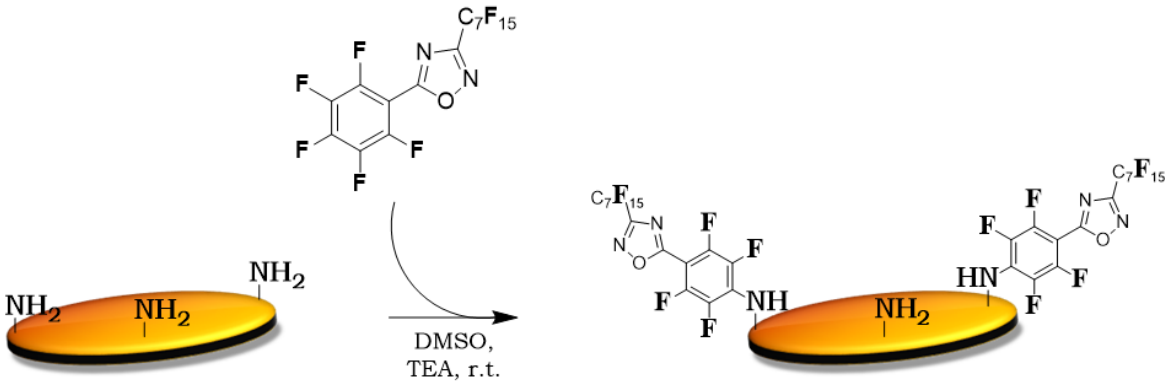

Pristine Collagen

Functionalized collagen with **compound 3.1**

Molar ratio (Lys-NH_2/ 3.1)	Time of reaction (hr.)	Conditions (Lys-NH_2/ 3.1_hr)
1/5	24 h.	1:5_24h
	48 h.	1:5_48h
	72 h.	1:5_72h
1/10	24 h.	1:10_24h
	48 h.	1:10_48h
	72 h.	1:10_72h
1/15	24 h.	1:10_24h
	48 h.	1:10_48h
	72 h.	1:10_72h

Scheme 3.1 upward represents a chemical strategy used for covalent functionalization, below (in the table) the condition which change as function of *i)* molar ratio between lysine and compound 3.1 *ii)* time of reaction.

In detail, three different molar ratios between lysine and compound **3.1**(Lys/30, 1/5; 1/10; 1/15) were set to produce a series of conditions. Further, for each molar ratio, three times of reaction were tested in order to study which are the best conditions (**scheme 3.2**, table). In order to follow reactions, from qualitative point of view, UV spectra of collagen derivatives scaffold were recorded in 200-400 nm range transmittance mode and converted in absorbance. In **figure 3.3** UV/Vis spectra were

reported in which functionalized collagen, with compound **3.1**, shows maximum peak at 325 nm, while unreacted oxadiazole presents a maximum peak around 249 nm. These data are in accordance with those already reported, refers to analogue compounds highlighting, on one side, characteristic spectroscopic red-shift as consequence of fluorine para-SNar and, on the other side, success of covalently functionalization.[178]

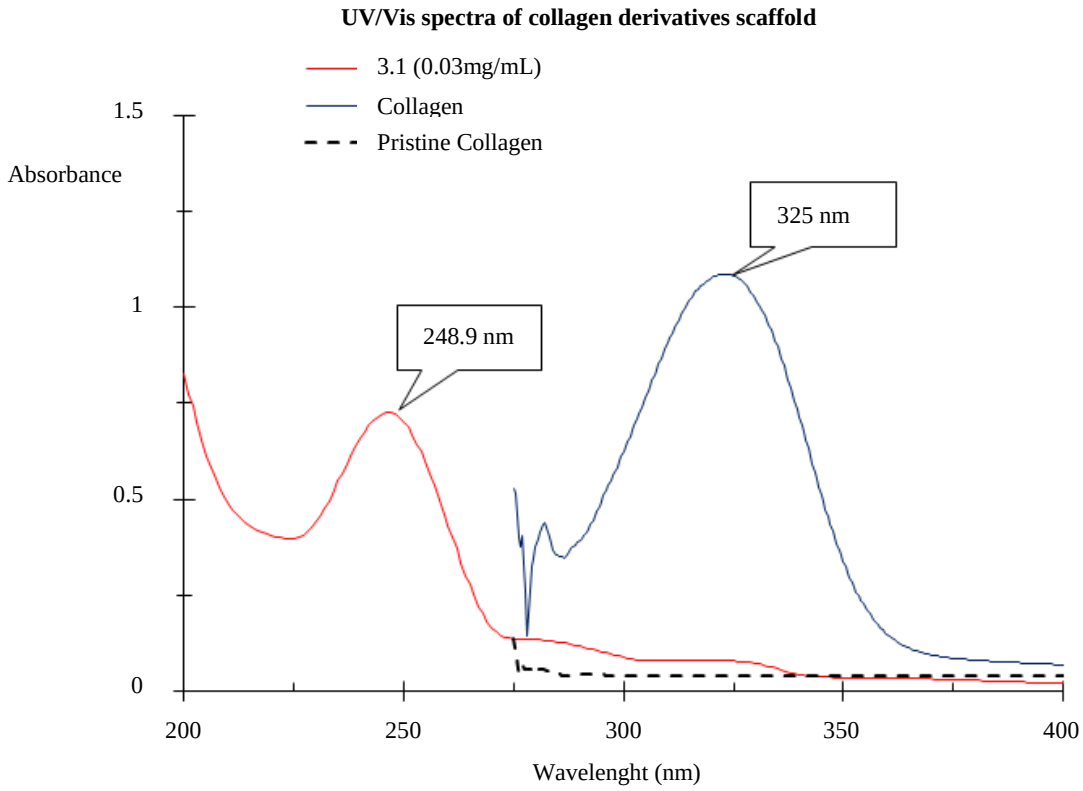

Figure 3.3 Absorbance graphs, red line represents the absorbance trend of unreacted compound 3.1; Black dashed-line: pristine collagen; blue line: absorbance of generic condition of collagen-3.1 functionalized material.

However, it hasn't been possible recording data under 275 nm due to notable background noise given by collagen and plastic support absorption. For these reasons we cannot exclude also the presence of 1,2,4-oxadiazoles fluorinated absorbed. Nevertheless, the observed differences between unreacted compound **3.1** and the functionalized collagen are enough to exclude interferences of the medium and experimental setup. Subsequently FT-IR analysis were performed in order to evaluate

3.1. functionalization and collagen coating integrity. As possible observe in (**figure 3.4**, Stacked spectra), collagen scaffolds (functionalized and not) displayed almost superimposable IR spectra also in the amide I band, which is due to the CO stretching vibrations of the peptide bond. This result indicates the maintenance of the overall protein secondary structures after chemicals conjugation. In the red line has been displayed 1,2,4-oxadiazoles fluorinated characteristic spectra, which give characteristic absorption bands with properties fingerprint regions.

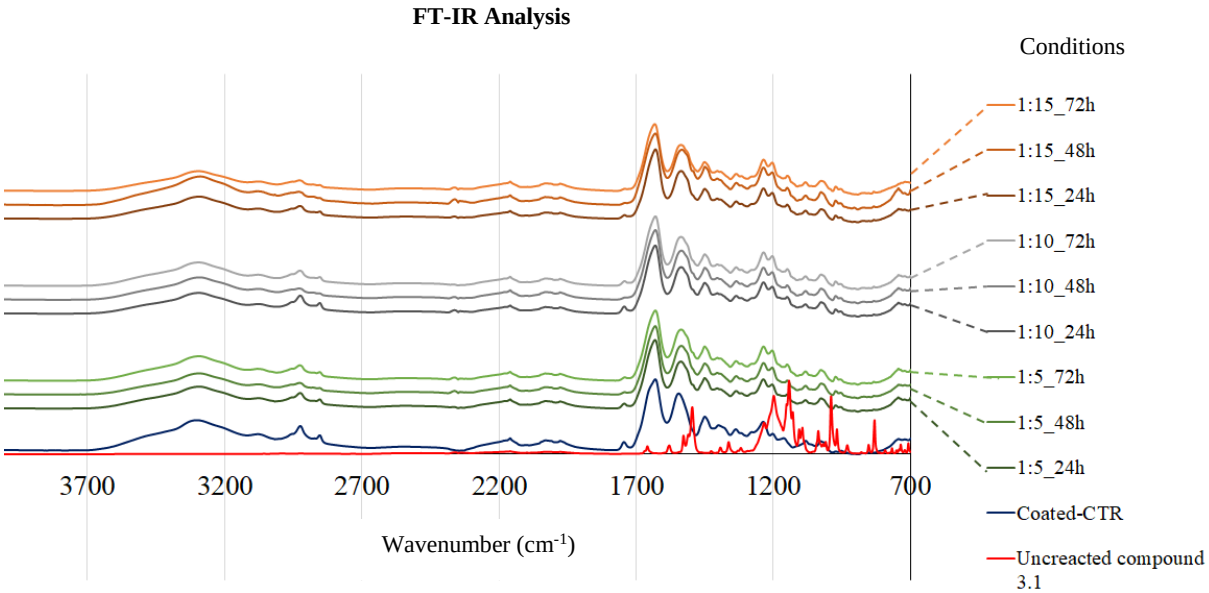

Figure 3.4 FT-IR spectra of fluorinated collagen coated. Red line represents **5-(2,3,4,5-Pentafluorophenyl)-3-perfluoroheptyl-1,2,4-oxadiazole (3.1);** blu line unreacted collagen, other colours describes FT-IR spectra of different conditions as described in scheme 4.1. In detail the first two number describe molar ratio between Lys content and Compound 30, the third number describes time of reactions.

As reported in **figure 3.5** (a zoom of **figure 3.4**, range 1160-1100 cm^{-1} and 900-700 cm^{-1}) C-F(ar) stretching band and CF_2 stretching vibration band (of fluorinated oxadiazoles, red line), respectively at 834.06 cm^{-1} and 1145 cm^{-1} (a e b), appear also in collagen functionalized samples and concur as previously reported.[179,180] However, due to high complexity of proteins IR spectra, these peaks appear weak and with low intensity. Second derivative analysis confirm observed differences, if compared with controls (**figure 3.5**, c. and d.); quantitative relative evaluation of these peak suggests an

important difference between unreacted collagen and functionalized samples. A signal inversion, due to new introduced peak, if compared with control collagen were seen (**figure 3.4 d**, 834.06 cm^{-1}). Nevertheless, no appreciable differences between fluorinated collagens with themselves are seen (**figure 3.4** e. and f.).

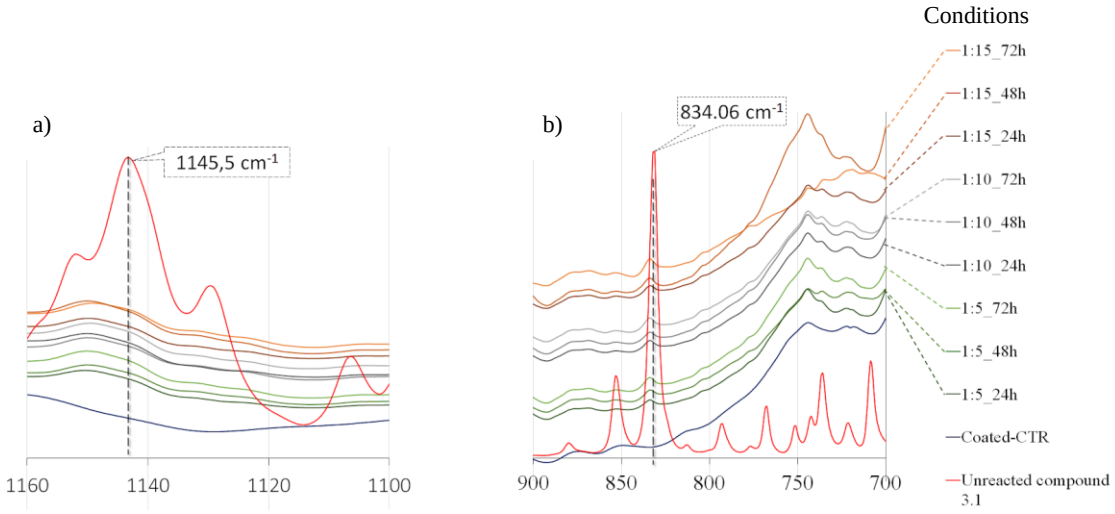

Analisis of Secondary Derivativevs

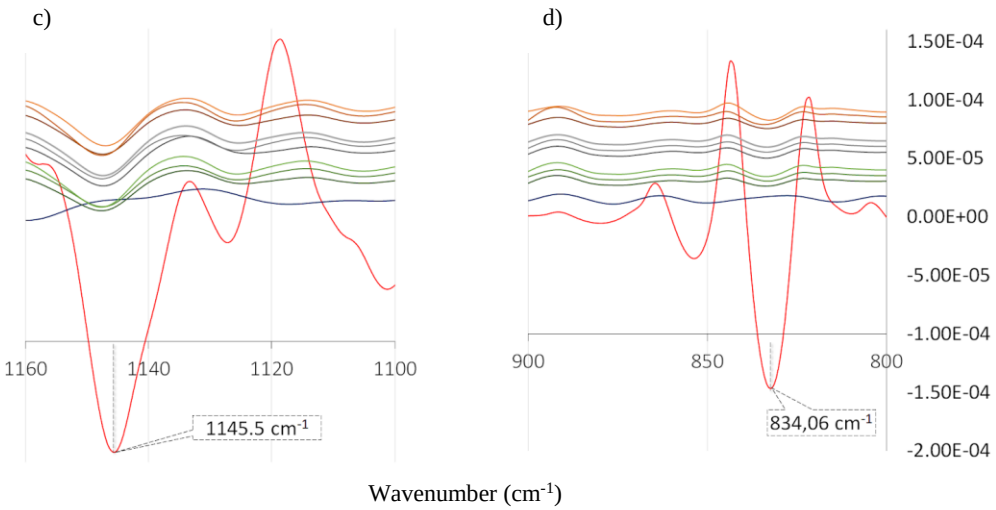

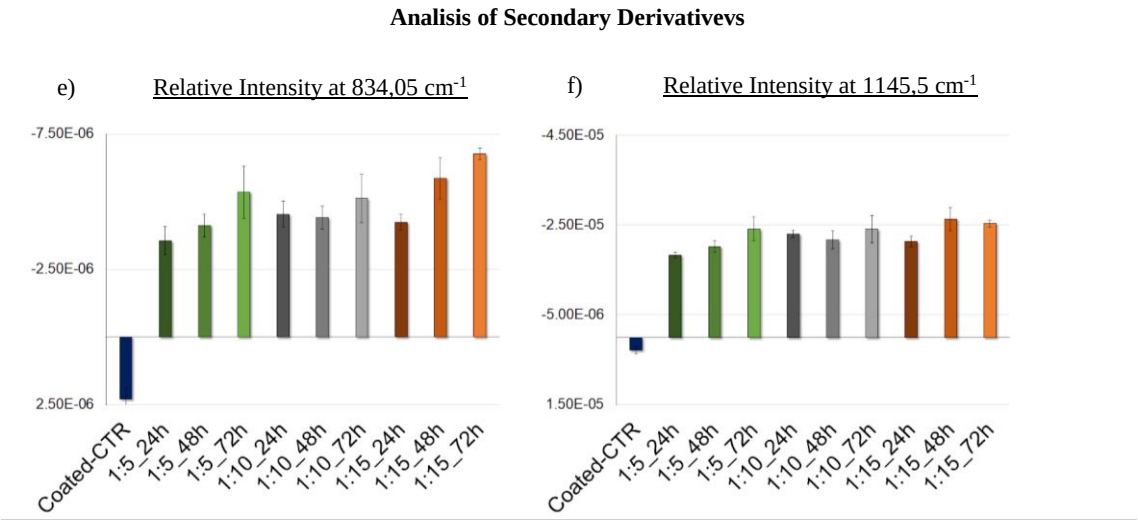

Figure 3.4 FT-IR spectra of fluorinated collagen scaffold. As shown **figure 3.3**., Red line represents **5-(2,3,4,5-Pentafluorophenyl)-3-perfluoroheptyl-1,2,4-oxadiazole (compound 3.1);** blue line unreacted collagen, other colors describes FT-IR spectra of different conditions described in (**scheme 3.1**). a. zoom between 1160-110 cm^{-1} shows overlapped peaks of fluorinated oxadiazole around 1145.5 cm^{-1} and several functionalized collagen b. a. zoom between 900-700 cm^{-1} with a peak around 834.06 cm^{-1}. c and d represent second derivatives analysis of a and b, where respectively peaks are confirmed. e and f highlight a relative quantification of the peak 1145.5 and 834.06 normalized to control value. (bars indicate deviation standard).

Furthermore, ^{19}F-NMR were performed on media reaction in order to quantify via NMR the degree of compound **3.1** bounded and then calculate the functionalization degree for each conditions. Reaction mixtures were collected and fluorurated oxadiazoles quantified using hexafluorobenzene as internal standard with coaxial tube method; in which a coaxial insert containing a standard solution of hexafluorobenzene is placed into the sample tube. In this way is possible introduce a reference standard with analyte without mixing them, avoiding any chemical interaction. Knowing the molar content of starting compound into reaction media and through remaining compound quantification, is possible find how much oxadiazole binds lysine amino groups (**figure 3.5**).

As NMR signal intensities represent the total number of their respective nuclei when acquired under quantitative conditions, they also represent the concentration of the corresponding component contained within the NMR sample tube.

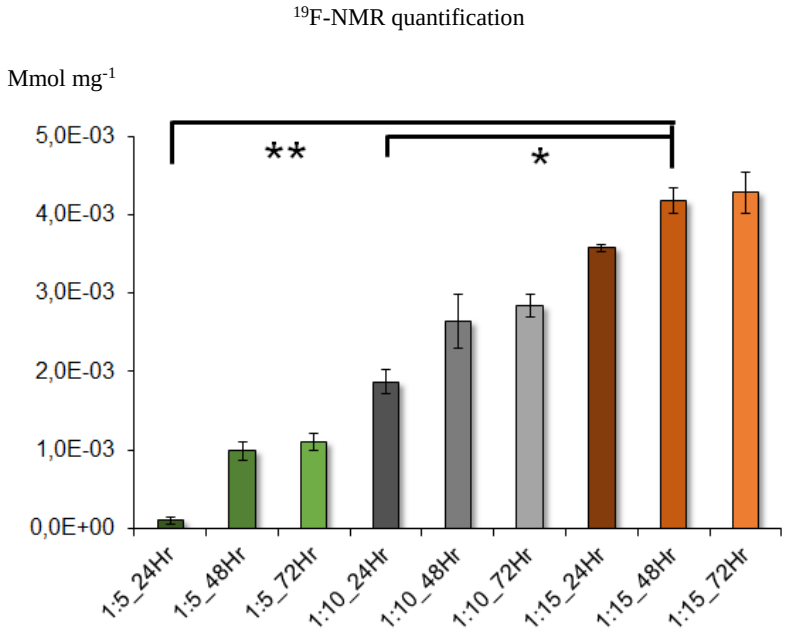

Figure 3.5 ^{19}F-NMR retro quantification for each conditions, the colours follow the same legend used in fig. 4.3. Histogram show an increasing trend toward higher value. (bars indicate standard deviation, t-student test for **p<0.05, *p<0.01).

As observed by ^{19}F quantification (**figure 3.5**), an increasing trend until plateau depending on molar ratio between lysine content and compound **3.1** results appreciable.

Concluding, no difference between 48 or 72 hrs time of reaction were seen for each condition. It was suggested that an equilibrium over 48 hrs could be presents between bonded or absorbed forms. Equilibrium not present at low molar ratio. The value of first condition (around zero), suggests us that washing procedure is enough to washout completely the unreacted oxadiazoles. Nevertheless, further analysis are necessary to discriminate absorbed compound from bound it.

3.5. Materials and Methods.

All reagents and solvents were purchased from Sigma-Aldrich and used without any further purification. **5-(2,3,4,5-Pentafluorophenyl)-3-perfluoroheptyl-1,2,4-oxadiazole** were provided by Prof. Andrea Pace (Department of Biological, Chemical, and Pharmaceutical Sciences and Technologies, University of Palermo).

FT-IR spectra of gelatin specimens were collected with the Varian 670-IR spectrometer equipped with the Quest (Specac) ATR device.The absorption spectra were reported after baseline correction between 1800 and 900 cm^{-1} and normalization at the amide I band intensity to compensate for the different protein content. The ATR-FTIR absorption spectra of the different collagen coating samples display the typical spectral features of polypeptides and are characterized by the Amide I and Amide II bands.
NMR spectra were recorded on a Varian Mercury instrument at 400 MHz (^{19}F- NMR). Chemical shifts are reported in parts per million downfield from $CFCl_3$ as an internal standard. Hexafluorobenzene has been used as further internal standard in order to quantify as seen. For 1:10 and 1:15_24/48/72hr conditions, 600 µl of Hexafluorobenze (10.7 µmol/ml) as been prepared and used as coaxial standard. For 1:5_24/48/72hr conditions, hexafluorobenzene as been used at 1.07 µmol/ml concentration.

Collagen Preparation (coated-CTR).

Type I collagen coating from bovine Achilles tendon (Sigma-Aldrich, catalog no. C9879, CAS no 9007-34-5) were produced by a solvent-casting method; as describe in Chapter 3.

Collagen 5-(2,3,4,5-Pentafluorophenyl)-3-perfluoroheptyl-1,2,4-oxadiazole functionalization (compound 3.1).

In order to functionalize collagen coating and evaluate functionalization degree, several conditions were thought and performed. Following a general scheme for each condition, an appropriate amount of **5-(2,3,4,5-Pentafluorophenyl)-3-perfluoroheptyl-1,2,4-oxadiazole (3.1)** was solubilized in DMSO (dry conditions) and an adequate aliquote added to each coated collagen. Than, trimethylamine added to neutralize hydrofluoric acid.

Conditions explored change based on molar ratio between lysine amino groups (as previously reported in **chapter 2, 2.5**) and compound 3.1 and time of reactions. (See table in the scheme **3.1**). At the end of reactions each condition was extensively washed, first with 1 ml of DMSO for 15 minutes, then three times with deionized water (1ml x 15 minutes) and last time with ethanol (1 ml x 5 minutes).

a. Conditions 1 (1:5). 13 mg of compound 3.1. weas solubilize in 1.2 ml DMSO (dry conditions, $2.1*10^{-2}$ mmol, $1.7*10^{-2}$ M). Then, 0.1 ml of this solution was added to collagens coated ($1.7*10^{-3}$ mmol, 5 eq. referred to lysine content), and volume adjusted to 0.3ml of DMSO. In addition, 50 µl of a solution of triethylamine 0.03M was added ($1.7*10^{-3}$ mmol, 5 eq.)

b. Conditions 2 (1:10). 25 mg of compound 3.1 were solubilize in 1.2 ml DMSO (dry conditions, $4.1*10^{-2}$ mmol, $3.5*10^{-2}$ M). Then, 0.1 ml of this solution was added to collagens coated ($3.5*10^{-3}$ mmol, 10 eq. referred to lysine content), and volume adjusted to 0.3ml of DMSO. In addition 50 µl of a solution of triethylamine 0.03M was added ($1.7*10^{-3}$ mmol, 5 eq.) and solutions leading to react for different times (24, 48, 72 hours).

c. Conditions 3 (1:15). 38 mg of compound 3.1 were solubilize in 1.2 ml DMSO (dry conditions, $6.3*10^{-2}$ mmol, $5.2*10^{-2}$ M). Then, 0.1 ml of this solution was

added to collagens coated ($5.2*10^{-3}$ mmol, 15 eq. referred to lysine content), and volume adjusted to 0.3ml of DMSO. In addition 50 µl of a solution of triethylamine 0.03M was added ($1.7*10^{-3}$ mmol, 5 eq.) and solutions leading to react for different times (24, 48, 72 hours).

For each of these conditions three times of reactions were tested in order to identificate the best reaction condition, in detail were tested 24, 48, 72 hours.

NMR quantitative study.

In order to quantify functionalization degree, quantitative 19F-NMR was performed using coaxial tube containing Hexafluorobenze (0.01 M, -164.9 ppm, s, 6F, C-F) as reference standard.

For each sample, supernatant was collected and 0.1ml of new DMSO was added to washing sample. Subsequently, also this volume it was collected and added to 350 ul previously token. NMR quantification was performed on this media and fluorurated oxadiazole quantity calculated as described.[181] Briefly, with coaxial method, the concentration of analyte (C_a) can be calculated directly by following equation:

(**Eq 3.1**)

$$C_a = \left[m_r \frac{1}{(MW_r * V_a)}\right]\left(\frac{I_r}{I_a}\right)$$

Where: "m_r"represents the mass of reference compound, "MW_r"its molecular weight, and "V_a" volume of analyte added to the NMR sample tube. "I_r "and "I_a" indicate respectively the integral of reference signal CF and analyte CF_3.

3.6. Conclusion

The collagen coated scaffold has been treated with fluorinated 1,2,4 oxadiazoles to obtain a new biomaterial, in principle able to increase solubility of oxygen when used for cell culture applications. Our synthetic approach is based on Aromatic substitution, exploiting amino groups of lysine side chain. In this way, we obtained a set of derivatives with different compound 3.1 derivatization degree based on reaction conditions. In particular conditions 1:15_48hr and 1:15_72hr, by our data, result best conditions for these systems generating good candidates to be employed for further test regarding gas solubility and releasing in cell culture conditions. Gasses release test and biological evaluations are in due course in order to test both oxygen solubility, and biocompatibility or citotoxicity.

Chapter 4 - Gelatine-based Hydrogels.

4.1. Introduction

An interesting further approach to drive cell fate or control cells behaviour in *vitro* conditions is the use of natural or synthetic polymers, able to form hydrogels (such as alginate or gelatine) which can be injected into the body and mimic extra-cellular environment, as a 3D "ECM-like structure". Hydrogels are structure able to retain a large quantity of water with a certain similarity to ECM macromolecular components, [182] finding numerous applications in drug delivery, and in the last years in tissue engineering.[183] As mentioned in the **chapter 1**, also hydrogels can be subdivided in three main categories, natural, synthetic or made of copolymers in accordance to their provenance. Among which gelatine, a form of hydrolysed collagen, has emerging as powerful and biocompatible tool for these purpose.

In the last decades, hydrogels have become one of the possible strategies for three-dimensional (3D) cell cultures and kinetics drug delivery studies. Furthermore, 3D cultures are applied for studying cellular physiology, stem cells differentiation, tumoral models and for the investigation of interaction mechanisms between extracellular matrix and cells.[184] In the field of medicinal chemistry and tissue engineering, hydrogels should have traditional properties such as biocompatibility, cells spreading and promote tissues formation. The properties include, also, traditional physical parameters, such as hydrogel degradation, enzymatic stability and good mechanical features, as well as described biological parameters. Certainly, one of the most critical parameters is the biocompatibility of hydrogels, which is based on the material's ability to stay within the body without causing detrimental effects, supporting at the same time, cells life. Furthermore, another important key feature of hydrogels is represented by their

stability. Hydrogel structural integrity depends on cross-links generated between polymeric chains, with different chemical bonds and physical interactions. Often chemists and physics work together to ensure the desired stability degree in order to avoid premature degradation or by-products liberation, which could involve harmful side effects. From chemical/physical point of view hydrogels are composed by hydrophilic and hydrophobic polymeric chains that can be either synthetic or natural in origin. As mentioned previously, hydrogels structural properties are designed in order to mimic as close as possible ECM, and they can be delivered in a minimally invasive manner.

4.1.1. Hydrogels composition

Nowadays, a great variety of natural or synthetic hydrogels are produced starting from several sources. In the first case, typical naturally derived polymers include gelatin, collagen, alginate, chitosan, fibrin, and hyaluronic acid (HA), meanwhile in the case of synthetic materials, hydrogels often are based on synthetic cross-linked network obtained from polymerization steps.[185] In biological field, **naturally derived** materials find much more applications in tissue engineering than synthetic based materials being either components of ECM or having macromolecular properties similar to the natural ECM. Collagen fibers and scaffolds can be created and their mechanical properties improved by inserting various chemical crosslinks (e.g., glutaraldehyde, carbodiimide), or physical treatments (e.g. UV irradiation, and heating), and by the combination with other polymers (e.g. hyaluronic acid, polylactic acid, poly (glycolic acid), poly(lactic-coglycolic acid), chitosan, PEO).

Naturally derived biomaterials can be divide in **protein based hydrogels** and **carbohydrate based hydrogels**.

Protein based hydrogels display interesting properties for use in the synthesis of 3D scaffold thanks to their excellent biocompatibility and biodegradability, due to higher degradability in the body than synthetic polymers. Gelatine, which is known as hydrolysed collagen, represents one of the most interesting starting material for hydrogels preparation due to its biocompatibility and facility of gelation. Gelatine based-hydrogels have been used for delivery of growth factors to promote vascularization of engineered new tissues. However, the weakness of the gels is still a problem, and this is a practical case of study in which multidisciplinary scientists (from chemist to physic) co-work in order to developing methods able to ameliorate the chemical stability and mechanical properties of gelatine based-hydrogels.[186]

On the other side, **carbohydrates based hydrogels** show particular structural forming self-assembled carbohydrate-rich networks in which specific small-molecule drugs can released more slow down than protein based hydrogels, [187] among which the most famous is hyaluronic acid. Hyaluronic acid (HA) is the simplest glycosaminoglycan (GAG) and is found in almost every mammalian tissue and fluid. It was found prevalently during wound healing and in synovial fluids of joints. It is a linear polysaccharide composed of a repeating disaccharide of (1–3) and (1–4)-linked β-D-glucuronic acid and N-acetyl-β-D-glucosamine units. HA hydrogels were produced by covalent crosslinking and stabilization for example with hydrazide derivatives [188], by esterification, and by annealing[189]. Among polysaccharides, alginate represents another alternative due to its ability to gelify under mild conditions, and low cytotoxicity. This polysaccharide is a linear copolymer of (1–4)-linked β-D-mannuronic acid (M) and α-L-guluronic acid (G) monomers which are sequentially distributed in either repeating or alternating blocks. Hydrogels are produced when divalent cations such as Ca^{2+}, Ba^{2+}, or Sr^{2+} cooperatively interact with blocks of "G monomers" to form ionic-bridges between different polymer chains; in this case gelation process is driven by physical interactions and could be easily manipulated by using different M and G ratio and molecular weight of the polymer chains.[190] Another interesting bio-polymer is chitosan, which is similar to naturally occurring GAGs and is degradable by human enzymes. This polysaccharide, formed by of (1–4)-linked D-glucosamine and N-Acetyl-D-glucosamine

residues, can be gelled just working on pH variation during its solubilisation. Nevertheless, several chemical strategies of crosslinking, based on glutaraldehyde[191], UV irradiation[192] and thermal variations[193] were optimized in last years, making them stable and fine tuneable.

On the other side, **Synthetic hydrogels** produced by building blocks, possess chemical properties which can be easily controlled, making them more reproducible then naturally derived hydrogels. Starting from specific monomers, synthetic polymer based-hydrogels can be produced by polymerization steps creating hydrogels which components possess specific molecular weights, also here using chemical or physical strategies. Consequently, properties such as gel formation, density, viscosity or more simply mechanical and degradation properties can be regulated easier than protein or polysaccharide based-hydrogel, in order to obtain desired products. Examples of synthetic materials are PEO ((poly(ethylene oxide)), PVA (poly(vinyl alcohol)), and P(PF-co-EG) (poly(propylene fumarate-co-ethylene glycol). PEO and other poly(ethylene glycol) (PEG) are hydrophilic polymers that can be crosslinked by modifying each end of the polymer with either acrylates or methacrylates and, then, by photo-initiator is possible drive cross linking processes via UV light exposure.[194] Furthermore, thermally reversible hydrogels can also be produced from block copolymers of PEO and poly(l-lactic acid) (PLLA) and PEG and PLLA.[195] Another synthetic hydrophilic polymer largely used in space filling and drug delivery applications is PVA; it can be physically crosslinked by repeated freeze-thawing cycles of aqueous polymer solutions or chemically crosslinked with glutaraldehyde or succinyl chloride to form hydrogels.[196]

Nevertheless, several classifications have been employed to hydrogels. Below (**Scheme 4.1**), briefly are reported the main categories used to describe hydrogels.[197]

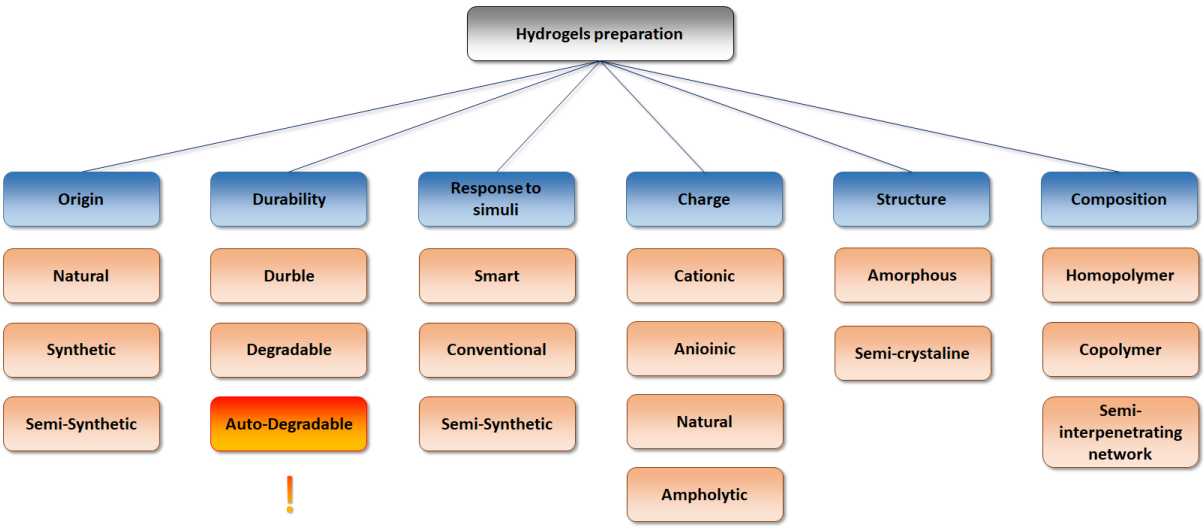

Scheme 4.1 Hydrogels classifications. In red, reported auto degradable hydrogels which are gained more interest in the last years.

4.1.2. Hydrogel preparation

Hydrogels preparation represents certainly one of the main challenges in the last decades Various methods were reported and extensively optimized in literature, depending on the designed structure and applications. Hydrogels preparation methods can be divided into "Chemical strategies" or "Physical methods", obtaining consequently new covalent bonds formation or physics interactions (**scheme 4.2**).

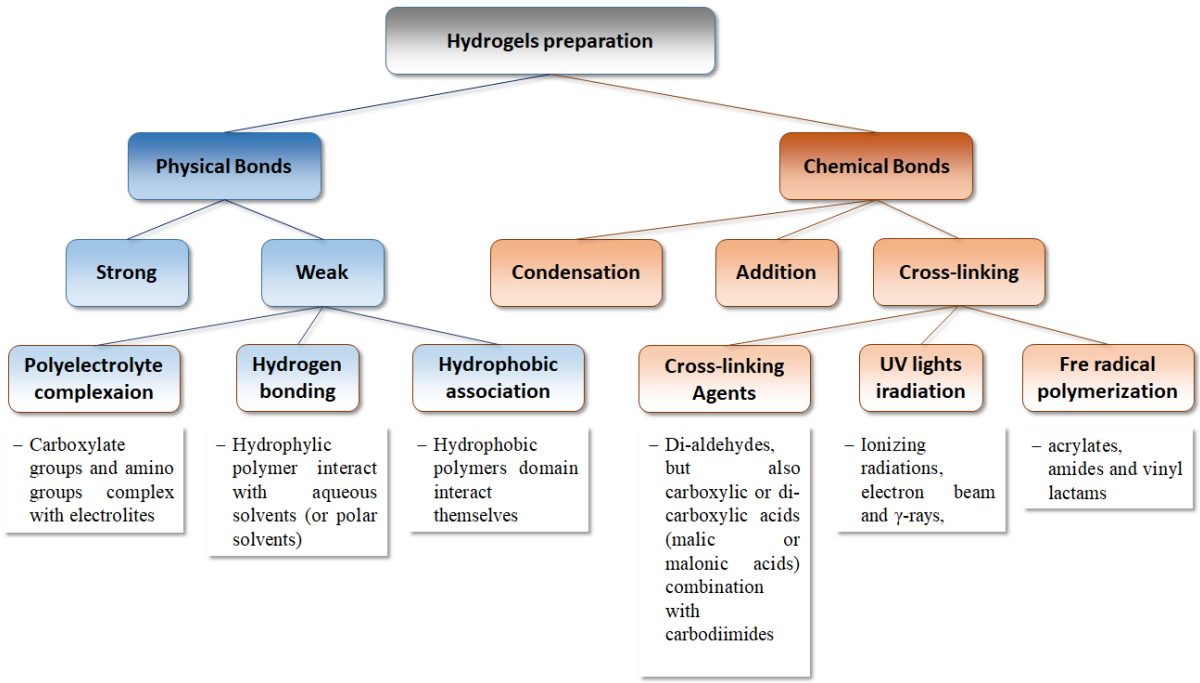

Scheme 4.2, major strategies to hydrogels preparation, based on physical or chemical approaches, in the last years.

Among chemical strategies, crosslinking agents represent a strategy through which permanent gels are formed, thanks to the formation of new covalent and stable bonds between polymer chains. These types of gels attain an equilibrium swelling state in aqueous environment, which depends on the polymer–water interactions and crosslinking density.[198]

Physicals crosslinking or reversible gels, are formed when the networks of the system are held together by molecular entanglements, and or secondary forces including ionic, hydrogen bonding or hydrophobic interactions. In physically cross-linked gels the dissolution is prevented by physical interactions, which exist between different polymer chains.[199] Hydrogels that are formed through physical interactions are mostly reversible, and can be disrupted by changes in physical conditions or application of mechanical stresses.[200]

With respect to the hydrogels prepared with chemical strategies, which are mostly irreversible, physical gels can be subcategorized into strong and weak physical gels. Strong physical gels are mainly made up of strong physical bonds between polymer chains and they are effectively more stable at a given set of experimental conditions. For these reason, they are basically similar to the chemical gels. Some examples of strong physical gels might be those of lamellar microcrystals, glassy nodules or double and triple helices. On the other hand, weak physical gels are mainly composed of reversible links that are formed from some temporary associations between chains, and they are categorized by finite lifetimes, able to breaking and reforming continuously, depending on the conditions at which they are subjected. Some examples of weak physical bonds are hydrogen bond, block copolymer micelles and ionic associations.[201]

In the field of Chemical treatments to hydrogel development we find:

a) free radical polymerizations, which is the favourite technique based on monomers such as acrylates, amides and vinyl lactams.[202,203] In these case, starting material have appropriate functional groups or can be decorated with radically polymerizable groups useful for free radical polymerization. The method typically requires several free radical polymerizations steps, which are: initiation, propagation, chain transfer and termination. In the initiation step, thermal, ultraviolet and red-ox initiators can be utilized for radical generation; these radicals then can react with monomers transforming them into active forms that react with more monomers and so on in the propagation step.[204]

b) A second technique for hydrogels preparation is based on photoreaction; hydrogels crosslinking by irradiation is very efficient, especially when ionizing radiations, such as electron beam and γ-rays, ionize simple molecules either in air or water. As a matter of fact, during irradiation processes, active sites are created along the polymer strands and bring to generation of a wide number of crosslinks. Hydrogels production, using these techniques can be achieved via irradiation of the polymers in bulk or in solution.[205]

c) One of the main techniques used for hydrogel preparations is represented by the use of crosslinking agents, for polymeric precursors functionalization. In this case, a bi-functional crosslinking agent is added to a solution of a hydrophilic polymer, which should have appropriate functionalities, able to react with the agent; this technique is adequate for generation of hydrogels from both natural and synthetic hydrophilic polymers. For example, gelatine–based hydrogels were produced using di-aldehydes as crosslinking agents[206] and, since, this is one of focal point of my work, below, a section will be dedicated to use of crosslinking agents.

On the other side, physical crosslinking with physical interaction is one of the general reverse techniques used for hydrogel development. Often, physical interactions are based on polyelectrolyte complexation, hydrogen bonding and hydrophobic association, weak interactions obtainable under mild conditions, without chemical treatments.

a) Polyelectrolyte complexation (ionic interactions) is based on systems where links are generated between pairs of charged sites on the polymer backbones. Carboxylate groups of sodium alginate and amino groups of chitosan chains are often used to complexation with electrolytes (as previously cited, Ca^{2+}, Ba^{2+}), in this way polysaccharide based hydrogels are obtained from polyelectrolyte complexation hydrogels.

b) Hydrogen bonding is represented by polymer chains which can be subjected to weak interaction with aqueous solvents contributing to hydrogel development. For example, producing gelatine-based hydrogel, the association of an electron deficient hydrogen atom and a functional group, with high electronegativity, involve into hydrogen bond formation. Hydrogels generated by this method could be altered by many factors: swelling process, polymer concentration, molar ratio of each polymer, type of solvent, solution temperature, and the degree of association between the polymer functionalities. For these reasons, in the case of gelatine, structure need to be furthermore stabilized by chemical treatments.

c) In hydrophobic association, polymers and copolymers, generally form disconnected structures with hydrophobic micro domain, can associate themselves generating physical crosslinking points toward polymeric structure. Hydrophilic poly (hydroxyethyl methacrylate) (PHEMA) based hydrogel, often were obtained in association with a small amount of hydrophobic poly(methylmethacrylate) (PMMA) as a long branch. Typically, the mechanical features of these hydrophobically combined polymers are poor because of the poor interfacial adhesion. Nevertheless, this technique for hydrogels formation have some advantages such as the low cost of the system.

4.1.3. Preparation of protein based hydrogel

In biological field, collagen (and its hydrolyzed forms such as gelatines), owns excellent properties among which are well known biocompatibility, good cell-adhesion, good spreading properties, biodegradability and low immunogenicity. For these reasons chemically modified gelatin with other natural or unnatural (macro)molecules have been extensively used in the field of regenerative medicine, developing new 3D biomaterials able to support cell-culture, engineering new tissues in order to restore injured state or failed organs,[207] finally, developing new drug release systems.[208]

However, gelatine and related natural proteins (such as elastin, fibrin, etc…), once gelified (naturally or by physical treatments) don't possess adequate mechanical properties, in fact, their high degradability in physiological conditions bring to several difficulties in gelatine-based hydrogels design with mechanical and chemical desired features. [209,210, 211]

In order to overcome these drawbacks, gelatine starting materials are usually modified with physical, enzymatic or chemical processes. The most used strategy, developed to improve cited features, is based on cross linking procedures (enzymatic or chemical).[212,213,214,215] In this case bio polymer functional groups react with crosslinker chosen affording 3D network with a well-defined architecture..

Moreover, with chemical cross-linking may be possible exploit either the intrinsic reactivity of functional groups present in the biopolymers (i.e. amino acids side chain, such as tyrosine or lysine)[216,217] and further reactive groups introduced specifically, which can be lately reacted bio-orthogonally.[218] Another approach often relies on click-reactions,[219,220] already analyzed, such as thiol-ene coupling,[221,222] or Huisgen-type cycloaddition (see chapter 1).[223]

Several crosslinking strategies have been developed in the last decades, for example, aldehydes, di-aldehydes, but also carboxylic or di-carboxylic acids (malic or malonic acids) have been used in combination with carbodiimides (EDC, DCC..., See **scheme 4.3**) to crosslink proteins through amidic bonds formation between lysine side chains and carboxyl/carbonyl functionalities. In these case gels enzymatic stability, toward collagenases or more generally proteases (in the case of proteic gels), is fundamental property to testing, and it was seen that an increase of crosslink degree results an improvement of swelling degree, thermal and enzymatic stability, promoting then cell adhesion and growth.[224,225]

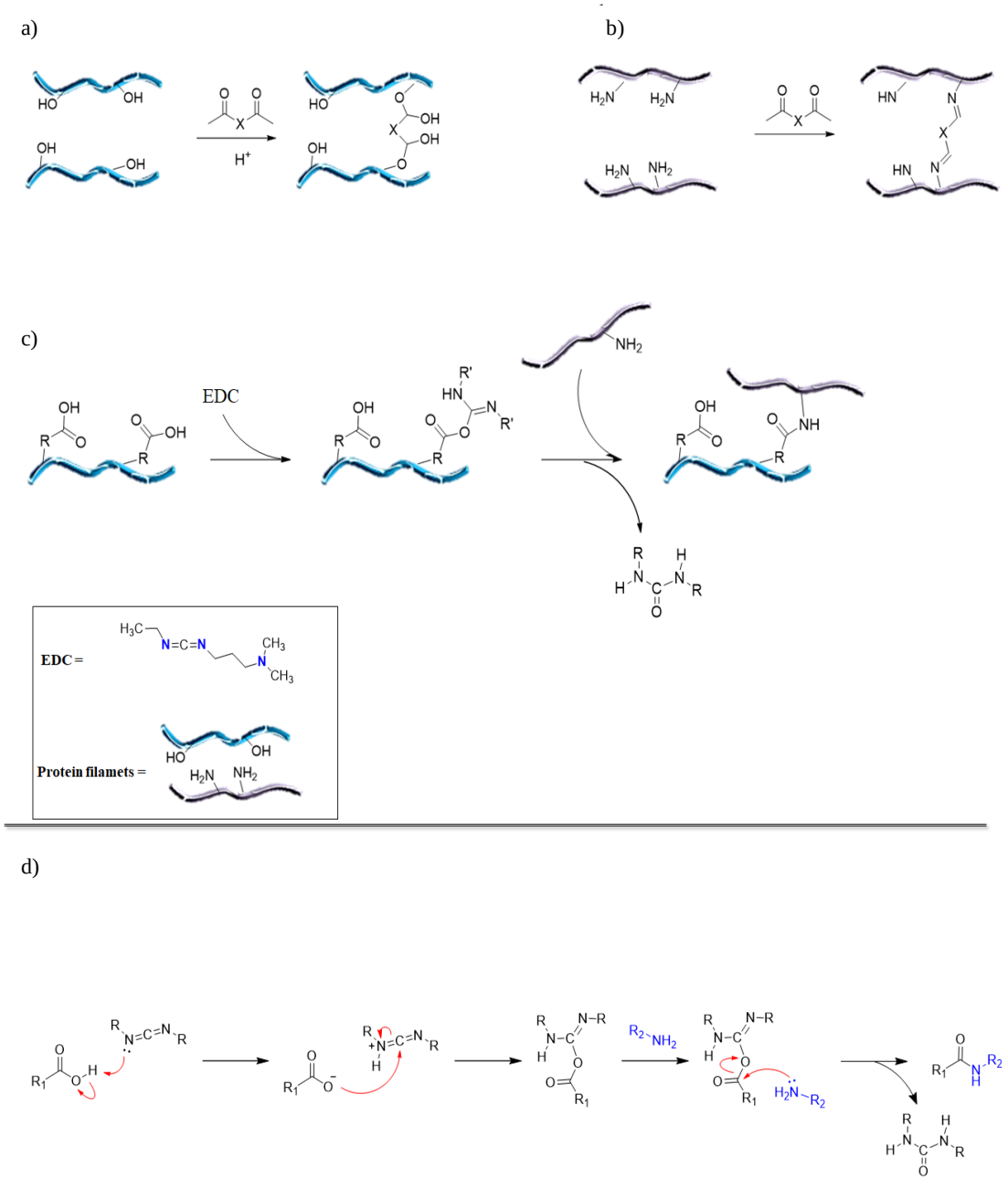

Scheme 4.3 Representative scheme of a generic di-aldehyde which reacts simultaneously with proteic hydroxyl groups (H^+ conditions, a) and amino groups (neutral conditions, b). c, An example of condensation between an hydroxyl group and amino group EDC mediated. EDC in this case work as activator. d, reaction mechanism of EDC activation.

Otherwise, enzymatic cross-linking, by transglutaminases (**scheme 4.4**), catalyzes new bonds between same or different functional groups. In the case of transglutaminase

(more used), glutamine side chains and lysine amino groups represent principal substrates, giving new amidic bonds stabilizing overall hydrogel structure. In addition, it was demonstrated how this innovative approach could be used to allow a controlled release of proteins (i.e. serum albumin, BSA) as tool for protein delivery. In this case, amino groups crosslinking was confirmed by denaturation temperature of hydrogel which increases from 38 °C to 68 °C.[226]

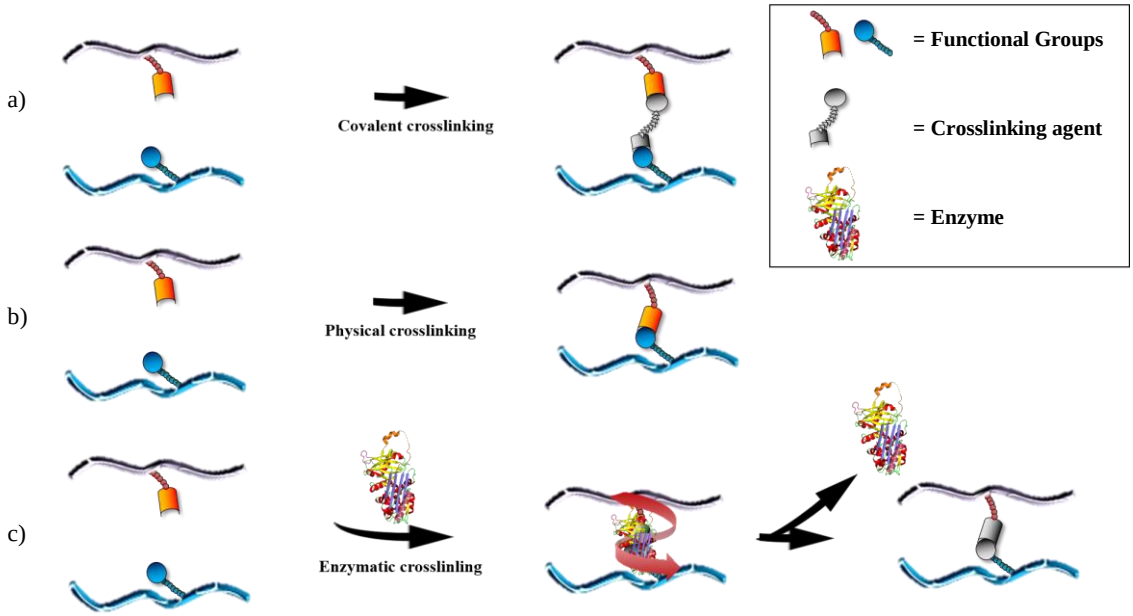

Scheme 4.4 Representative scheme of a generic cross-linking based on chemical methods (a), physical methods (b) and enzymatic methods (c).

However, all mentioned cross-linking agents react exploiting amino, hydroxyl or carboxyl groups in the amino side chains, excluding aromatic ring of tyrosine or tryptophan. To including aromatic rings ligation, oxidative cross-linking of tyrosine phenolic groups need to be proposed, based on oxidation processes of phenolic moieties.[227,228,229] In addition to the oxidative coupling affording zero-length dityrosine adducts, very recently triazoledione chemistry has been proposed to chemoselective conjugations to tyrosine residues, without use of metal mediated catalyzer or drastic conditions.

4.1.4. Protein-based hydrogel, Swelling ability

Another important hydrogel application regards controlled release of molecules, including drugs, therapeutic peptides, proteins, and nucleic acids.[230] The high water content of most hydrogels, for drug delivery systems, results in rapid drug release over a few hours to several days, carrying eventually harmful side-effects.[231,232]

Nowadays great efforts focus on extending the duration of drug release, and expanding the range of molecules which can be delivered.[233] A large number of parameters participate to the result, such as the geometry of the delivery system, hydrogel swelling capacity, and the type and amount of release medium.[234] In addition, release kinetics can also take large time and the sampling can last up from few hours to several days making them time-consuming and expensive, if referred to large drug loads.[235] To overcome these troubles, screening large libraries of potential drug delivery formulations results necessary as well as improve analytical methods that directly asses drug diffusivity, improving certainly the development of new hydrogel-based drug delivery systems.

Generally, hydrogels drug release mechanism involve simultaneous absorption of solvent/cell-culture medium and desorption of drugs via swelling/de-swelling controlled mechanism.[236] When a dried hydrogel comes into contact with water or any other compatible medium, solvent penetration into free spaces on the surface promote swelling process. When enough water has absorbed by the scaffolds, hydrogels reach, so called, water equilibrium. In this situation, an increase of end-to-end distance of polymer molecules were observed. Swelling ability drive the factors mediating drug delivery.[237] Regarding bio-inspired hydrogel (such as collagen or gelatin based hydrogel), polar amino acids side chain, represent the first groups will be hydrate, leading to “primary bound water”. When the polar groups are hydrated, the network swells, changing its conformation and geometry, exposing hydrophobic groups, which also interact with water molecules; leading to hydrophobically-bound water, or

'secondary bound water'. Primary and secondary bound water are often referred as 'total bound water'. After complete interaction between hydrophobic or polar amino-acids side chain, the structure (or swollen network) will imbibe additional water, due to the osmotic driving force of the network chains. However, this process called "additional swelling", is opposed by covalent or physical crosslinks; in this way, hydrogel will reach an equilibrium swelling level. As the network swells, if the network chains or crosslinks are leaky, the gel will begin to disintegrate and dissolve, at a rate depending on its composition. It should be noted that a gel used as a tissue engineering matrix may never be dried, but the total water in the gel is still comprised of 'bound' and 'free' water. There are a number of methods used by researchers to estimate the amounts of water, as fractions of the total weight of the hydrogels.[238,239]

Among numerous methods to evaluate swelling ability, gravimetric analysis results the easiest and fastest method. Dried cross-linking hydrogels are placed into specific volume of solvent (in the case of hydrogels, aqueous-solvent); the samples, removed, are quickly blotted free of surface water and then weighed on an analytical balance. The weigh collected in this manner can be represented by Dynamic Swelling Graphs, build on calculated Swelling Degree from follow equation.[240]

(**Eq. 4.1**)

$$\text{Swelling Degree} = \frac{1}{Dw\,(\,Sw - Dw\,)}$$

Where Sw symbolizes "Swallen weight of the sample" and Dw "Dry weight of the sample". The absorbed water can be quantitatively represented by the equilibrium water content (EWC), the ratio of weight of water in the hydrogel to the weight of the hydrogel at equilibrium hydration, expressed as a percentage.

(**Eq.4.2**)

$$\underline{\text{Equilibrium Water Content (\%EWC)}} = 1Sw(Sw_e - Dw) * 100$$

Sw_e = Swelling weight of the sample at equilibrium, (total weight of hydrate gelatin); Dw = Dry weight of the sample"; and "Sw_e- Dw" represents the total weight of hydrate gelatin.

The hydrogel water-swelling ability can find several applications in several drugs delivery systems and cellular growth model. As a matter of fact, hydrogels with high degrees of swelling could provide rate-controlling barriers to the diffusion of water-soluble drugs allowing the highest attainable fluxes from polymers. Several authors have reported on the diffusion of a wide variety of species through water-swollen hydrogels and shown that both in vitro and in vivo the diffusion coefficients can be calculated from the following semi-empirical expression:

(**Eq.4.3**)

$$D_p = D_0 \exp [-0.05 + (10^{-6} M) P]$$

In this equation, D_p, represents the diffusion coefficient of the specified diffusing species of molecular weight "M" in the water-swollen hydrogel of percentage polymer content of P. D_0, is the diffusion coefficient of the identical compound in pure water. From this equation it is possible to estimate the hypothetical change in the diffusion coefficient D_p, for an hypothetical drug, when some condition have been changed.[241]

4.1.5. Protein-based hydrogel, Applications

There are a lot of applications where hydrogels found efficacy. Hydrogels, in regenerative medicine, traditionally have been used as scaffolds to supply structural integrity for cellular organization, but at the same time several application as barriers and bio-adhesive, cell encapsulation or drug depots were studied.[242]

Hydrogels as barriers. There are lot of consequence caused by surgical procedures, among which restenosis and thrombosis, caused by post-operative adhesion formation, appear as most problematic issues[243]. In this field hydrogels were introduced as a thin layer intravascularly where they are able to inhibit restenosis, reducing intima thickening and thrombosis. The thin layer is able to decrease intimal thickening avoiding the contact with platelets, coagulation factors and plasma proteins with the vascular wall. The contact between these factors and vessel walls stimulates smooth muscle cell proliferation, migration and ECM synthesis events, involving restenosis. Furthermore, hydrogels barriers were tested to prevent post-surgical adhesion formation, by intraperitoneal insertion, or ovoid over fibroblast attachment at the tissue surface.[244]

Hydrogels as drug delivery systems. As will be described later, hydrogels with drug delivery capabilities are often thought to localized drug depots, and then, drug release rates can be controlled, and triggered smartly after physical or chemical stimuli, which can be physiological or not.[245,246] Often, hydrogels can be made of proteins that are hydrophilic. As described, monitoring swelling degree, crosslinking thickness and degradation rate, kinetics of drug delivery, can be modulated in accordance with the desired drug release plan. Alternatively, photopolymerizable hydrogels possess the ability to adhere to tissue and polymerize *in vivo* and *in situ*. Drug delivery systems and hydrogels as barriers can be used simultaneously to release specifics drug, and at the same time, avoid post-surgical effects.[247] In this field, hydrogels were formed in bilayers with different permeability. Inner layer is less permeable than the outer layer, in

this way we are able to improve, on one side, the delivery of released drugs into environment, meanwhile, on the other side we can avoid undesired cellular adhesion, just working on hydrogels preparation. Moreover, different drug concentrations can be encapsulated into each layer during synthesis of a multilayer matrix device to obtain excellent release behaviour.[248]

Cell encapsulation. In certain conditions, hydrogels can be used to supply immunoisolation, while still enabling oxygen, nutrient, and metabolic products to distribute with facility into the hydrogel. With this aim, several PEG diacrylate (PEGDA) hydrogels have been formed for cells transplantation applications. For example, islets of Langerhans to restore pancreas deficiency. working on this thema, researchers was able to suspend islet cells in a photopolymerizable PEG di-acrylate prepolymer solution, and the solution was used to create PEG-based microspheres with captured islets.[249]

4.2. Targeting tyrosine residues through homobifunctional triazolediones.

As widely described, gelatine, due to its properties such as: biodegradability, biocompatibility, cell-adhesion and low- immunogenicity, have been extensively employed as biomaterial for tissue engineering and drug delivery systems.[250,251,252]In addition, gelatine modification could give a plethora of products find several applications in field of regenerative medicine. However, pristine gelatine, without further modifications (both chemical or physical) doesn't possess mechanical properties which can be used, for example, its short degradation time prevents developing hydrogels with stable morphology.[253,254,255] For these reasons, physical, enzymatic, or chemical cross-linking[256,257,258,259] are often necessary to improve desired mechanical properties.

In respect of all previously cited methods, chemical cross-linking is generally preferred, since it affords stable covalent bonds and better reproducibility of the process. In order to provide new covalent bonds between amino acids chains, intrinsic reactivity of functional groups or extrinsic reactivity of introduced groups, can react bio-orthogonally. Bio-orthogonally chemistry relies on click-chemistry strategies[260,261], offering advantages (for example high yield) but also some disadvantages such as the necessity of two step chemical processes.[262] During the last years gelatine were cross-linked both taking advantage of extrinsic functional groups[263,264,265,266,267] or through direct cross-linking based on intrinsic amino acid reactivity.

In biological chemistry lysines provides primary amine groups and although their side chains are protonated under physiological pH, they can still react as nucleophiles making them the most suitable aminoacids groups for biological functionalization in order to introduce new biological properties.[268] For the same reasons, is reasonable thinking that using these groups to improve hydrogels mechanicals properties, through cross linking strategies, results in an impoverishment of the groups themselves for further functionalizations. These are the reasons why, nowadays to find new strategic ways to functionalize several amino acids side chains is great interest. In addition to traditional methods previously described, oxidative cross-linking of tyrosine phenolic groups has been proposed through triazoledione chemistry.

Triazoledione chemistry recently emerged as a click-reaction for the chemoselective bioconjugation to tyrosine residues, mediated by cyclic monofunctional diazodicarboxamides, such as 4-phenyl-1,2,4-triazole-3,5-dione (PTAD).[269,270,271,272] Hetherobifunctional triazolediones (TADs), have been used for the synthesis of DNA−protein conjugates,[273] while homobifunctional TADs have been applied to the cross-linking of synthetic polypetides.[274] In the present work, we propose, for the first time, the use of homobifunctional TADs for gelatin cross-linking towards the production of stable hydrogels.

4.2.1. Results and discussion

New bio-orthogonally strategies has been developed by the use of two different homobifunctional reagents with two terminals 1,2,4-triazole-3,5(4H)-diones groups, namely 4,4'-hexane-1,6-diylbis(3H-1,2,4-triazole-3,5(4H)-dione) compound **4.2** and 4,4'-[methylenebis(4,1-phenylene)]bis(3H-1,2,4-triazole-3,5(4H)-dione) compound **4.4 (Figure 4.2.1**) were chosen as cross-linking agents. Compound **4.2** and **4.4** were synthesized following literature methodologies.[275,276]

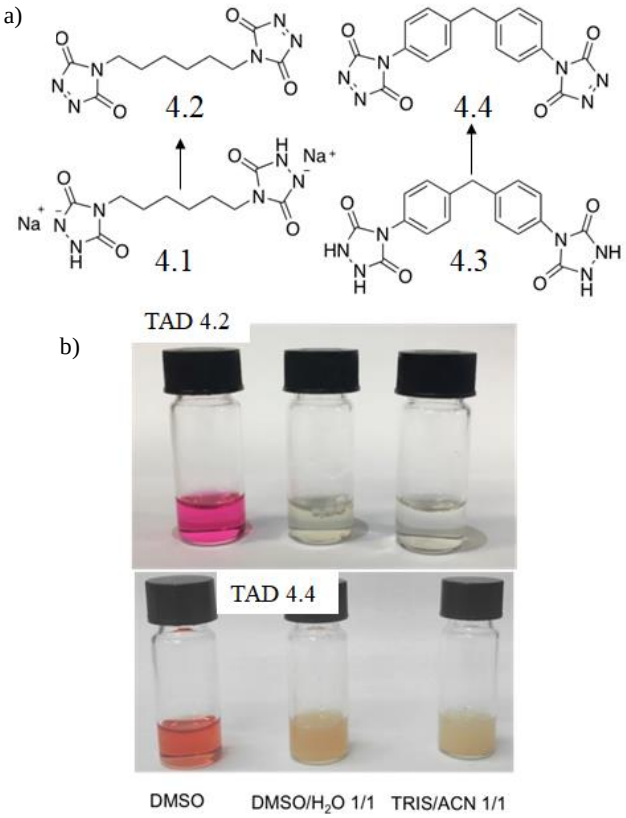

Figure 4.2.1 a) The gelatin cross-linkers TADs **4.2** and **4.4** and the corresponding reduced forms **4.1** and **4.3,** respectively; b) TADs stability in different solvents (DMSO, 1:1 DMSO/H_2O, 1:1 TRIS Buffer solution-pH= 7.4/acetonitrile). The disappearance of the fuchsia colour indicate the degradation of **4.2** and **4.4.**

First, we tested TADs stability in three conditions in order to find best operative conditions. While pristine gelatine can be easily dissolved in aqueous solutions above 37 °C; TADs degrades in aqueous medium as indicated by the disappearing of their characteristic fuchsia colour in a few seconds (**Figure 4.2.1 b**). Thus, suitable reaction conditions should be found for effective gelatine cross-linking by TADs, in order to allow the cross-linking agents to react with tyrosine residues present in the protein, affording the desired chemical reaction towards network formation.

In our study, DMSO shows compatibility with gelatine solubility (12 mg/mL at 37°C) and TADs stability (for several hours) as proven by our solubility tests in **figure 4.2.1 b**. As a matter of fact, in these conditions characteristic fuchsia colour is maintained, confirming the stability of the two cross-linking agents in this medium (**figure 4.2.1 b**). In this way DMSO was selected as solvent for the reactions.

Given the amino acid composition of porcine gelatin, tyrosine is expected to be present from 3 to 4 mmol per 100 g of dry gelatin[277]. In order to study cross linking reactions, 4TADs/tyrosine molar ratios were experimented, in detail 0.5:1, 1:1, 2:1, 5:1. During the reactions characteristic fuchsia colour of TADs disappears, under continuous stirring, indicating the progress and the end of reaction. Upon completion reaction products were recovered by precipitation (adding methanol in the case of **TAD 4.2**, and acetone in the case of **TAD 4.4**).

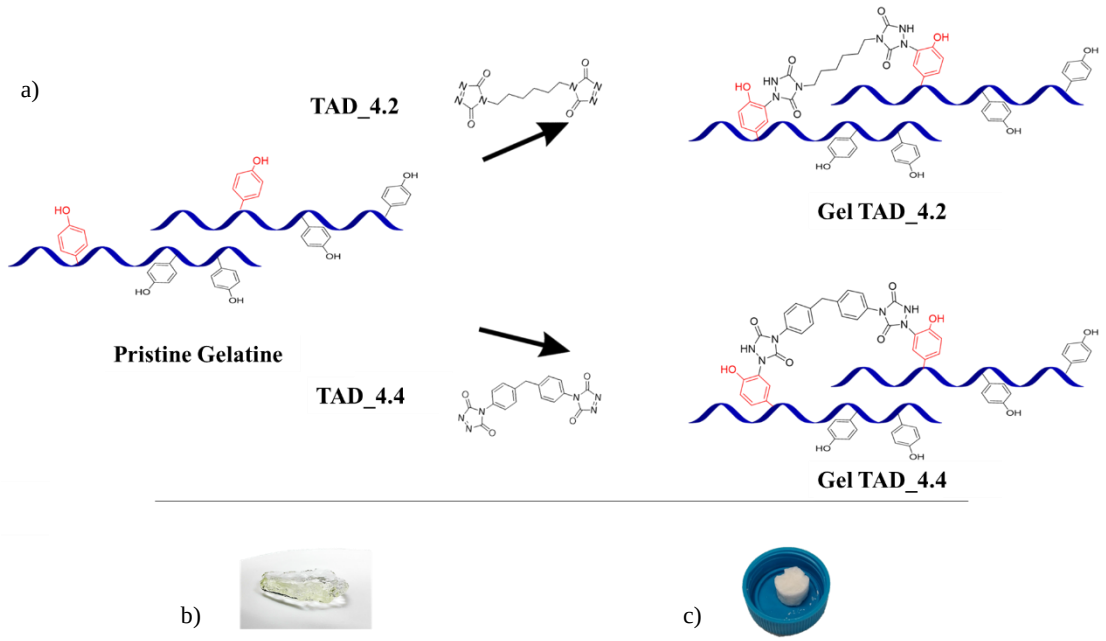

Scheme 4.2.1. a) cross-linking reaction between gelatin and **TAD 4.2** or **TAD 4.4**; b) recovered hydrogels; c) cross-linked gelatin scaffolds after freeze-drying of hydrogels.

After recovery of the products, thermal resistance at pH 7.4 and 37° C, swelling properties, FT-IR spectroscopy, and SEM image data were collected. All of this to demonstrate the effectiveness of the cross-linking methodology. Cross-linked gelatine shows improved thermal stability as TADs/tyrosine ratio increases, in accordance to SEM images (**figure 4.2.5**), showing increase in reticulation.

Subsequently it was demonstrated that cross-linked occurs prevalently through covalent bonds formation (chemical cross-linking), instead of non-bonding interactions (i.e. hydrogen bonds, physical cross-linking). In fact, treated gelatin with the reduced form (urazole) of the TADs (compounds **4.1** and **4.4 Figure 4.2.1, a.**), in a 5-fold excess in respect to tyrosine for 30 minutes (as for the treatment with **4.2** and **4.4**) and identically worked up, doesn't show any improved properties in terms of thermal stability or swelling ability. Thus gelatin treated with **4.1** and **4.3** was soaked in water at 40° C: the specimen promptly dissolved in water at 40° C, indicating that physical cross-linking did not occur. This demonstrate that chemical covalent cross-linking is actually occurring with TADs **4.2** and **4.4**.

Then, thermal stability was tested in order to evaluate the compatibility with cell culture conditions. Freeze-dried cross-linked gelatin specimens were rehydrated with 1 ml of PBS buffer (pH 7.4) and placed in a 37 °C chamber to test their thermal stability (**Figure 4.2.2**), and compared with pristine gelatin samples. As expected, pristine gelatin dissolved almost immediately; cross-linked gelatin with TADs/tyrosine 0.5:1 ratio displayed better resistance when compared to untreated gelatin, dissolving in about 1h for TAD **4.2** and 2h for TAD 4.4**,** respectively. In general, it was observed that the increase of TADs/tyrosine ratios affords better performing cross-linked gelatin. For TAD/tyrosine ratio 5:1, cross-linked gelatin was stable over a month.

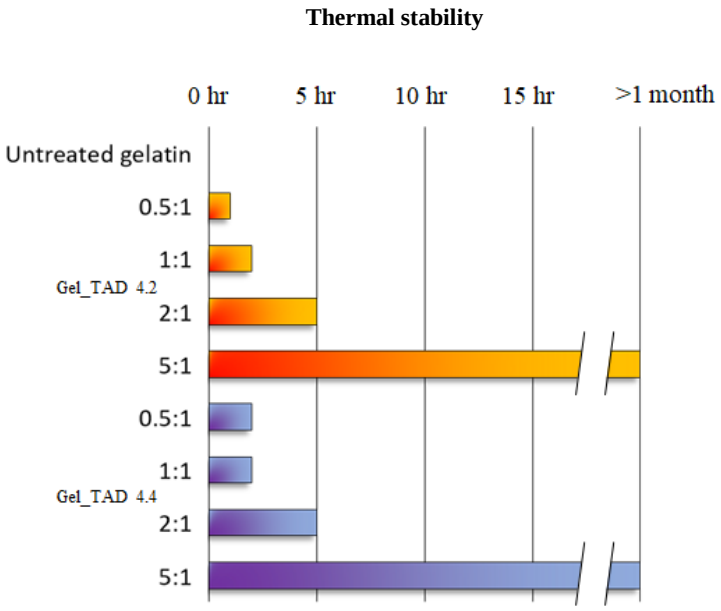

Figure 4.2.2 Thermal resistance of hydrogels at 37°C; results for any TAD/tyrosine ratio are means of 3 independent experiments.

Considering thermal stabilities, cross-linked gelatin with TADs/tyrosine 2:1 and 5:1, which result more stable, were tested for their swelling abilities in an aqueous medium by gravimetric technique. Thus, lyophilized freeze-dried cross-linked gelatin 2:1 and 5:1 (**figure 4.2.3**) were placed in 4 ml of deionized water, and weight changes over time collected. From these data the swelling degree can be extrapolated. In literature swelling

degree is defined as weight change due to solvent absorption and it can be represented by kinetics curves (see **figure 4.2.3 a.**).[278]

Although all specimens tested show water retaining ability at room temperature, without dissolving, swelling degree assays highlight differences related to cross linked ratios (2:1 and 5:1). Interestingly, TAD **4.2** affords hydrogels featured with lower water retaining properties than TAD **4.4** (**figure4.2 a.**), suggesting a better cross-linking degree.

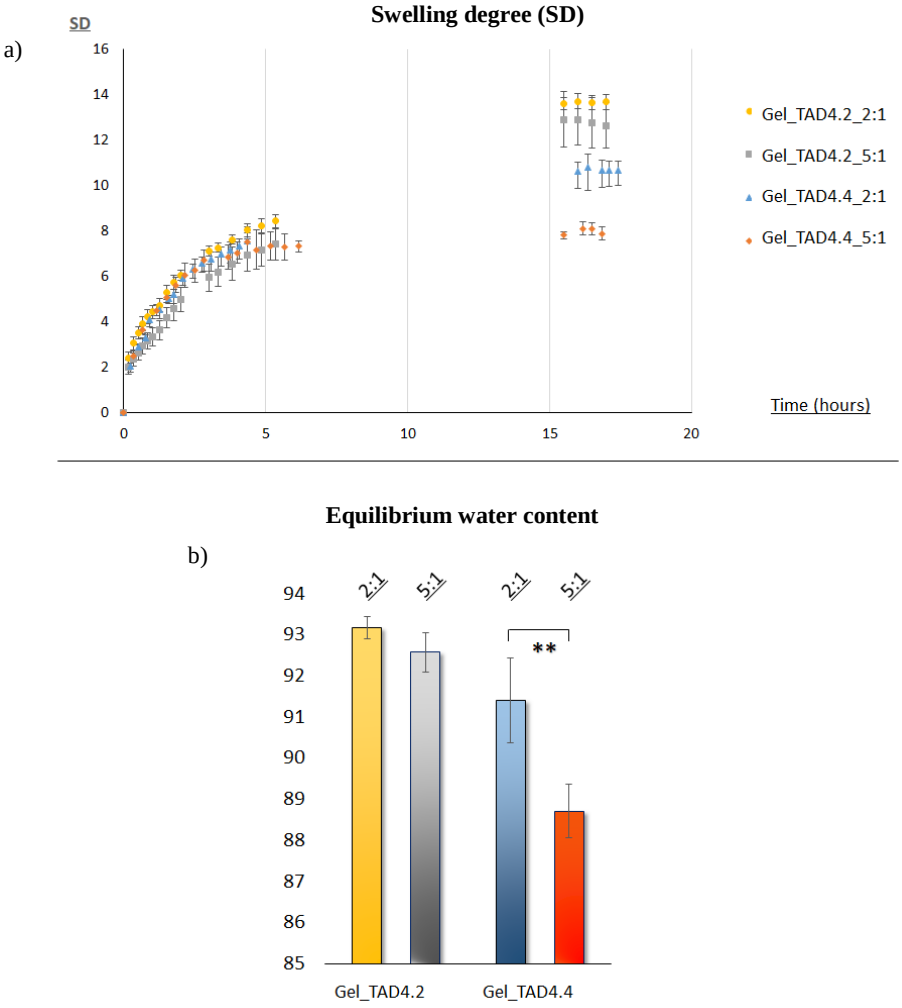

Figure 4.2.3 a) Swelling degree for lyophilized hydrogel cross-linked either with TADs **4.2** or **4.4** at TAD/tyrosine molar ratio 2:1 and 5:1; b) equilibrium water content (graphs and histograms represent average values of three independent measures, bars indicate standard deviation and statistical analysis were performed with t-student with **p<0.01; *p<0.05)

As possible see in **figure 4.2.3 b.** increasing ratio between cross link agent and tyrosine, results in a swelling degree decrease, as general consideration. In addition, analysing Equilibrium water content, at steady state, it is possible note that: samples Gel_TAD **4.2** (both 2:1 and 5:1) absorb approximately 92-93% w/w of water, meanwhile; Gel_TAD **4.4** (2:1) get to 90% of its weight. Finally, Gel_TAD **4.4** (5:1) reaches just 85%, absorbing smaller volumes of water.

Afterwards, gelatin specimens were analyzed by FTIR measurements in attenuated total reflection (ATR). The ATR-FTIR absorption spectra of the different gelatin samples display the typical spectral features of polypeptides and are characterized by the amide I and Amide II bands and several partially overlapped components in the fingerprint region around 1500-800 cm-1 (Figure **4.2.4**, insets a-1 and b-1). Small spectral changes were observed after TAD **4.2** and TAD **4.4** treatments. The intensity variations were evaluated by second derivative analysis that enable to discriminate among overlapped components of the absorption spectra. In particular, a significant increase of the 1013 cm-1 and 952 cm-1 peaks was observed in the 5:1 TAD **4.2**/tyrosine ratio (**Figure 4.2.4**, insets a-2 and a-3). These components, which are also present in the neat TAD **4.2** cross-linker (**Figure 4.2.4**, inset a-1), were tentatively assigned to the CN vibrations.[279],[280] In the case of TAD **4.2** cross-linker, a strong increase of the 1512 cm^{-1} component was observed in the 5:1 TAD **4.4**/tyrosine ratio (**Figure 4.2.4**, insets b-2 and b-3). This component is typically assigned to the CC vibrations of the aromatic ring.[281] The FTIR data thus confirm the gelatin cross-linking through TAD **4.2** and TAD **4.4.**

FT-IR Analysis

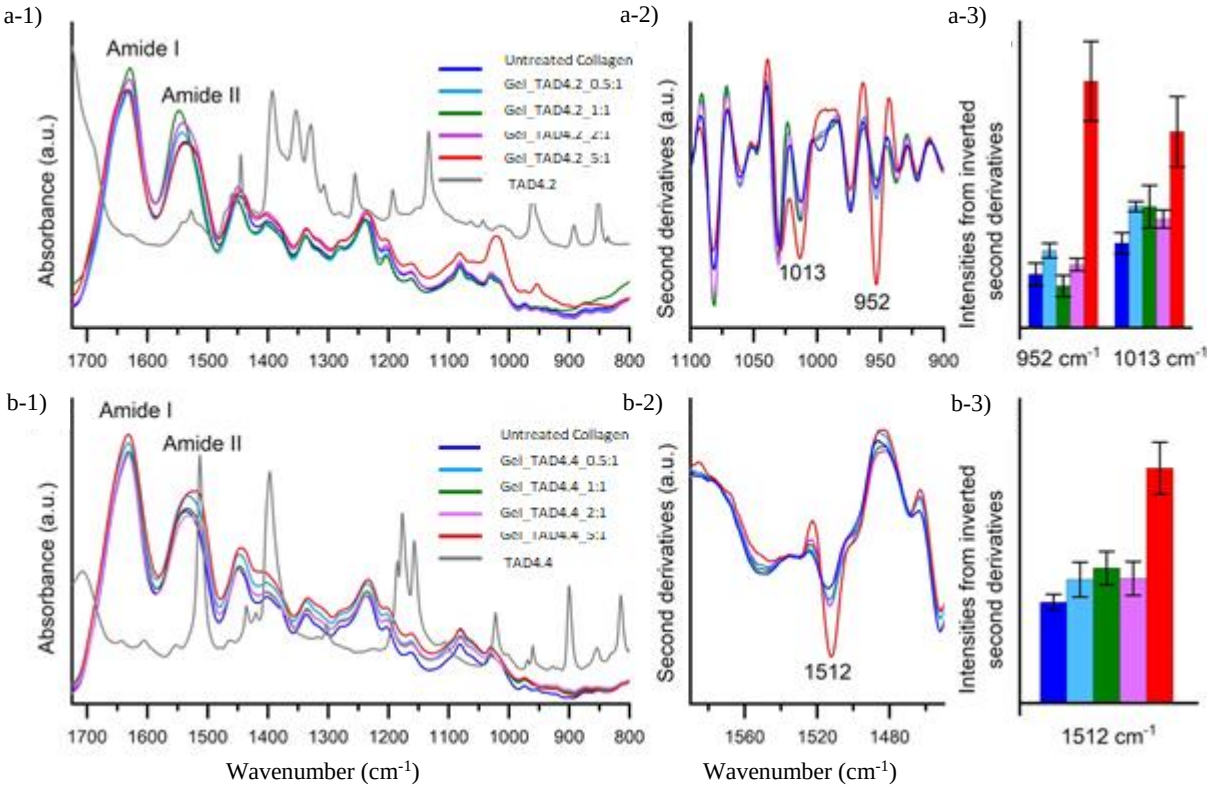

Figure 4.2.4 Insets a1 and b1: ATR-FTIR absorption spectra of untreated gelatin, TADs and cross-linked gelatin specimens reported in the 1725-800 cm-1 region.; the second derivatives of TAD **4.2** (inset a-2) and TAD **4.4** (inset b2) cross-linked samples are reported in the spectral regions where the contributions of the TADs moieties can be detected. The intensities of the indicated components were evaluated from the second derivative spectra (insets a-3 and b-3). Error bars refer to three independent measurements. Spectra are shown after normalization at the Amide I band area.

Finally, low-vacuum scanning electron microscopy was used in order to investigate the surface morphological changes induced by the different TADs cross-linking ratio used. A porous structure along with the foam-like morphology was easily recognizable and measurable in all specimens (**Figure 4.2.5**). As a general trend, moving from 0.5:1 to 5:1 TAD/tyrosine ratio (**Figure 4.2.5**) the increased cross-linkers amount results in an increase in the reticulation texture and a less heterogeneity in porosity and pore size due to increased cross-linking, while pristine gelatin shows a heterogeneous texture with open pores ranging from 5 to 20 µm (Figure **4.2.5 a**). The addition of the cross-linkers increases the interconnected porosity and the pore size shrinks down ranging from 5 to 2 µm.

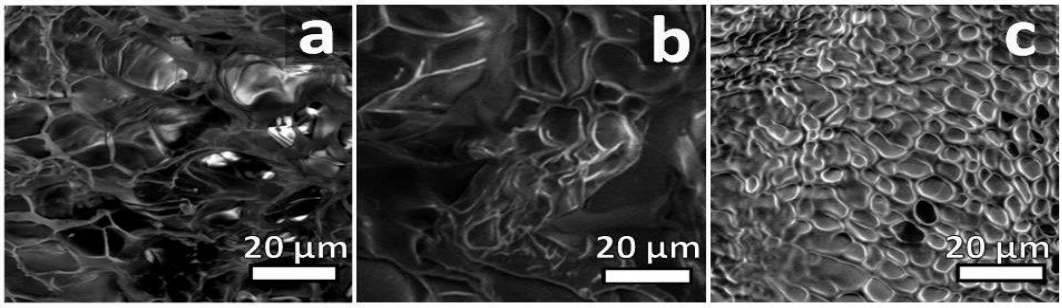

Figure 4.2.5 - Representative SEM micrograph of gelatin samples (a) pristine gelatine and cross-linked with **1** in (b) 0.5:1 and (c) 5:1 TAD **1**/tyrosine ratio respectively.

4.2.2. Materials and Methods

All reagents and solvents were purchased from commercial sources (Aldrich Chemical Co. and Fluorochem) and used without further purification (Gelatin is purchased from by Sigma-Aldrich, catalog no. G2500). ^{1}H NMR spectra were recorded with a Bruker Avance 500. ATR-FTIR spectra of TAD **4.2** and **4.4** and related synthetic intermediates were recorded with a Perkin-Elmer Spectrum 100; ATR-FTIR spectra of gelatin specimens were collected with the Varian 670-IR spectrometer equipped with the Quest (Specac) ATR device.[282]

Cross-linked gelatin was freeze-dried by a Christ alpha 1–2 freeze dryer (Christ, Osterode am Harz, Germany). Melting points were measured with a Stanford Research Systems Optimelt apparatus.

Synthesis of cross-linking agents.

Cross-linkers **4.2** and **4.4** were kindly provided by Prof. Antonio Papagni, dept. of material science, University of Milano-Bicocca.

Gelatin cross-linking

*Synthesis of 4,4'-hexane-1,6-diylbis(3H- 1,2,4-triazole- 3,5(4H)-dione) (compound **4.2**) cross-linked gelatine (**Gel_TAD 4.2**)*

100 mg of gelatin were added to 8 mL of DMSO at 37°C until complete dissolution. Then, starting from tyrosine content (3.68 µmol on 100 mg of gelatin, referred to Eastoe, J. E. *Bioch. Journal* **1955**, 589); a starting solution of TAD1 was prepared in DMSO (5mg/ml). Depending on TAD/tyrosine desired ratio, 103, 206, 412 µl and 1.030 ml were added to gelatin solution (respectively 1.84, 3.68, 7.36, 18.4 µmol, corresponding to 0.5:1, 1:1, 2:1 and 5:1 molar ratios).

The solutions were kept at r.t. and in the darkness, and reacted under stirring until the purple solution becomes colorless (30 min). Then, gelatin was precipitated by addition of 8 ml of methanol, then the precipitate was centrifuged (6500 rpm, 45') and extensively washed for 1 time with methanol (5ml) and two times with deionized water (2 ml for each times). The hydrogels formed on the bottom of centrifuge tube were lyophilized

*Synthesis of 4,4'-[methylenebis(4,1-phenylene)]bis(3H- 1,2,4-triazole- 3,5(4H)-dione) (compound **4.4**) cross-linked gelatine (**Gel_TAD4.4**)*

At the same manner previously described, a starting solution of TAD **4.4 (**5 mg/ml) was prepared and then 133, 266, 532 µl and 1.030 ml (respectively 1.84, 3.68, 7.36, 18.4 µmol, corresponding to 0.5:1, 1:1, 2:1 and 5:1 molar ratios µmol), added to a gelatin solution, previouslyprepared.

On the contrary, TAD 4.4 Cross-linked gelatin was recovered by acetone addition (8 ml), also here the suspension was centrifuged with the same protocol used for TAD 1 cross-linked gelatin, using this time acetone for the washing procedure.

Thermal stability studies.

Lyophilized Gel_TAD (ca 90 mg) specimens were hydrated with 2 mL of PBS buffer, pH=7.4 (physiological conditions), placed in a 12 multiwell plate were left in hot room at 37°C. The samples were visually inspected to check sample dissolution. The thermal stability was esteemated on the basis of hydrogels integrity optical observation.

Swelling Degree studies.

Swelling measurements were made by gravimetric analysis. Dried cross-linked gelatin was placed in a well and 4 mL of water were added at room temperature. The sample, removed at different time intervals, was quickly blotted free of surface water using filter paper, weighed on an analytical balance (Analytical Balance 220g x 0.1mg, Radwag AS 220/C/2) and returned to the swelling medium.

SEM analysis.

Scanning electron microscopy (SEM) analysis were performed with a Philips XL30 ESEM, working at 8kV accelerating voltage and in low vacuum mode (1 torr). Sample were dried, cut, fixed with conductive carbon tape to standard SEM stubs and directly analyzed. Working at low vacuum condition, no conductive coatings were applied in order to preserve the original structure. Samples showed good stability under electron beam illumination at the operating conditions.

4.2.3. Conclusions

A new cross-linking methodology for proteins such as gelatin useful for the preparation of hydrogels has been proposed through the use of homobifunctional triazolinediones. The reaction is effective, as demonstrated by several characterisation techniques and thermostability of obiianed specimens if compared to untreated gelatin. TADs are expected to target mainly tyrosine residues, however reaction of TADs with tryptophan has been reported recently,[283] using an organic solvent as reaction medium.

4.3. Targeting Lysine residues as a new method for gelatin cross-linking.

Nowadays, just few hydrogels can find application as drug delivery systems. In this context, beyond the swelling abilities, also "situ gelation" property represent a key point for success of hydrogel development. More efficient gelation strategies are based on chemical cross-linking (see **chapter 4, paragraphs 1 and 2**), often related to chemical functionalization, UV polymerization or click chemistry. The several strategies offer gelation time-dependent triggered by several kind of stimulus (e.g. pH, temperature, light, etc.).[284]

Nowadays, hydrogels, as drug delivery systems don't find many application, however, sometimes can be used with this purpose. One of the applications of hydrogels, regards glioblastoma treatments (GBM), where, several kind of anticancer drugs are, *in situ*, provided by these systems. In this way, side effects due to drugs overdose are lower than classical formulations. However, in these case hydrogels need to be directly administered in the brain (or more general, *in situ*). In this way, drugs can be released intratumorally or in the surgical resection cavity.[285]

Some loading strategies have been developed in the last years, in some cases, the drug is directly loaded in the hydrogel matrix, while in other cases nan-devices loaded with drugs are necessary to support hydrogel formulation, in order to prolong the sustained release of the drug. Furthermore, hydrogels need to sustain drug release over specific time sheet with initial controlled burst effect and, obviously, need to be compatible, non-immunogenic and biodegradable within 6 to 12 months and prevent cell infiltration.[286]

One of the most challenge in proteins bioconjugation and hydrogels development is related to find a correct amino acid side chain to bind molecules of interest. While, in previous chapter, we explored tyrosine chemistry, using triazolinediones, here, amino

groups of lysine side chains have been selected. It's our opinion that, consequently to a different amino acids distribution in collagen or gelatine matrix, it should be possible modulate mechanic properties of the product. Choosing cross-linking agents, with high chemo-selectivity, if referred to a specific amino acid side chain, we can control crosslinking degree and fine tuning physical properties. In this case lysine, as reported previously, represents the most amino-acid present in collagen sequence. In this optic is reasonable thinking that: with appropriate cross-linking strategies we can modulate mechanical properties in order to stimulate specific biological response. for these reason, lysine side chains functionalization offers a great starting point to work on with the aim to develop new hydrogels with interesting properties, each ones useful for specific applications.

4.3.1. Aim of the work

In this section it was proposed a new methodology to crosslink gelatine in order to obtain new, biocompatible hydrogel for drug release system. In this case amino groups of lysine side chains were selected of target groups to generate a network based on chemical interaction between carboxyl groups of 3,4-dihydroxy-3-cyclobutene-1,2-dione (SQ, compound **4.3.1**) and lysine amino groups.

In this way, we obtained a new lysine cross-linked hydrogel and its mechanicals, chemicals and physical properties were evaluated. Then biocompatibility and drug release abilities were assessed in order to understand the potentialities, and eventually, applications of these systems providing an overview behind protein based hydrogels. Here, the reaction gives products with interesting properties which were deeply studied from chemical, mechanical and physical point of view. Moreover, reactions can be

conducted in aqueous environment (with controlled pH), making them available for further biological studies,

4.3.2. Results and discussion

Lysine cross-linked hydrogels were prepared by two different conditions which give two products with different chemical, physical and mechanical properties. The different conditions regard the concentration in which gelatine were solubilized. In the first case pristine gelatine were solubilized keeping a concentration of 5% (w/w, "Gel_SQ 5%"), in the second case, concentration was set to 10% (w/w, "Gel_SQ 10%") (for experimental detail see below). As cross-linking agent was selected **3,4-Diethoxy-3-cyclobutene-1,2-dione** (SQ, **scheme 4.3.1**), which has been added after gelatine solubilisation at different concentrations.

a)

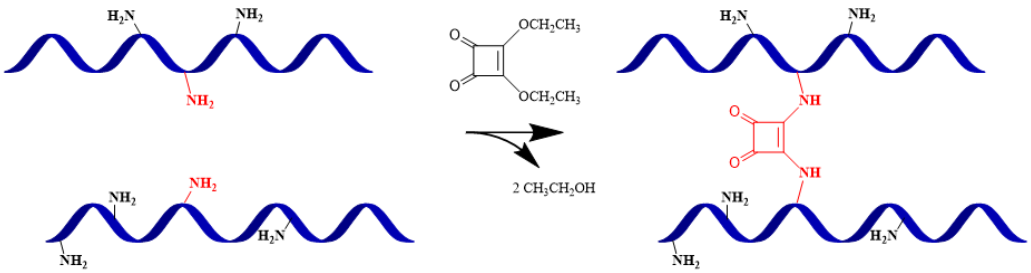

b)

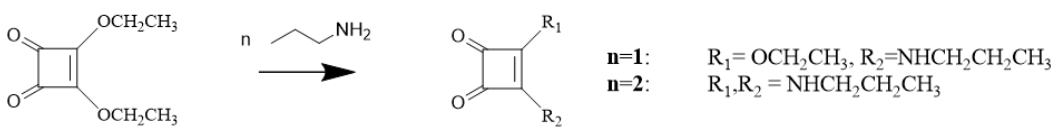

Scheme 4.3.1- reaction representation, at the top has been illustrated lysine side chains reacting with 3,4-Diethoxy-3-cyclobutene-1,2-Dione (acid Squaric or SQ). Down, has been illustrated the same reaction carry on as model with 1-Aminopropane (AP) at different molar ratios.

After reactions, FT-IR analysis were performed in order to evaluate chemical modifications and check secondary structure of protein. As shown in **scheme 4.3.2**, after reactions, hydrogels 5% show overall almost superimposable IR spectra, if compared to control (Gel_SQ 5% vs Pristine gelatine, **figure 4.3.2)**. However, a new absorption band has been detected around 1804 cm^{-1}, probably due to stretching of new introduced CO. In addition, this new group is placed near to C double bond, normally absent in pristine gelatine or collagen. This result was further confirmed by second derivatives analysis in which, is appreciable the inversion of the peak.

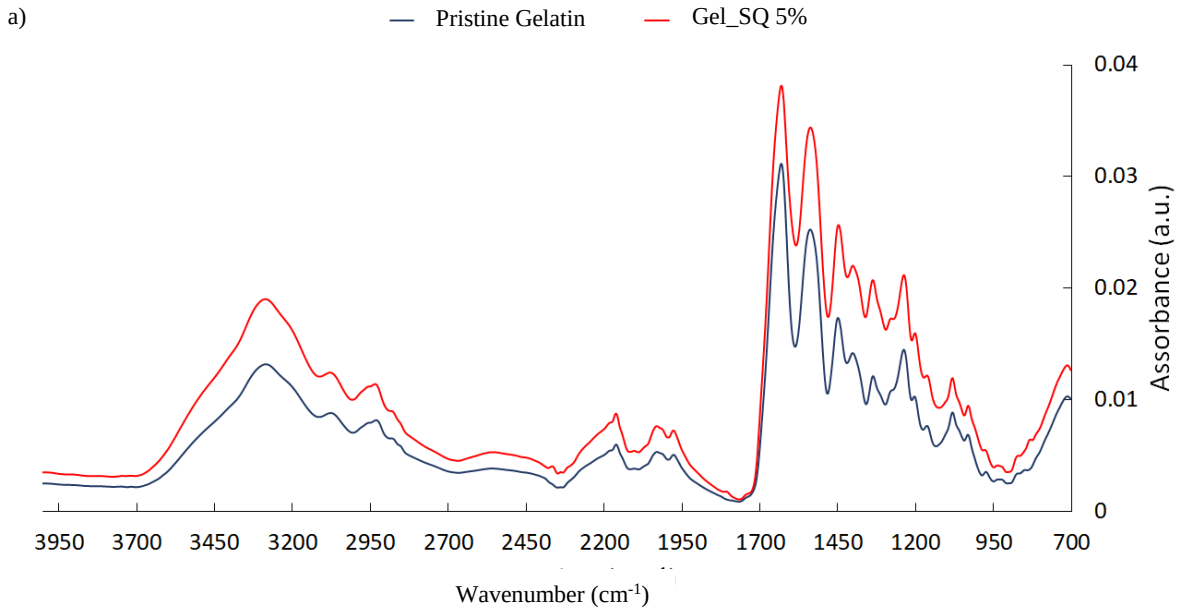

Figure 4.3.2 -a global view of FT-IR spectra; a. has been shown comparison between hydrogel obtained from reaction product with gelatin 5% (Gel_SQ5%, blu line) and pristine gelatin (red line).

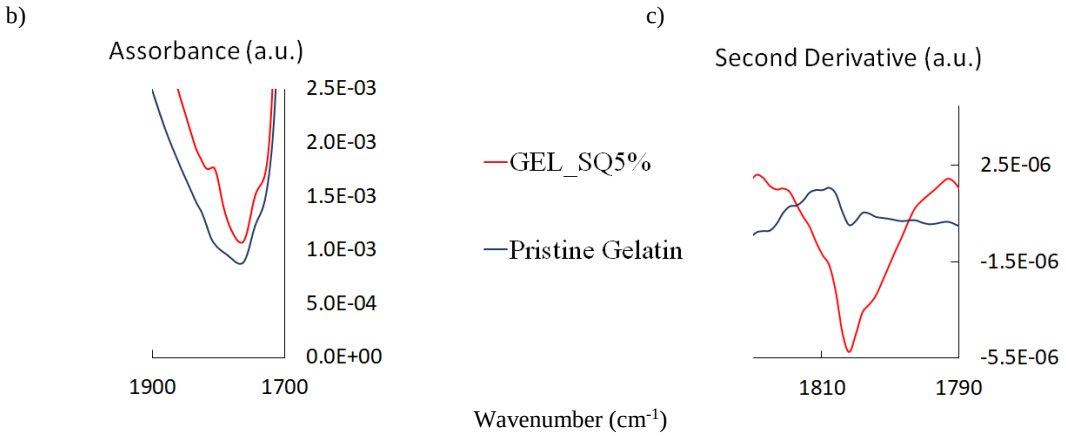

Figure 4.3.2 – continued - b. is a zoom of the same situation seen in **Figure 4.3.2 "a"** around 1900-1700 cm^{-1}, c. represents second derivative of the peak described, at 1804 cm^{-1}.

With the aim to confirm further as reported, a model of study was proposed to follow the reaction with FT-IR analysis. In detail 3 reaction conditions were set up with 3,4-Diethoxy-3-cyclobutene-1,2-dione (SQ) and N-aminopropane (AP) to mimic and simplify our case of study. The reactions were prepared exploring several molar ratios between SQ and AP and evaluate through FT-IR analysis the stretching of CO bond, and how its chemical shift change as result from amino groups insertion (**Figure 4.3.3**).

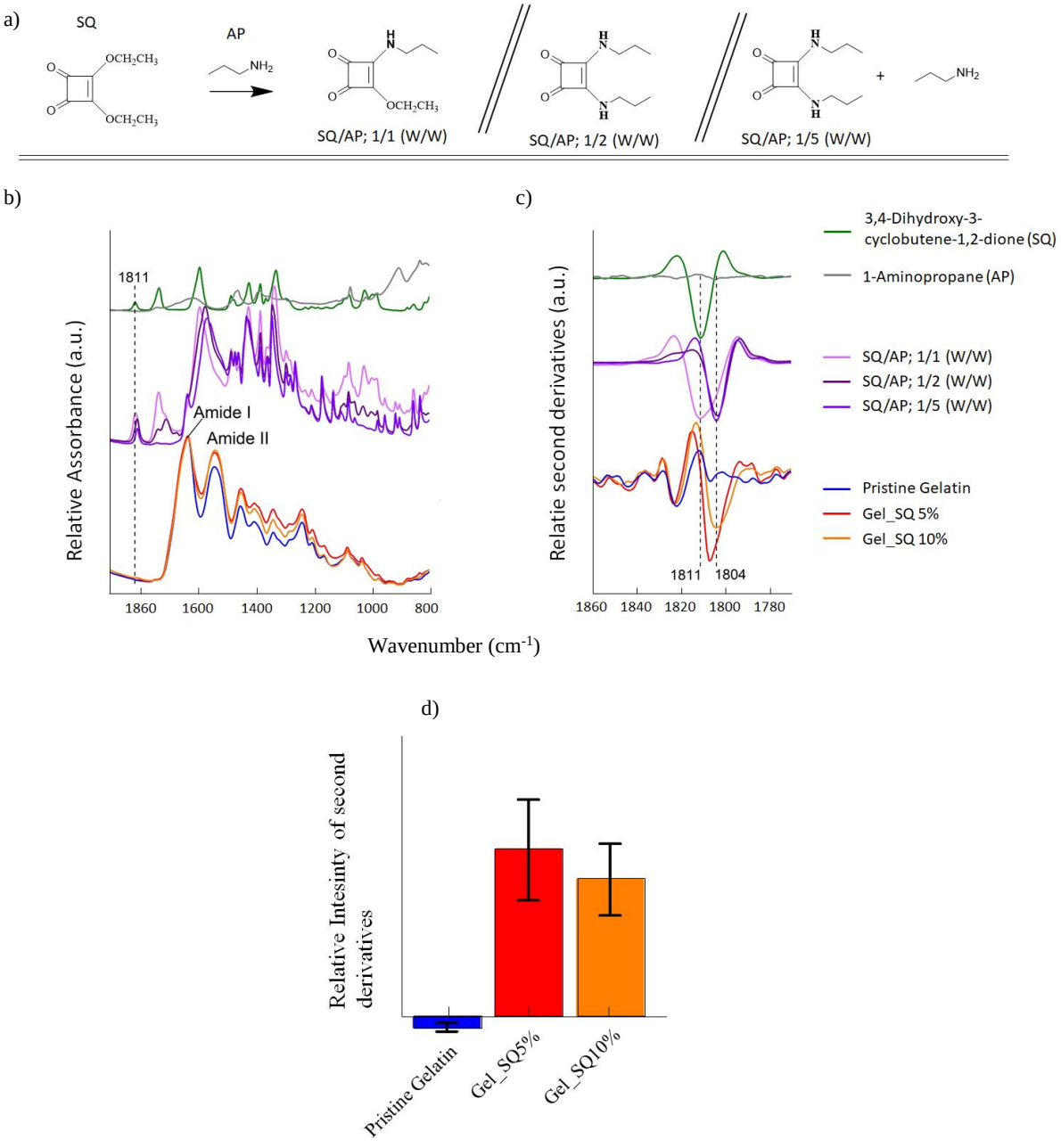

Figure 4.3.3- in a. it has been reported a reaction scheme between SQ and AP with different molar ration and the respectively products. In b. respectively FT-IR spectra of compounds shown in "a" with a generic control. In c. second derivatives of spectra collected in "b". In d. relative quantification of 1804 cm^{-1} absorption band.

As reported by our FT-IR analysis, SQ possesses a typical absorption band around 1811 cm^{-1} due to CO stretching, while 1-aminopropane doesn't possess this band (**figure**

4.3.3, b and c; respectively green and grey lines). In the case of reaction product SQ/AP 1/1, (**figure 4.3.3**, **b** and **c**, light purple line) this band appears with a small shoulder shifted of some cm^{-1} units (from 1811 cm^{-1} to 1804 cm^{-1}). In SQ/AP 1/2 (**figure 4.3.3**, **b** and **c** purple line), a shift of CO stretching peak toward lower wavenumber is observed (1804 cm^{-1}); data were confirmed by second derivatives analysis (**figure 4.3.3**, **b** and **c** dark purple). The same result was also collected for SQ/AP 1/5 (**figure 4.3.3**, **b** and **c**, dark purple), confirming further the shift. Interesting, in second derivatives, this band is completely superimposable with Gel_SQ 5% and Gel_SQ 10% and it is completely absent in pristine gelatine sample, (**figure 4.3.3 c**, line blue). It's our opinion that, the observed shift is due to insertion of aminic groups; since these groups are adjacent to carbonyl moiety, chemical makeup changes, involving minimal shift of CO absorption peak toward lower wavenumber. In addition, being this group normally absent in pristine collagen, we are able to confirm the success of reaction.

Moreover, other assay was also performed in order to confirm cross linking reactions and evaluate physical and mechanical properties of hydrogels and how these change, dependently, from substrates concentration. Since one of the most studied hydrogels properties is the resistance by enzymatic degradation, *in vivo* conditions, it was performed collagenase assay with the aim to obtain further informations about it.[287] As shown in **figure 4.3.4 a**, gelation products were treated with a solution of collagenase and weight collected over the time until complete sample degradation. In these conditions hydrogel 5% show a lower stability than hydrogels 10%, degrading in less than one hour, meanwhile hydrogel 10% resists over two hours confirming cross linking greater degree. In addition, also preliminary two parallel plate test rehometry suggests a greater crosslinking degree. As a matter of fact, as shown in **Figure 4.3.4 b**, increasing shear rate value, the viscosity of the system decrease preferentially with Gel_SQ 5%.

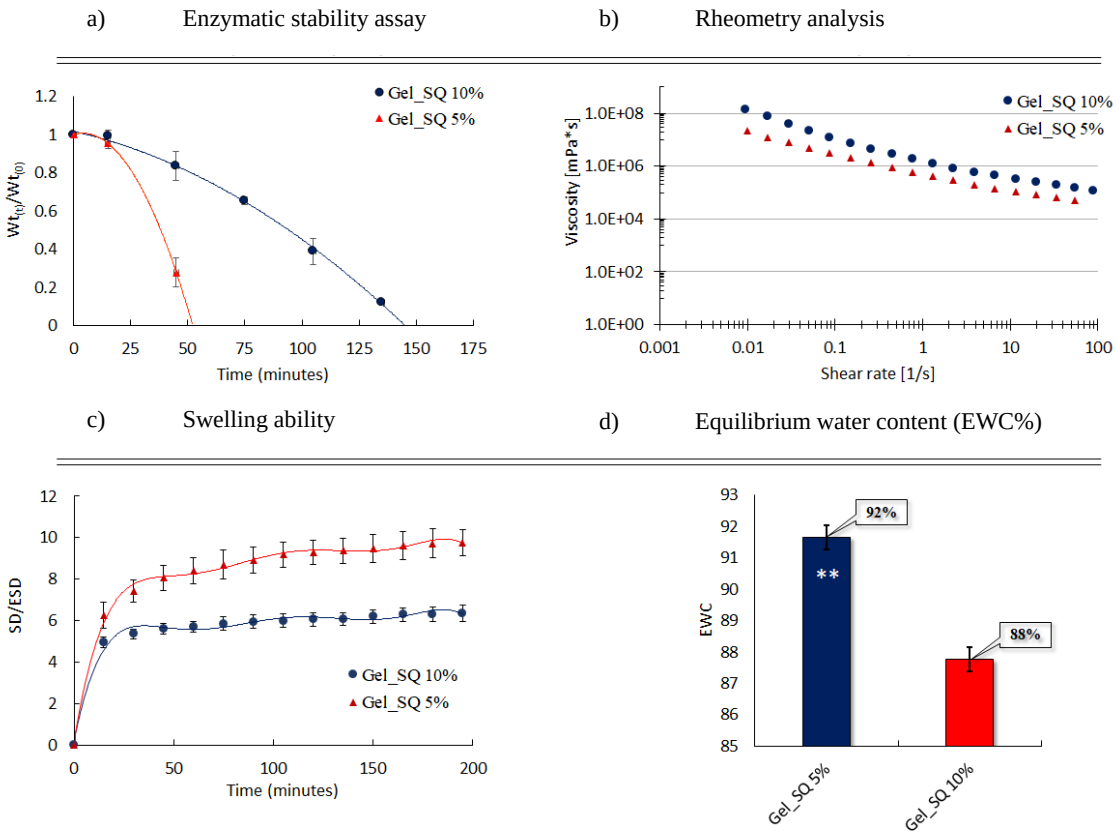

Figure 4.3.4, in this figure has been shown an overview of principal techniques used to evaluate globally hydrogels resistance. in a. Enzymatic stability assay shown the difference of two gel toward protease. in b. has been illustrated rheometry analysis, c. swelling ability and d. extrapolated equilibrium water content determined as previously described. (Gel_SQ 5%: gelatin starting concentration 5%; Gel_SQ 10%: gelatin starting concentration 10 %; bars indicate standard deviation, t-student test for **p<0.01).

Dried gelatine hydrogels were then tested for their swelling abilities in an aqueous medium by gravimetric technique (with analogue procedure seen in previously paragraph). Thus, carefully weighted freeze-dried cross-linked gelatine (with cylinder shape, 100mg for Gelatin SQ 5% and 200 mg for gelatin SQ 10%) (**Figure 4.3.4, c**) were placed in 40 ml of deionized water, and weight measured over the time until equilibrium. From these data, the swelling degree can be extrapolated, as further confirmation of effective cross-linking and gel stability toward water absorption.[288] Although all two dried samples tested show water retaining ability at room temperature, without dissolving, Gel_SQ 5% show higher retaining water ability if compared with

Gel_SQ 10%. Furthermore, it was possible calculate, as reported in previous chapter, equilibrium water content from which, greater crosslinking degree involves as consequence lower water absorption (**Figure 4.3.4, c)**. All These data suggest that, changing gelatin concentration and gelatine/cross linking molar ratio, we are able to modulate finely enzymatic stability, dynamic viscosity and swelling features, With the aim to verify our hypothesis on different water retaining behaviours, the two dried hydrogels (Gel_SQ 10% and Gel_SQ 5%) were analyzed by SEM microscopy following the indicated sections in **figure 4.3.5**. As observed in **figure 4.3.5**, both Gel_SQ 5% and Gel_SQ 10% show characteristic porous structures with misurable average diameters. In the case of gel_SQ 5%, **figure 4.3.5**, a. porous average diameter is around to 30-35 μm, whereas in the case of Gel_SQ 10% rarely diameter exceeds over 20 μm. These value are verified for two different sections (figure **4.3.5**, section A and **4.3.6**, section B).

a) Section A of Gel_SQ5%

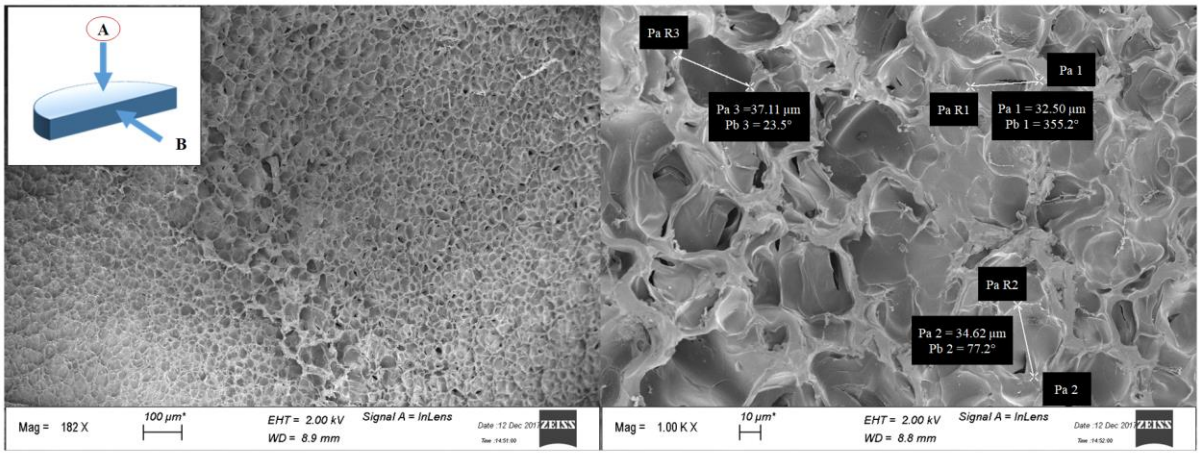

b) Section A of Gel_SQ10%

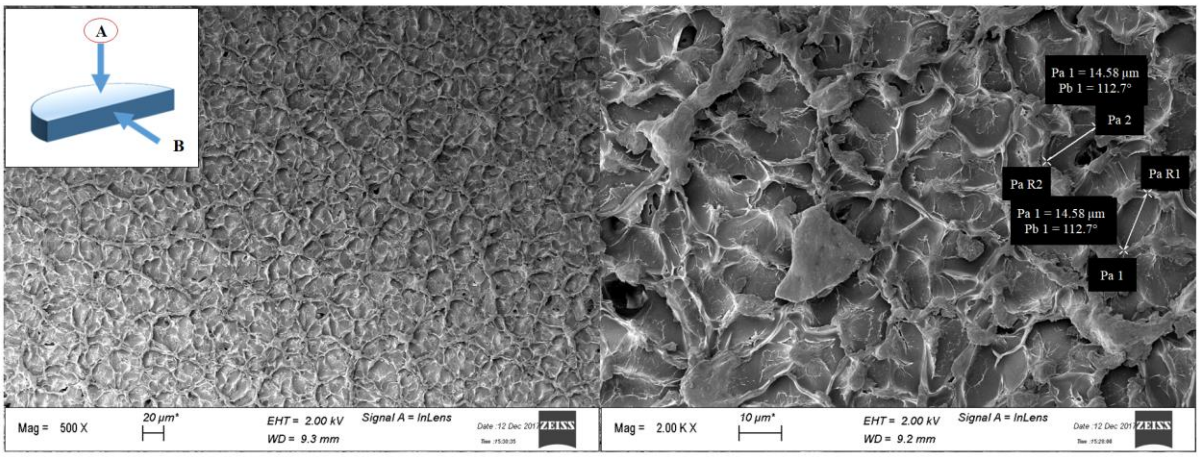

Figure 4.3.5, SEM images of Section A of Gel_SQ 5% a; and Gel_SQ 10%. b;. On the right of each pictures have been reported average pores diameter

a) Section B of Gel_SQ5%

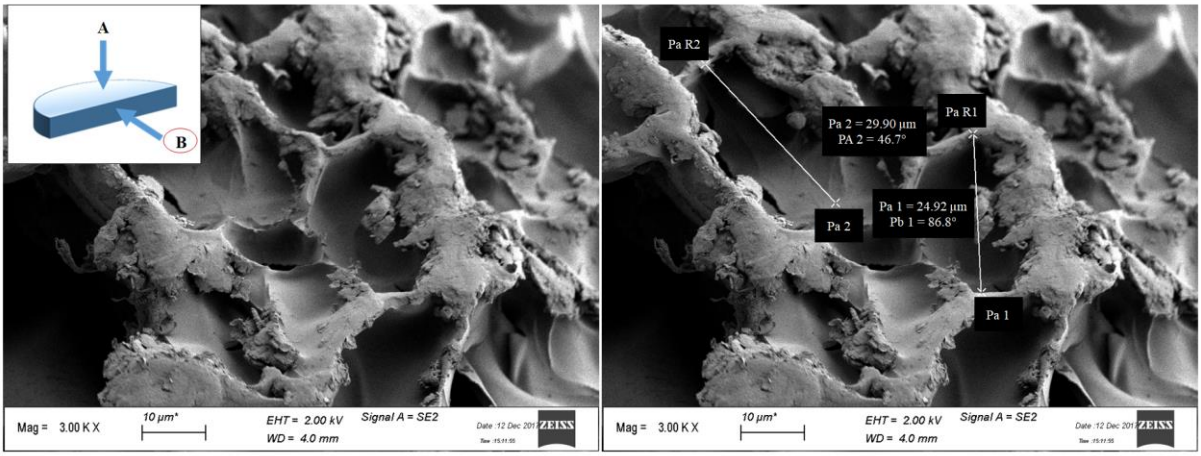

b) Section B of Gel_SQ10%

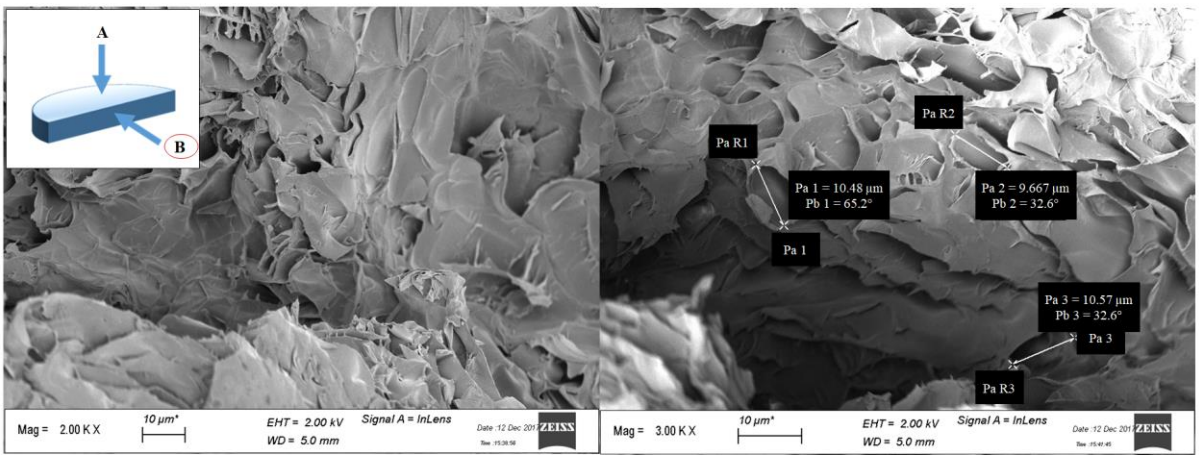

Figure 4.3.6, SEM images of Section b of Gel_SQ 5% a; and Gel_SQ 10%. b;. On the right of each pictures have been reported average pores diameter

Both swelling tests and SEM images suggest how, modifying reaction conditions (Gel_SQ 10% and Gel_SQ 5%) we can alter porous average diameters. In detail, an increase of starting gelatin concentration involve to decrease of porous diameter, meanwhile, decreasing concentration imply an increase of diameters.

Subsequently, in collaboration with Michela Ceriani (assistant professor, Dept. Biosciences and biotechnologies of Milano Bicocca), two cells cultures were prepared in order to evaluate cell hydrogel permeability and biocompatibility, using primary Human Cartilage Cells (C28/I2), and secondary human embryonic renal immortalized cell line (HEK293 cells). C28/I2 represents a good cellular model for tissue engineering in regenerative medicine, useful for biocompatibility studies of hydrogels. In fact, C28/I2 on 3D matrices are known to grow up with difficulties, for these reason they represent a good starting point to test also other cell lines. On the other side, HEK293 cells, have been used due to their lowest dimension.

Dry gelatin sponge were placed in each well of a 24-well plate, here C28/I2 suspension (5×10^6 cells/mL) or HEK293 suspension (5×10^6 cells/mL) were incubated for 4 h at 37°C with 5% CO_2 and cultures were conducted for 2 weeks. Then hydrogels were cut into thin slices and stained with of Phalloidin-TRITC and DAPI to stain at the same time cytoskeleton and DNA. With the first stain it was possible study the morphology of the cells, and through second it was possible observe DNA by two photon microscopy.

a) Chondrocyties, Hydrogel 5%

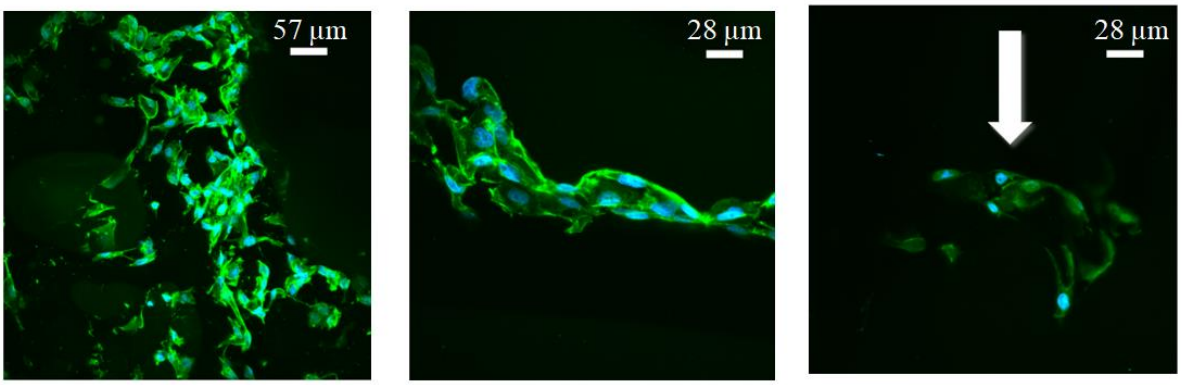

b) Chondrocytoes, Hydrogel 10%

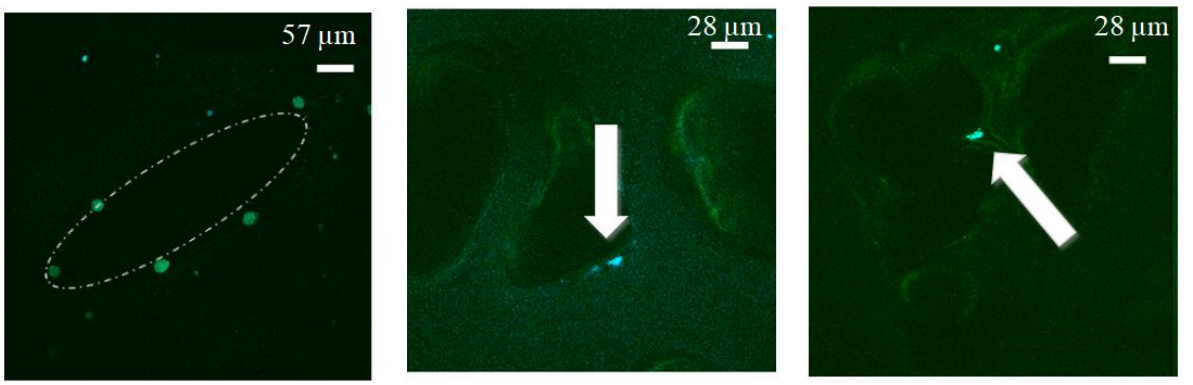

Figure 4.3.7 Confocal microscopic images of Gel_SQ 5% a. and Gel_SQ 10% b. Each pictures shows the difference in cellular growth of C28 Chondrococytes.

As possible observe in **figure 4.3.7**, after 2 weeks' chondrocytes colonize our 3D matrices, into images is possible observe chondrocytes adhere toward the walls of the pores. It is interesting observe the variation of cells colonization between hydrogel_SQ 5% and 10%. In fact, in the second case the number of the cells seen is lower than first case (**figure 4.3.8, a** and **b**). Changing starting gelatin concentration, SEM analysis highlights a narrowing of pores at high concentrations, reaching to 20 µm. Since chondrocytes diameter is around 30 µm is our opinion that, in the second case, pores are too small to allow cell growth. Finally, as general consideration, observing the images can be noted how pores diameter increase from SEM images to confocal acquisition, both 5% and 10%. This fact could be explained by swelling process that involves into

increase pores dimensions. At the same time also cytoskeletal morphology looks different from Gel_SQ5% to Gel_SQ10%, but this is just preliminary macroscopically observation, further analysis are in due course to evaluate this point.

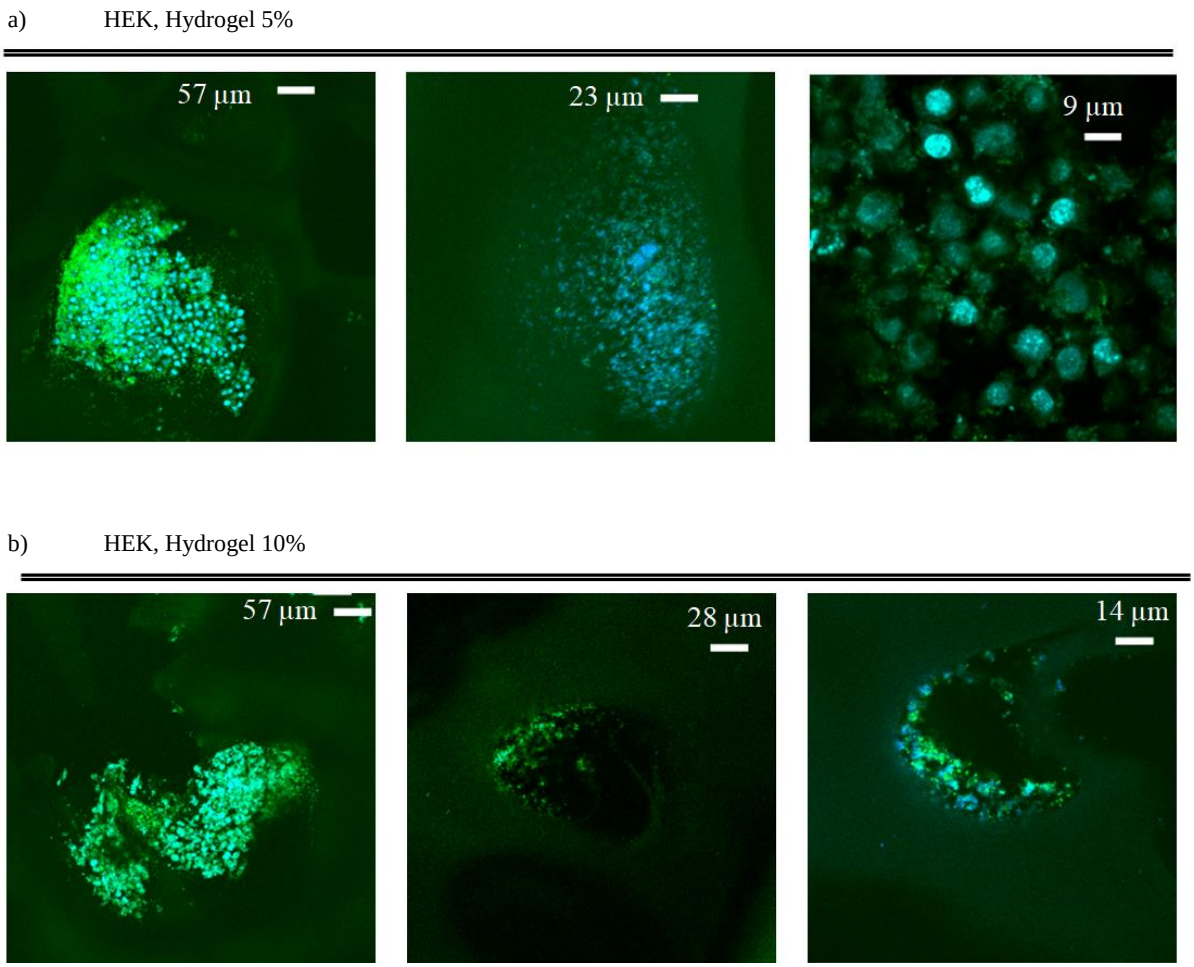

Figure 4.3.8 Confocal microscopic images of Gel_SQ 5% (above the line) and Gel_SQ 10%. (under the line). Each pictures shows the difference in cellular growth of Hek 293 cells.

As further confirmation of what has been seen, HEK 293 cells also have been seeded. As well known in literature this embryonic cells are really smaller than chondrocytes, reaching also 10-15 µm. As a matter of fact, HEK cells appear numerous in the porous structure, in some case it almost seems like they close the pores highlighting, by DAPI stain, an important DNA volume. No appreciable differences appear between

Gel_SQ5% and Gel_SQ10% confirming the hypothesis in according to key role of average diameter pores.

As seen before, most hydrogels applications are based on water absorption. Therefore, the equilibrium swelling degree and the study of drug delivery kinetics are essential from the point of view of their application in the biomedical field. For these reasons, and based on the fact that hydrogel prepared to 10% doesn't result compatible with cells penetration (by preliminary biological assay), we chosen to proceed only with hydrogels obtained by 5% condition; testing drug delivery and diffusion properties.

The first step to study diffusivity and eventually release properties of drugs, is improve the knowledge behind swelling ability and evaluate at the same time the kinetics of drug loading process at the same conditions. In this case, it has been chosen to load drug directly on produced gel, but to do this, first for all it has been reported a second curve of swelling ability, obtained directly on gelation products without further lyophilisation processes (**Figure 4.3.9**, **a**). Then, rhodamine uptake kinetic was studied (**Figure 4.3.9**, **b**). Rhodamine uptake was followed spectrophotometrically using Beer-Lambert law, by soaking the hydrogel samples in Rhodamine-6G solution. By means of a spectrophotometer, we check the absorbance decrease of the solution and then it has been possible estimate that, hydrogels absorb about 61 % of initial concentration. All these data were collected thanks to Prof. Maddalena Collini (University of Milano Bicocca, dept. of physics "Giuseppe Occhialini").

Since swelling and absorption processes in hydrogel have the same characteristic time, it may be supposed that drug diffusion is swelling controlled.

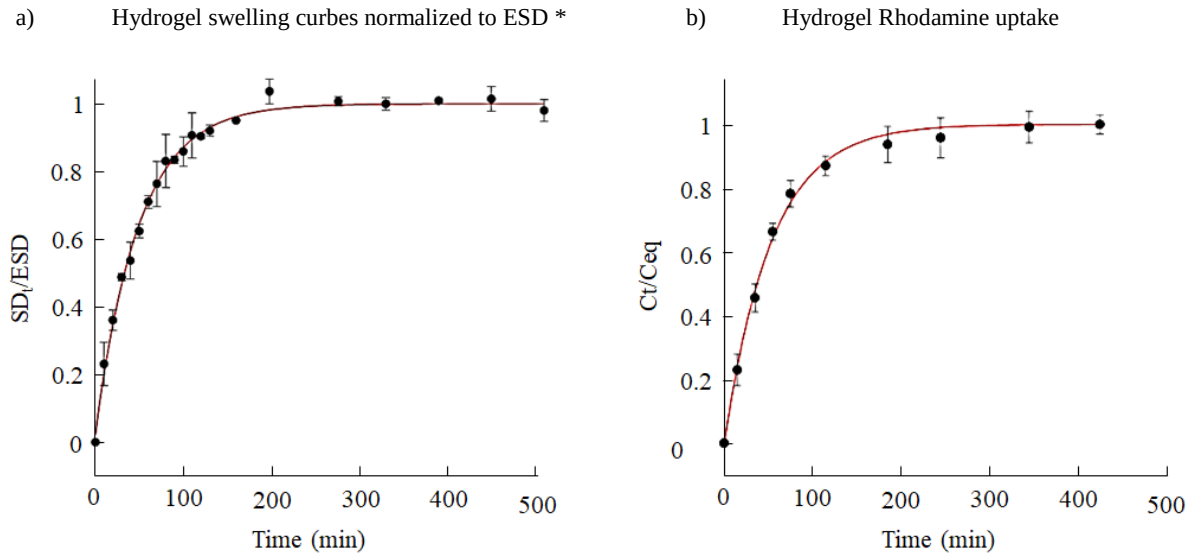

Figure 4.3.9 Dynamic swelling curves of hydrogels (without further treatments, a), and hydrogel rhodamine uptake over the time (b).

The release kinetics is followed by soaking the hydrogel samples, containing rhodamine solution, in water. Also here, we measured the absorbance over the time, changing the water every time. We obtain that hydrogel can release 24 % of the absorbed Rhodamine concentration in less than 36 hours (**figure 4.3.10**).

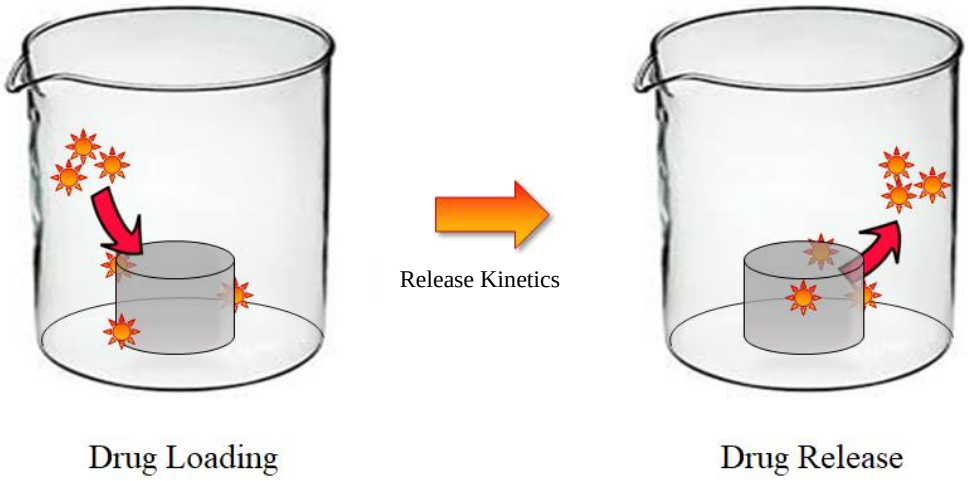

Rhodamine release concentration curves

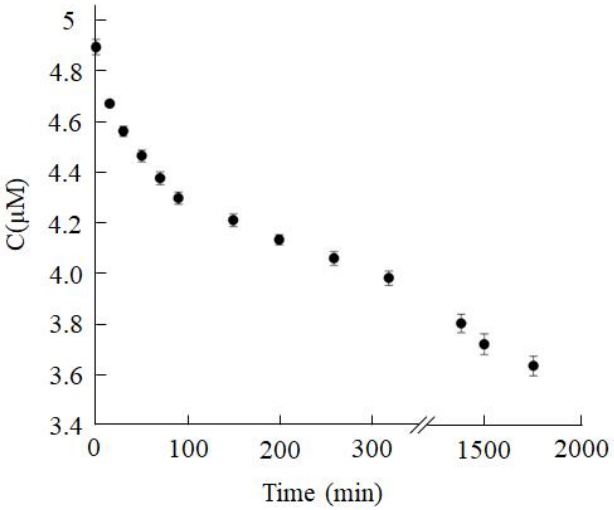

Figure 4.3.10 Up side, schematic figure of drug release kinetics, below rhodamine release concentration curves over the time.

4.3.3. Materials and Methods

General

All chemicals were purchased from Sigma-Aldrich and used without any further purification.
Gelatin from porcine skin is provided by Sigma-Aldrich, catalog no. G2500, CAS Number 9000-70-8. For the drying procedure, a Christ alpha 1–2 freeze dryer (Christ, Osterode am Harz, Germany) was used. All samples were immersed in liquid nitrogen for about an hour before the drying procedure.

Chemistry

10 % hydrogel preparation.

To prepare 10% gelatin based hydrogels, gelatin powder type A (CAS Number 9000-70-8, catalog. N° 2500)) was dissolved in sodium carbonate-bicarbonate buffer (pH 8,5) in 100 mg/mL concentration (2mL) at 40 C°. Then, the crosslinker, 3,4-Diethoxy-3-cyclobutene-1,2-dione (Sigma-Aldrich, CAS Number 5231-87-8) was dripped to solution with a final concentration of 0.016 M (0.032 mmol, 5 µl 0.5 eq., lysine eq. 1). After reaction 2 ml of solution were placed in 24-multiwell, to make a hydrogel mold, then samples were incubated for 90 minutes at 37 °C and then left at room temperature until complete gelation.

5 % hydrogel preparation.

To prepare 5% gelatin hydrogel, an aliquot (1ml) of previous 100 mg/ml gelatin standard solution was prelevated and diluted to reach a final concentration of 50 mg/ml. Then the crosslinker was added as described above (0.008M, 0.0.16 mmol, 2.5) . Also

here, 2 ml of the samples were incubated for 90 minutes at 37 °C and then left at room temperature until complete gelation.

FT-IR spectra.

ATR-FTIR spectra of gelatin specimens were collected with the Varian 670-IR spectrometer, for final dried hydrogel, 3,4-Diethoxy-3-cyclobutene-1,2-dione, 1-Aminopropane and the described reaction products. The instrument was equipped with quest (Specac) ATR device following the parameters indicate in: https://doi.org/10.1016/j.ijbiomac.2016.01.051"

Collagenase assay.

Collagenase assay was performe using *Clostridium histolyticum* collagenase type I(≥125 CDU/mg solid, CAS: 9001-12-1, EC: 3.4.24.3, Sigma-Aldrich). All samples (directly after gelification, without further treatments) were incubated with 1 mL of a solution of Tris-HCl buffer (0.1M, pH 7.4) e $CaCl_2$ (0.05M) at 37 °C for an hour. Then, 1 mL of enzyme solution (0.5 mg/mL in Tris-HCl 0.1M, pH 7.4) was added. All samples were kept at 37 °C and the degradation was followed by gravimetric analysis with analytical balance[289].

Swelling test.

Swelling tests were performed immerging each sample in 40 ml of deionized water at room temperature. over the time (each 15 minutes approximately), the samples were removed from aqueous solvent, quickly dried from surface water using filter paper, weighed on an analytical balance (Analytical Balance 220g x 0.1mg, Radwag AS 220/C/2) and returned to the swelling medium.

Rheometer analysis.

Without further manipulation, hydrogel recovered from reaction were submitted to rheometric analysis. All the analysis were performed using a MCR 52 rheometer (Anton Paar, Graz, Austria). Samples were analyzed with a plate-plate system (5 cm diameter) and a standard thickness of 1 mm. During the analysis were collected viscosity data, in graph it was shown shear rate as a function of viscosity.

(**Eq. 4.3.1**)

$$\text{Shear Stress}(\boldsymbol{\tau}) = \frac{F}{A}$$

F = force applied between the plate (N),

A= cross-sectional area of material (mPa)

(**Eq. 4.3.2**)

$$\text{Shear rate} = \frac{1}{\tau}$$

$$\text{Viscosity} = mPas * S$$

Cell Culture:

For the cells cultures were used Human chondrocytes and Human embryonic kidney cells (**C28/I2** and **HEK293**). Human cartilage cells C28/I2 were cultured in Dulbecco's

modified Eagle's medium/ Ham's F-12 (DMEM/F-12) (BioWest the serum specialist, USA) supplemented with 10% heat-inactivated fetal bovine serum (FBS) (Euroclone spa, Pero, Italy), 100U/mL penicillin, 100 mg/mL streptomycin, 4mM L-glutamine, 17mM of D-glucose (BioWest the serum specialist, USA). C28/I2 cells were maintained at 37°C in a humidified atmosphere with 5% CO_2 in 100 mm Petri dishes. The medium was changed every three days. Cells were cultured in monolayer, grown sub-confluence (80%) and passaged at a ratio of 1:8.

HEK293 cells, were grown and cultivated in 100 mm Petri dishes that contained DMEM supplemented with 10% FBS, antibiotics (100U/mL penicillin, 100mg/mL streptomycin) and 4mM L-glutamine. HEK cells were maintained at 37°C in a humidified atmosphere with 5% CO_2 in 100 mm Petri dishes. The medium was changed every three days. Cells were cultured in monolayer, grown sub-confluence (80%) and passaged at a ratio of 1:8.

Briefly, for cellular inoculation into hydrogels, confluent monolayer cultures of both cell lines were released by Trypsin-EDTA from mother culture and cells were counted and re-suspended in growth medium at a density of 5×10^6 cells/mL.

Cellular inoculation.

Before seeding C28/I2 and HEK293 cell lines, lyophilized hydrogels were sterilized in 75% ethanol for 20 min, followed by 30 min UV irradiation and several washing with 1mL PBS. After sterilization, sponges were equilibrated in 1 mL culture medium (DMEM/F-12 for C28/I2 and DMEM for HEK293) for 12h. All samples were dried by aspiration prior to cell seeding to ensure the removal of remaining ethanol. The dried gelatin hydrogel were placed in each well of a 24-well plate. Each gelatin sponges were seeded with 200 µL of C28/I2 suspension (5×10^6 cells/mL) or HEK293 suspension (5×10^6 cells/mL) and were incubated for 4h at 37°C with 5%CO_2 in a humidified atmosphere to allow cells to attach to the material. Subsequently, 1 mL of culture medium was added in each well. The culture was conducted for 2 weeks, maintained at

37°C in a humidified atmosphere with 5% CO_2 and medium was changed twice a week. Cells were observed daily using an inverted microscope (CK40, Olympus, Tokyo, Japan).

Immunofluorescence.

After two weeks of culture, gelatin sponges containing cells were fixed with PBS-4% paraformaldehyde for 2 h at 4°C and washed twice with PBS. Afterwards, gelatin sponge were cutted into thin slices sections of 300 µm or 250 µm (with 10% gelatin sponges was possible to obtain 100 µm section) using vibratome (VT1000S, Leica, Wetzlar, Germany). The slides were permeabilized with 1mL of 0.1% Triton X-100 in PBS for 15 min, blocked with 1mL of 1%BSA/PBS for 45 min, washed four times with 1%BSA/PBS and stained with 1µL of Phalloidin-TRITC (Sigma-Aldrich, Saint-Louis, Missouri, USA) in 1 ml of 1%BSA/PBS for 1h. After five washing with PBS, DNA was stained using DAPI (Sigma-Aldrich, Saint-Louis, Missouri, USA) and slides were washed four times with PBS. At the end, slides were mounted using Eukitt® quick-hardening mouting medium (Sigma-Aldrich, Saint-Louis, Missouri, USA) and were analyzed using two-photon confocal microscope.

Rhodamine loading study

Fresh Gelified hydrogel (5 %, obtained from 100 mg of substrates) were placed in 3 ml of Rhodamine-6G solution (7 µM) in milliQ water. Every 20 minutes the absorbance of solution were checked in order to estimate the concentration. The measures were performed in accordance with Lambert-Beer law using spectrophotometer. Rhodamine extinction molar coefficient as = 116000 $M^{-1}*cm^{-1}$ and the path length L = 0.2 cm.

The hydrogel sample concentration was reported as normalized data to the equilibrium value of $C_e = 4.5 \pm 0.1$.

Rhodamine release study.

The release kinetics is followed by soaking the hydrogel samples, containing Rhodamine solution, in 3 ml of milliQ water. We measured the absorbance at intervals of 15 minutes, changing the sample water every time at the same condition previously cited (molar extinction, path length). Also here, graph was reported as normalized data to equilibrium value.

4.3.4. Conclusion

In this section we developed new hydrogels using 3,4-Diethoxy-3-cyclobutene-1,2-dione as cross-linking agents specific toward lysine amino groups functionalization. Through its chemical structure, which imply a sort of conjugated system between carbonyl bond and C double bond, it was possible think a way to follow the reaction with FT-IR spectroscopy. As a matter of fact, this spectroscopic technique often doesn't give information about single bond formation (if applied on protein structure) but here, these system appears as a diagnostic tool, by which we can affirm the successful of crosslink. This data was further confirmed by several physico-chemical analyses, such as enzymatic stability toward collagenase or swelling properties, highlighting a series of fine modulating properties, depending on gelatin starting concentration. Increasing this parameter, characteristic porous structure of this systems undergoes a decrease of pores average diameter, as seen by SEM imaging and confirmed by two photon microscopy. Here, hydrogels network can support cell growth just if pores diameter appears compatible with dimension of cells, acting as a filter excluding big cells if compared with pores dimension. Preliminary rheological tests with two parallel plate suggest

changing starting concentration could help to obtain an ECM like structure with similar properties to native ECM if compared.

Regarding future applications, drug release systems represent an alternative. Here it was tested rhodamine release kinetics, highlighting a complete release in less than three days; making this system interesting, although further physical studies are necessary. In conclusion, it’s our opinion that the best result could be collected from these systems based on protein physiologically present in ECM structure, which possess biocompatibility, low cytotoxicity and no adverse effect arising from vivo degradation.

Chapter 5 - Dendrons, dendrimers and multivalency

Another important topic in regenerative medicine is knowing the deepest mechanisms of proteins interactions such as, carbohydrate-lectin interactions, which are based on multivalent interaction. The Affinity between a single glycol-residue and lectin is usually relatively low; to circumvent this issue, nature uses a so called “cluster effect”, in which multiple simultaneous weak interactions, between ligands and their receptors, reinforce one-another, yielding an higher affinity than the sum of the individual interactions.[290] Nowadays, the design of glyco-clusters with high affinity and selectivity for lectins may rely on rational design.[291] In addition lectins mediate several biological processes such as cell–cell communication, molecular recognition and molecular interactions between pathogenic microorganisms and viruses and the surfaces of mammalian cells.[292,293] For these reasons, developing new glycol-functionalized biomaterials is powerful progress in regenerative medicine. However, to make this, first, we had to study the role of carbohydrate as signalling molecule, in particular way the role of multivalent interaction between carbohydrate and lectins. In this context dendrimers and dendrons have been developed to provide multivalent glycoconjugates.[294,295] For over a century, dendrimers and other chemical structure, have been used to understand biochemical mechanisms behind cellular responses, but only last three decades these concepts have been aplicate in material engineering in order to replicate ECM micro-environmental.

5.1. Introduction

The binding events between the cells or cells-environment, as previously mentioned, are the basis of cellular communication, spreading a large informations amount about local or peripheral states. In these cases, the complexity of binding processes increases if multivalent partners are involved, especially when, at this level, the interactions occur also through different mechanisms (see **scheme 5.1**). An example could be represented by homomultimeric lectins, which can interact simultaneously with several ligands, arising from a multi-glycosylated molecule.[296] This mechanism is typical of multimeric lectins (such as AB5 toxins, hemagglutinins), which are membrane anchored proteins, able to interact with glycosylated partners. Furthermore, other mechanisms have been shown to be the base to multivalency. For example, are well known biochemical processes, referred as receptor clustering, in which monovalent lectins can associate on outer side cell membrane, by diffusion across dynamic lipid bilayer. Here, these cluster are tightened by the binding to the multivalent ligand, triggering signalling transduction events.[297,298,299,300] Moreover, an improvement can be caused by multivalent glycosylated structures, interacting with monovalent lectins, through an higher density of available ligands in proximity of the binding sites (statistical re-association).[301]

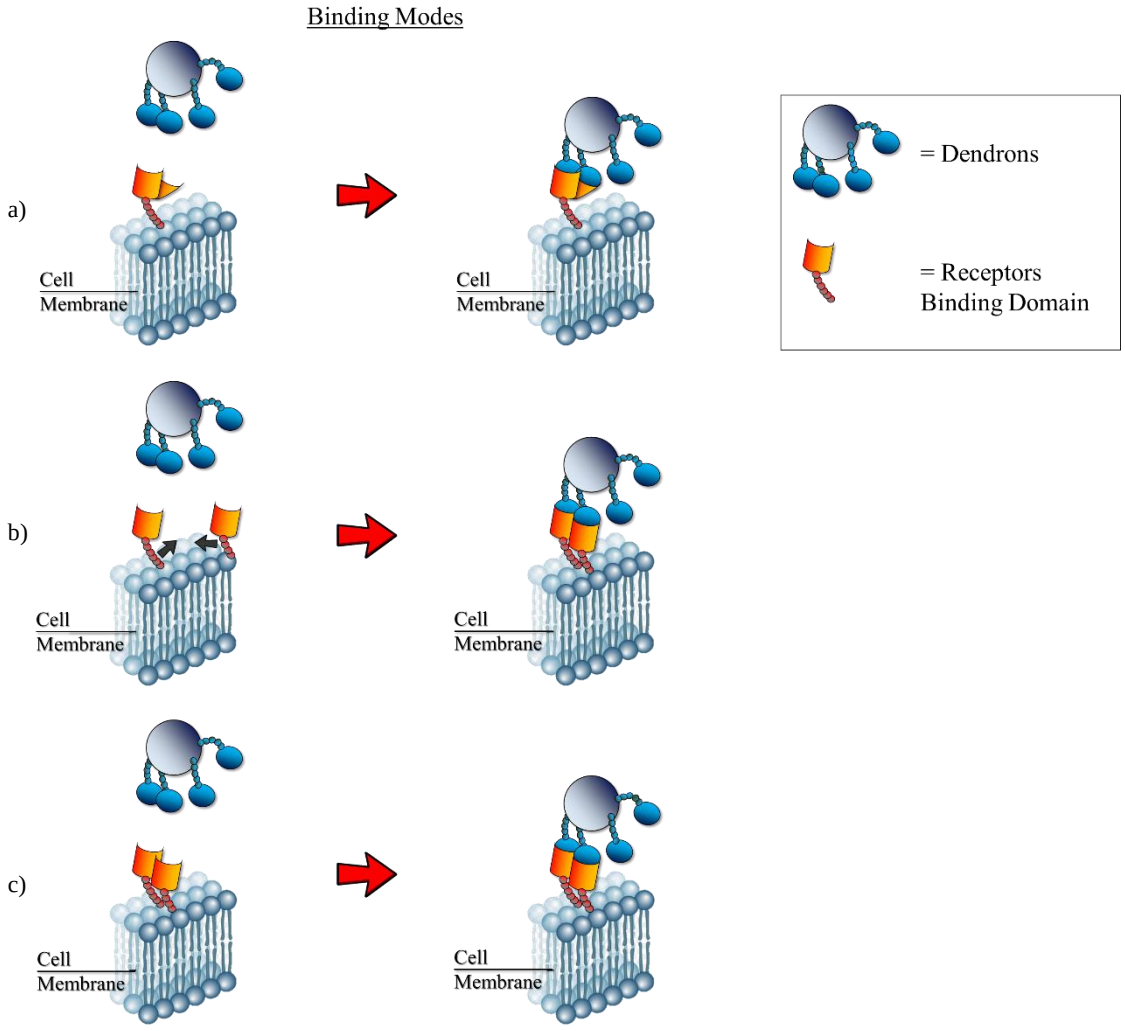

Scheme 5.1 Binding modes engaged by multivalent ligands, a. Multivalent ligands can bind homomultimeric receptors by occupying multiple binding sites, b. causing receptor clustering in the membrane, c. By monovalent lectins through an higher density of available ligands.

For these reasons, hyper-branched structure, has great promise in medicinal chemistry giving the basis of knowledge behind multifactorial binding events, exploring parameters such as density of exposure ligands; which is a necessary requirement to rational design of 2D scaffolds. While on one side, dendrons are defined as hyperbranched structures with a central core (like a “tree”), dendrimers represent an evolution of this structure. In detail are defined as structure with nano-size scale, structurally constituted by a central core covalently linked to repeated monomers,

forming consecutive layers called generations. Each generation expose an elevated number of functional groups on the surface, giving interactions with different kinds of biomolecules. Two main approaches can be followed in order to synthesize dendrimeric structures, often referred as convergent or divergent approaches. On one hand, convergent approach is based on synthesizing dendron monomers and then linking them on central core structure.[302] On other hand, divergent approach is focused on developing, first "the central core", proceeding towards the branches via step by step addition of suitably protected monomers.[303] Moreover, this strategy allows more strict control over dendrimer structures and their physical and chemical properties. Up to now, a wide variety of different cores and building blocks are used in dendrimers development, so this several subfamilies are defined with the aim to explore possibilities offered by organic chemistry, ranging from monodisperse dendrons and dendrimers to polydispersed dendrigrafts and dendritic linear hybrids (**Figure 5.1**).[304]

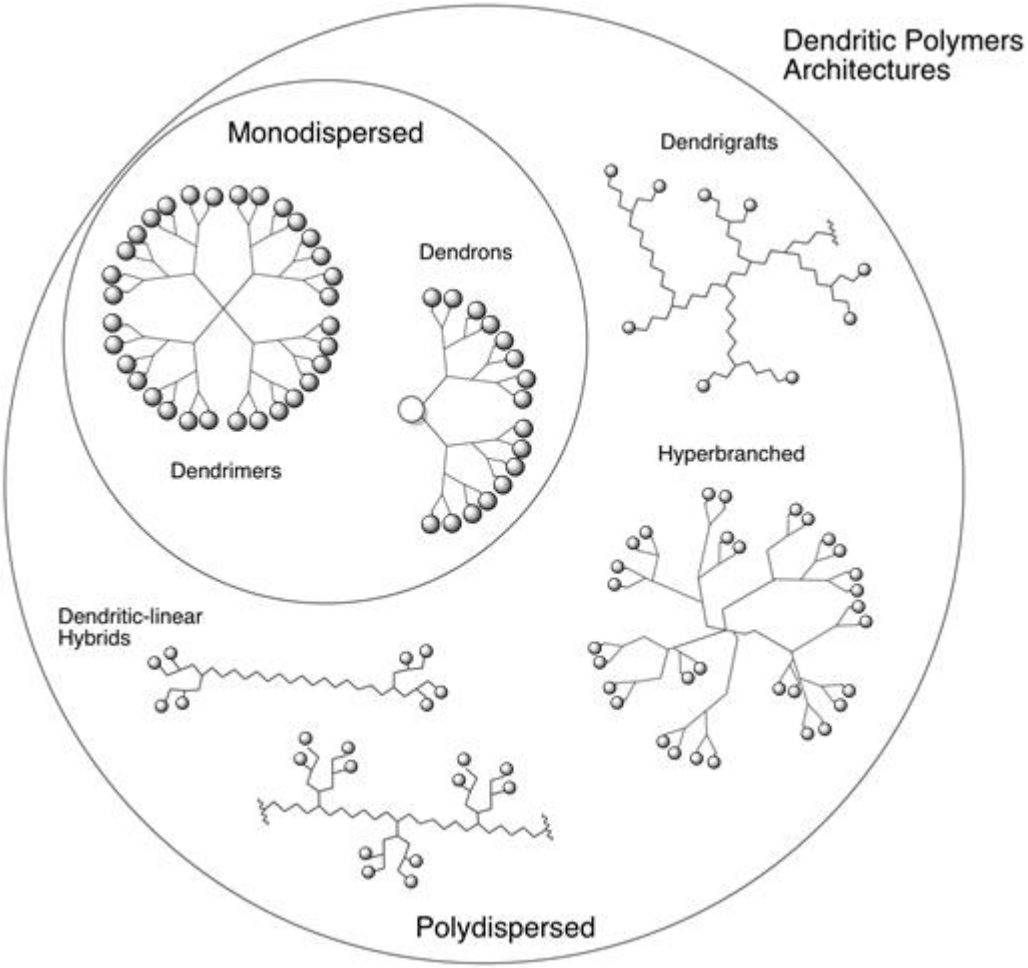

Figure 5.1 General architecture of dendrons, dendrimers and alternative hyperbranched structures.

The multivalent nature of dendrimeric structures represent an ideal scaffold for ligand presentation, moreover, their stability, low immunogenicity, monodispersity (favouring reproducible pharmacokinetics), and high cellular uptake levels (due to efficient cell-membrane permeability), make them excellent tools for biomedical applications, for examples drug and gene delivery.[305]

In the last decades, glycodendrimers are gained more interest as one of the most promising classes of dendrimers for biomedical applications. In fact it was seen that functionalization of hyper-branches dendrimeric structure, significantly involves a lowered cytotoxicity, improved biocompatibility and prolonged their blood half-

life.[306,307,308] Moreover, the glycosylation is one of the most important post translational modification in eukaryotic organism and that is involved in cell-cell interaction, cell-environment interaction and last but not least in self-recognition processes, in addition several proteins of ECM are glycosylated in order to control end promote cellular behaviour. On the other side, glycosyl-profile of cellular surface is a dynamic process and its alterations are indicative of changes in cellular environment and physiology. The biological events in cells and environment interactions, happen through lectin-sugar interaction so that any modification in Glycoprofile (both cellular surface or ECM) can lead different pathophysiological states such as cancer or host-pathogen interactions. The alteration in glycosignature has been associated with malignant transformation, cancer progression, and metastasis is very well documented. For example, in breast cancer cells, extension of O-linked glycosylation of MUC1 protein is defective and aberrant, resulting in increased expression of truncated O-linked glycans, known as T (*â*-D-Gal-[1f3]-D-GalNAc-R-Ser/Thr) and Tn (GalNAc-R-Ser/Thr) antigens.[309] Understanding the roles of glycans involvement and regulation in these pathological processes become increasingly urgent, as matter of fact, they have been shown mediate multiple functions both directly and indirectly, through post-translational modifications of proteins, conjugation of lipids and also as modulators of DNA/RNA activities. Therefore, how these systems explicate their functions are not fully understood and an improvement of that may be essential for basic research, tissue engineering and finally drug design.[310] Many studies have shown that lectins on cell surfaces mediate cell-cell interactions by combining with complementary carbohydrates promoting specific cellular processes such as proliferation, adhesion or differentiation. As seen before the affinity towards their carbohydrate ligands is rather weak so that, in order to increase the efficiency of interaction, different multivalent recognition process take place. For all these reasons, glycodendrimers provide an enhanced molecular recognition system due to the sugar-dependent interactions with lectins;[311,312,313] thus setting themselves as promising tools in the targeting of a variety of pathological states.[314] In addition, dendrimers offer also other therapeutics promises. For example, some scientists suggest that dendrimers of opportunely dimension and functionalization, in some circumstance

of pH or ionic activity, can suffer an important conformational change, assuming a structure like packed globular protein. From this point it has been proposed and discussed the potential of tuning dendrimers to develop macromolecules that can mimic some proteins, triggering then, a specific biochemical response.[315,316,317] This feature brings to many new technological applications in the field of regenerative medicine, for example, if these architectures are able to mimic globular proteins, reasonably, dendrimers may be a valuable tool for the development of synthetic serum-free culture media and adequate substratum for superior cell culturing in order to direct cellular fate. At the level of protein interactions, have been study several stable complex between these "nano-size machines" and proteins suggesting that both the structures and functions may be similar to native and original protein.[318,319]

5.2. Glycodendrimers classification

Although the huge backbone structural variety, glycodendrimers can be classified into:

a. carbohydrate-coated (**figure 5.2, a**);

b. carbohydrate-centered (**figure 5.2 b**); and

c. fully carbohydrate based glycodendrimers [320] (**figure 5.2 c**)

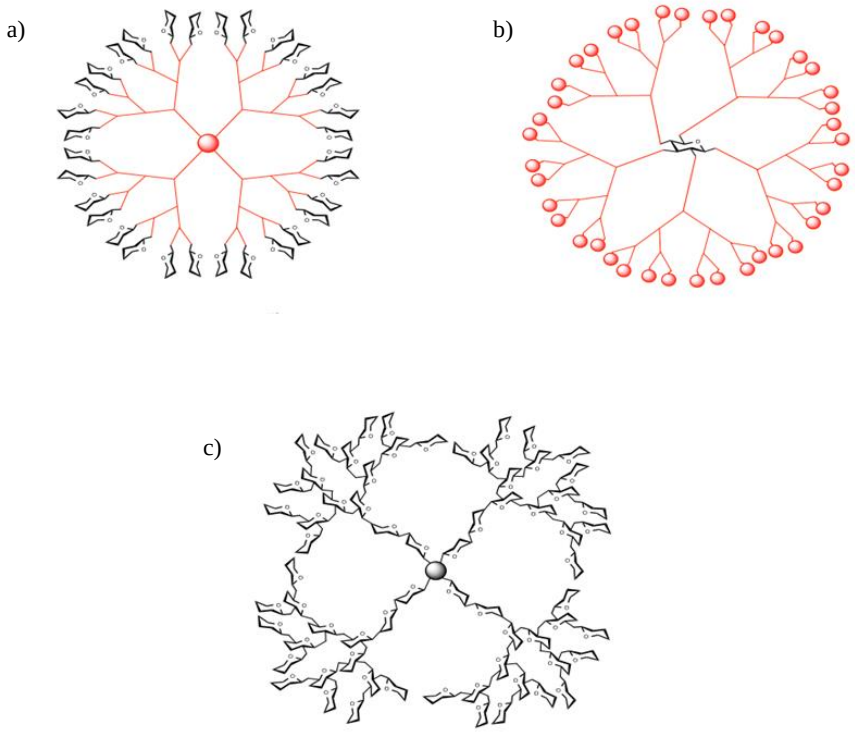

Figure 5.2 General subdivisions of glycodendrimers.

Among these subfamilies, there are wide range of possible hybrid structure, such as:

- Carbohydrate-coated glycodendrimers (**figure 5.3, a.**), which are constituted by non-saccharide central cores and linkers (i.e. polyamidoamine, PAMAM; poly(propylene)imine, PPI; poly(ethylene)imine, PEI; 2,2-bis-(hydroxymethyl)-propionic acid, bis-MPA or various aromatic scaffolds) functionalized with sugar moieties linked to peripheral functional groups.

- Carbohydrate-centered glycodendrimers (**figure 5.3, b.**), with a saccharide core, in which hydroxyl groups are exploited for functionalization with organic linkers to achieve a multivalent exposure of other sugars.

- Fully carbohydrate-based glycodendrimers concept (**figure 5.3, c.**), was inspired by the vast degree of structural diversity than can be achieved by natural polysaccharides, considering the variety of building blocks, the inherent

stereochemistry and regiochemistry of glycosidic linkages and the possibility of ramification through the polymer.

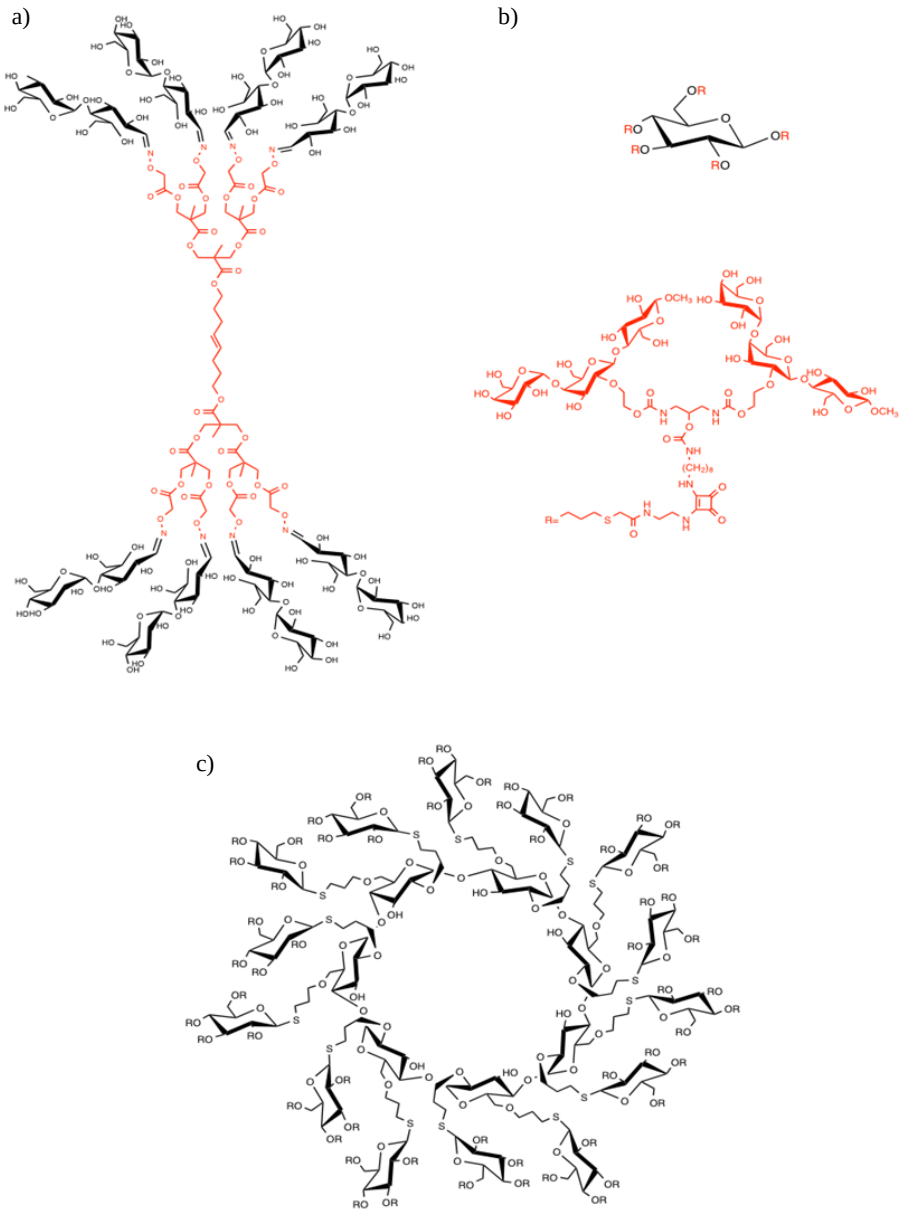

Figure 5.3 some examples of Glycodendrimers.

In this scenario, glycosylation appears to be first choice to create carbohydrate-based glycodendrimers, however, it is not a simple reaction and often requires extensive protecting group chemistry in order to ensure region- and stereo-selectivity.[321,322] To

overcome glycosylation troubles, introduction of unique functional groups in the monomers, such as peptides, has been proposed to allow other kinds of coupling, as in the case of glycopeptidodentrons synthesized by Sadalpure and Lindhorst, in which carbohydrate and dendrimer chemistries have been combined in order to design multivalent glycoconjugate mimetics (**figure 5.4**) In this case, the structure combine the binding properties, influencing, potentially, carbohydrate- protein interaction.[323]

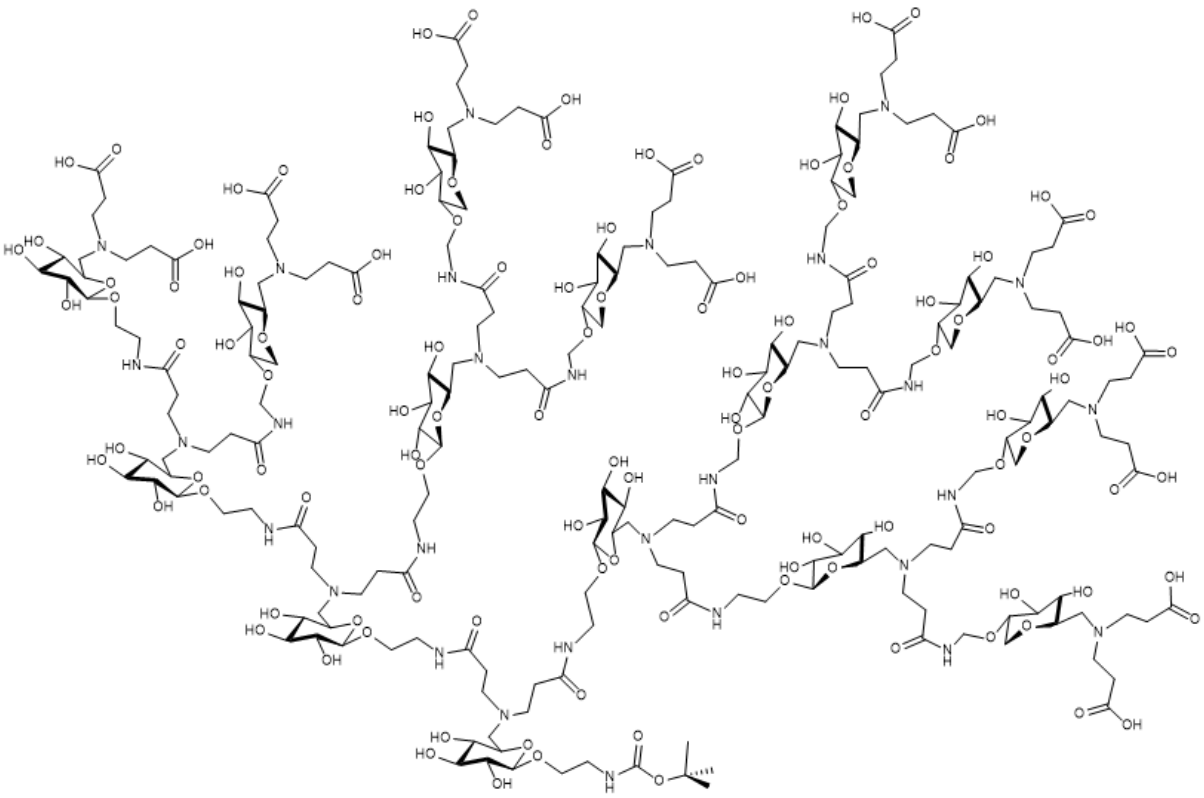

Figure. 5.4 An example of glyco-peptide dendrons (by *Chem. Int. Ed*. **2000**, 2010-2013)

Further, another different strategy to develop fully carbohydrate based dendrimers via click chemistry, could be Thiol-ene coupling. In this case thiol-ene is used to obtain interesting architectures (**figure 5.5 a**).[324] Alternatively, reductive amination, has also been used to give glycoconjugation, here, amine functions were used as substrate for reductive amination with other two saccharides derivatives producing glycoconjugates.

In this way, is possible synthesize an oligosaccharide-based glycodendron with reduced use of protecting groups with a controlled stereochemistry of anomerics bonds.[325,326] in fact, this strategy ensures a chemoselective exposure of glycosyl epitopes (**figure 5.5 b)**.

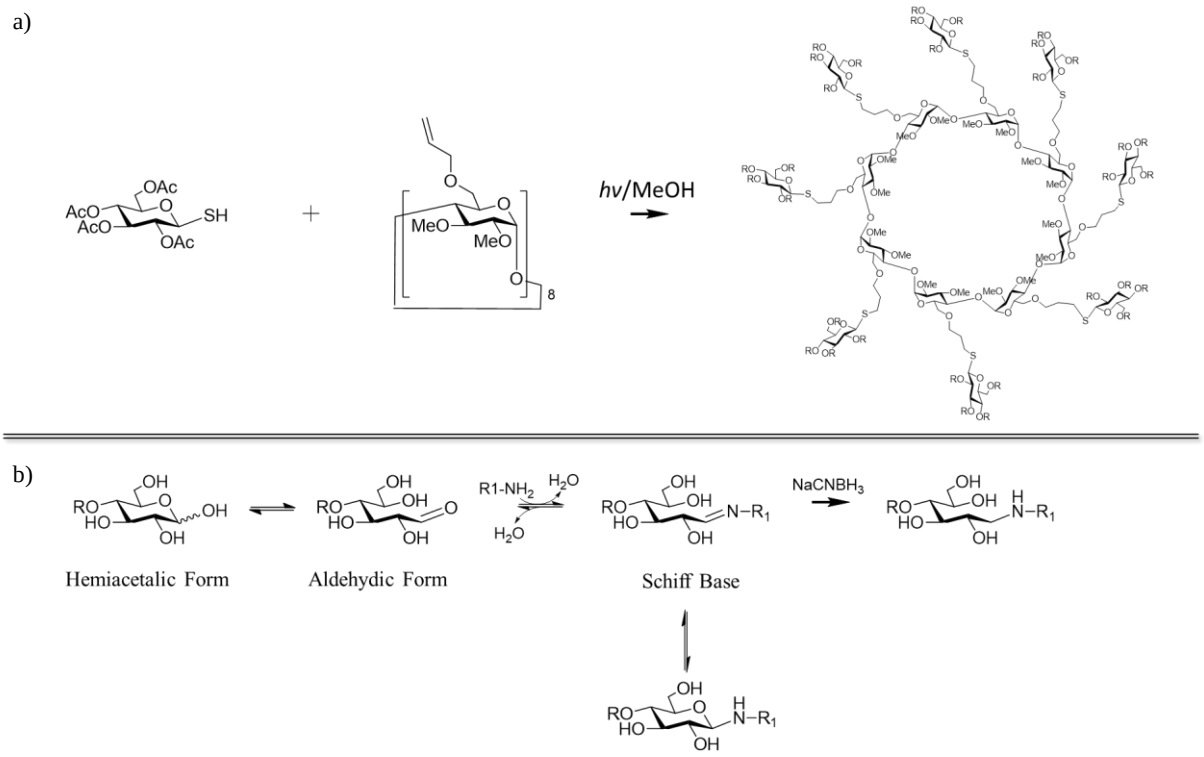

Figure. 5.5 In a. an example of applications of Thiol-ene chemistry (*Org. Lett.*, **2000**, 1113-1116), in b. a supposed mechanism for reductive amination.

In addition, the stereochemistry of this structure could also be modified substituting maltosyl units, for example, with cellobiose; changing, in this manner, anomeric configuration of the terminal glucose from α to β, or with others saccharides of biological relevance to broaden their interactions spectrum. All this in order to study the relevance of anomeric bond stereochemistry in biological field, also, developing where possible, power to pharmaceutical tools in the regenerative medicine.

5.3. Aim of the work

Given their peculiar structure and properties, dendrimers have been proposed for a variety of applications in the biomedical field [327,328,329,330] (i.e., for drug and gene delivery, anti-cancer agents, magnetic resonance imaging contrast agents, photodynamic therapy, biosensors) or as scaffolds for light harvesting, emission, and amplification.[331, 332]. However, as previously mentioned, working with carbohydrate often requires extensive protecting groups chemistry in order to ensure regio- and stereoselectivity of the last glycopeptiopes linked; here, we propose the synthesis of novel oxime-armed dendrimers structures which allow for the multivalent conjugation of carbohydrates in order to ensure a correct glyco-epitopes exposition. The dendrons architectures has been synthesized using cross-metathesis for focal point coupling, it was possible obtain dendrimer like structure.[333] On the other hand, maltose has been exploited as functionality for oxime coupling; as strategic way to ensure a correct alpha-glycoepitopes exposition. Hypothetically these structure could drive biological response modulating interaction events between lectin and appropriate sugar epitopes.

5.4. Results and discussion

As reported in literature, dendritic structures based on polyester structures, such as bis-MPA, are biocompatible, non-immunogenic, biodegradable, and bioproducts are not toxic, thus eligible as promising scaffolds for a wide collection of biomedical applications.[334,335,336,337] Moreover, these branched structures may provide good benefits to biomedical and tissue engineering applications, where high density of ligand exposure and spatial topographical presentation are crucial to bring desired biological

effects.[338,339,340] Here, carbohydrates represents one of the major biomolecules involved in the immune response, in cellular recognition, and in cellular adhesions.[341,342]

During my phD course, new methodology for the synthesis of multivalent glycodendrimers has been performed using a metathesis reaction with Hoveyda–Grubbs as second generation catalyst. In this way, by dendrons dimerization has been possible obtain several final structures with high branching degree. The terminal ends have been with aminoxy groups, which can be exploited for glyco-conjugation of unprotected sugars. In detail the final structures were synthesized starting from building block in **scheme 5.1**, obtaining respectively G1, G2 and G3 dendrons, with a double bond at the focal point and multiple alkoxy-amino termini.

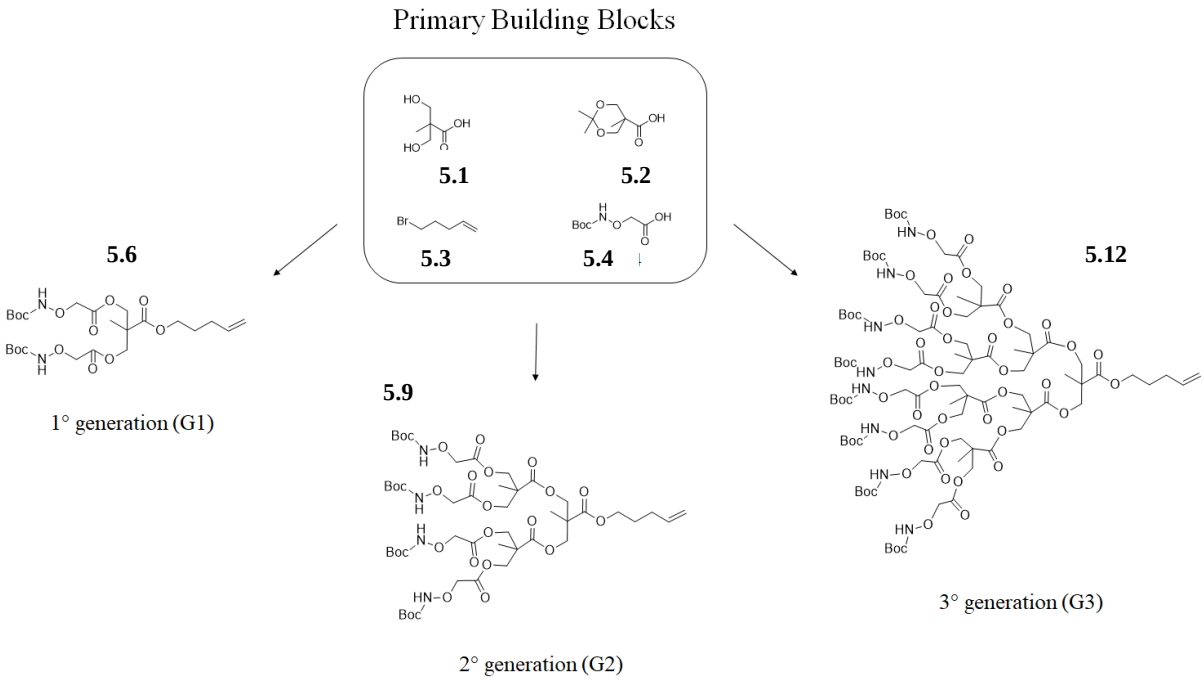

Scheme 5.1 Building Blocks 5.1, 5.2, 5.3, 5.4 for the synthesis of dendrons bivalent 5.6, tetravale 5.9, octavalent 5.12

First, second and third generation of heterobifunctional dendrons (compounds **5.6**-**5.9**-**5.12**) were synthesized starting from (Boc-aminooxy) acetic acid (compound **5.4**) and selected building blocks (compounds **5.1**-**5.2**-**5.3**, **Scheme 5.1**) through esterification and protection/deprotection steps (**Scheme 5.2**); in accordance as already reported.[343,344] The reaction of 2,2-Bis(hydroxymethyl)propionic acid (compound **5.1**) with 5-Br-pentene (compound **5.3**), in the presence of Cs_2CO_3, afforded compound **5.5**, which was coupled with (Boc-aminoxy) acetic acid in presence of DPTS (4-(dimethylamino)pyridinium p-toluenesulfonate) and DCC, giving compound **5.6** (40% overall yield). To obtain G2 dendron (**5.9**), compound **5.5** was reacted with protected Bis-MPA (compound **5.2**) in the presence of DPTS and DCC to promote coupling reaction giving compound **5.7**. After deprotection of **5.7** in acidic condition (to give **5.8**) a further coupling reaction was performed with the same condition seen previously to give **5.9** with 21% overall yield.

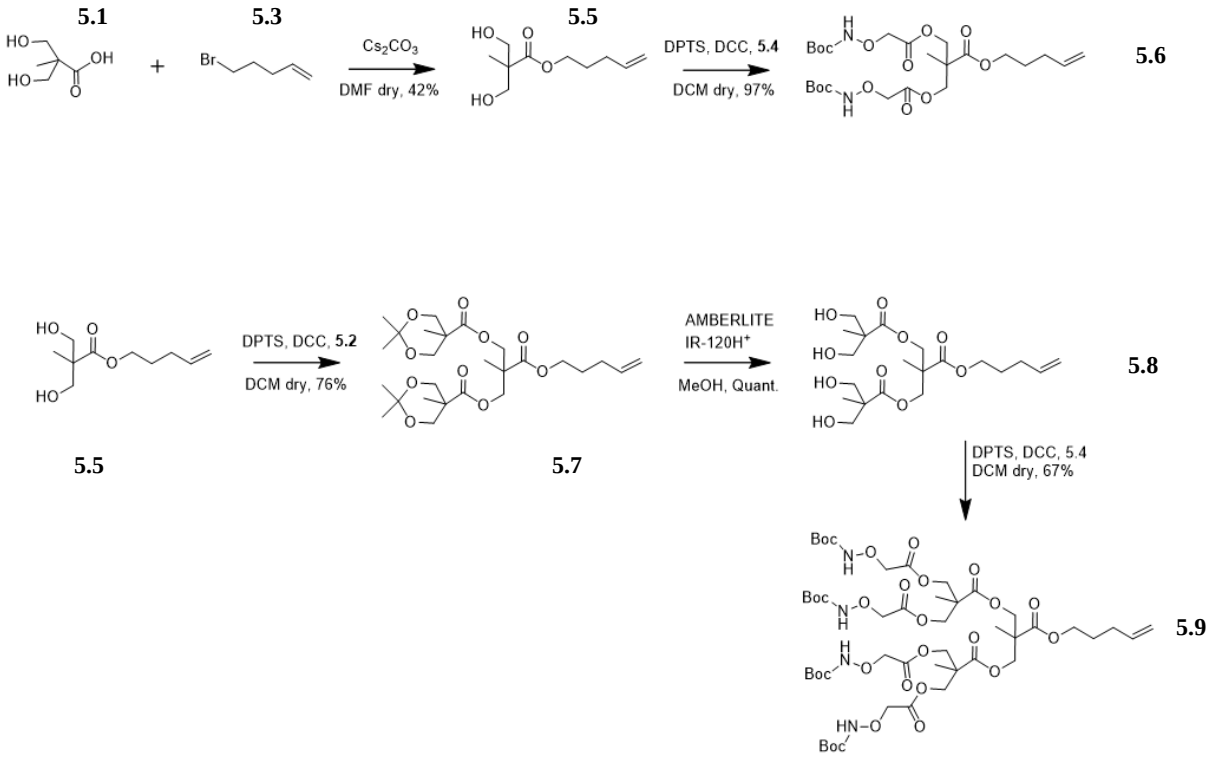

Scheme 5.2 Synthesis of dendrons **5.6** and **5.9**.

With the same strategy seen for the synthesis of dendrons **5.6** and **5.9**, was synthesized also third generation dendrons. In this case we started by compound **5.8** and after coupling and sequential deprotecting strategies we obtained also compound **5.12** (scheme **5.3**, 0.13% overall yield).

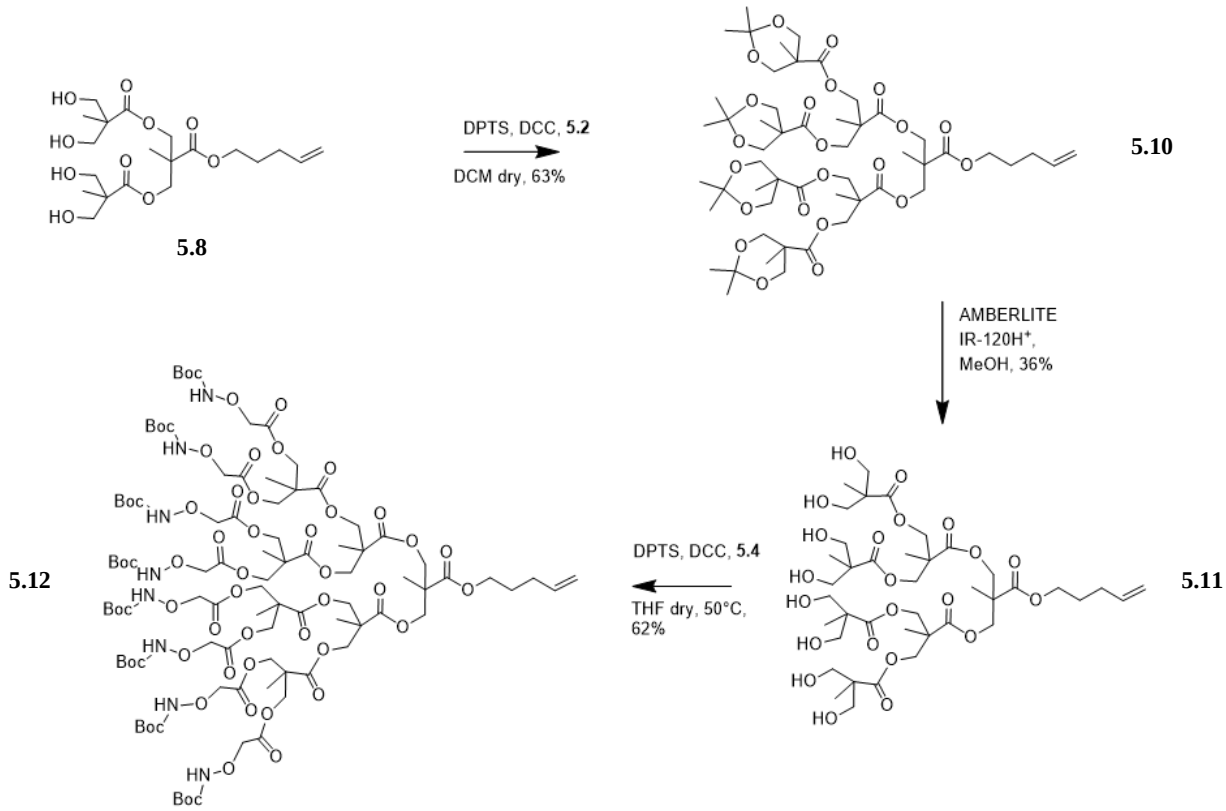

Scheme 5.3 Synthesis of dendrons **5.12**.

Subsequently, Dendrimers **5.13** and **5.16** were synthesized exploiting terminal double bond from dendrons **5.6** and **5.9**, by described metathesis reaction, using octafluorotoluene as solvent, because it permits a faster and more efficient reaction by boosting the activity of the catalyst.[345] Then, dendrimers **5.13** and **5.16** were reacted with trifluoroacetic acid to remove t-butoxycarbonyl (Boc) protecting groups, giving

dendrimers **5.14** and **5.17**. Then, it was demonstrated the efficacy of the metathesis reaction by synthesis of hexadeca-valent dendrimer **5.19** (**Scheme 5.4**) with the same procedure.

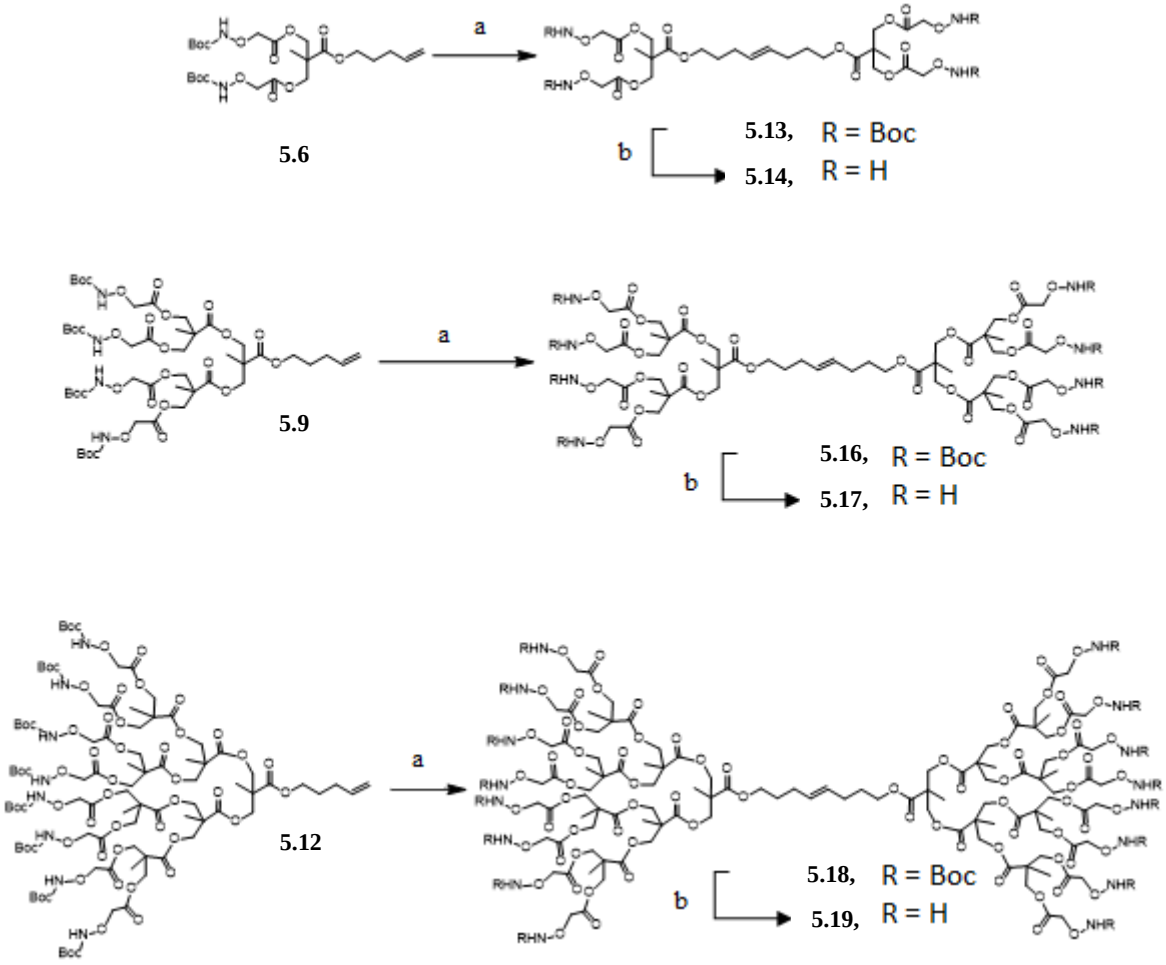

Scheme 5.4. Reaction conditions: (a) Hoveyda–Grubbs second generation, octafluorotoluene; (b) TFA 30%, dry DCM;

Now, glyco-conjugation were performed exploiting aminoxy arm (compound **5.14** and **5.17, scheme 5.4)** by reaction with maltose, as sample saccharide. In this case Aniline

were used as catalyst in acetate buffer at pH 4.5 yielding glycodendrimers **5.20** and **5.21** exposing multiple sugar moieties at their ends, potentially capable of eliciting a biological response in a biochemical context.

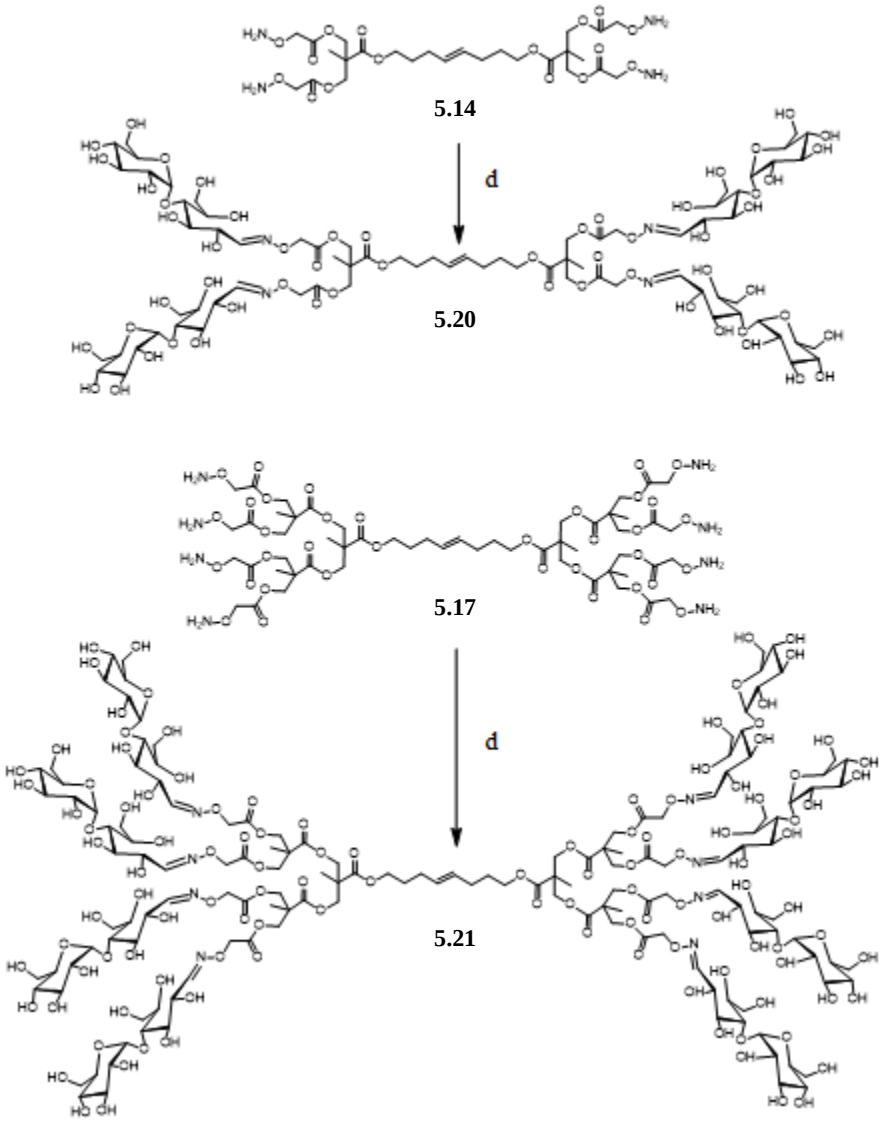

Scheme 5.5. glycoconjugation step to give products **5.20** and **5.21**, (d aniline in buffer solutions pH 4.5, for detail see experimental section).

The use of aniline for the aminoxy-carbonyl coupling allows the equilibrium to shift from the stable carbohydrate cyclic hemiacetal form towards a more reactive open chain

intermediate,[346] which can now react with aminoxy groups (proposed mechanism in scheme **5.6**).

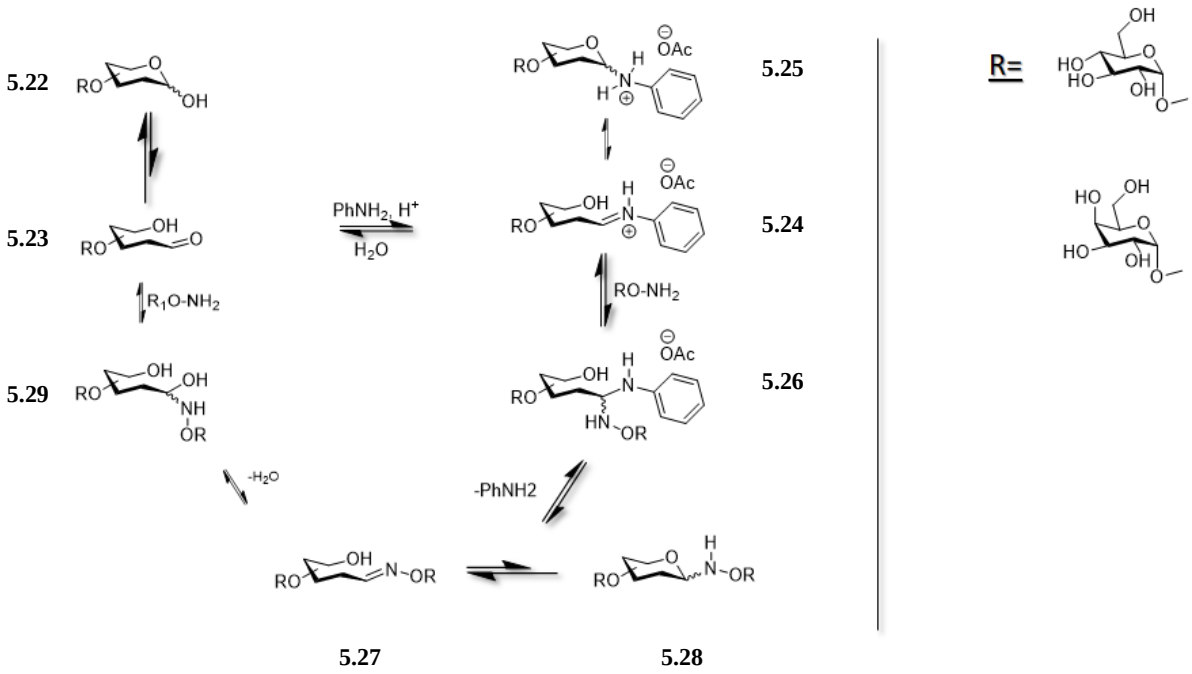

Scheme 5.6 Proposed main reaction pathways of nucleophilic catalysis of carbohydrate oxime Formation at pH 4-5. $R_1O\text{-}NH_2$ could represents a schematic view of alcoxy-amino arms of structure **5.14-5.17**.

In more detail, as suggested in carbohydrates chemistry, carbonyl coupling suffers additional equilibria due to the dynamic masking of the reactive aldehydic tautomer **5.23** as cyclic hemiacetals **5.22**(Scheme **5.6**; >99.9%). Moreover, in the presence of aniline, the trapping of iminium ions **5.25** as (protonated) glycosyl and amine **5.24** involves potentially further rate-limiting intermediates.[347,348] However it was also demonstrated an high reactivity by imine intermediates **5.26** toward carbonyl addition product **5.27.** These contradictory evidences are thought to be largely a result of the ease of protonation of these species relative to the carbonyl species, where subsequent elimination of aniline is fast.[349,350] Maltose, once exposed on the dendrimers, will

presents an alpha-glucoside epitope, which is a fundamental signalling moiety in a variety of biochemical interactions[351,352].

All compounds have been analysed by NMR spectroscopy and MS spectrometry. However, since the complexity of the dendrimeric structure increases, spectra show a high degree of overlapping signals. Nevertheless, most significant peaks have been identified. Glycosylated structures **5.20** and **5.21** (see **figure 5.7**), show complex NMR spectra, probably due to highly crowded pattern of signals belonging to the sugars and possible E/Z isomer of oxime bonds (**figure 5.7**). In addition, also, amphipathic nature of these molecules could give some problems in NMR spectra analysis. For the same reasons, since glycosylation proceeds in aqueous media, dendrimers may tend to aggregate into micellar structures, masking hydrophobic backbone. Regarding glycodendrimers **5.20**, ^{1}H-NMR spectra shows the oxime and double-bond signals with relative integral of 4:2 (**figure 5.7**, on the left), as expected from the presence of four sugar, instead, octavalent dendrimer **5.21**, ^{1}H-NMR spectra shows similar signals but with a ratio between oxime and double-bond signals 7:2(**figure 5.7**, on the right), suggesting a partial glycosylation.

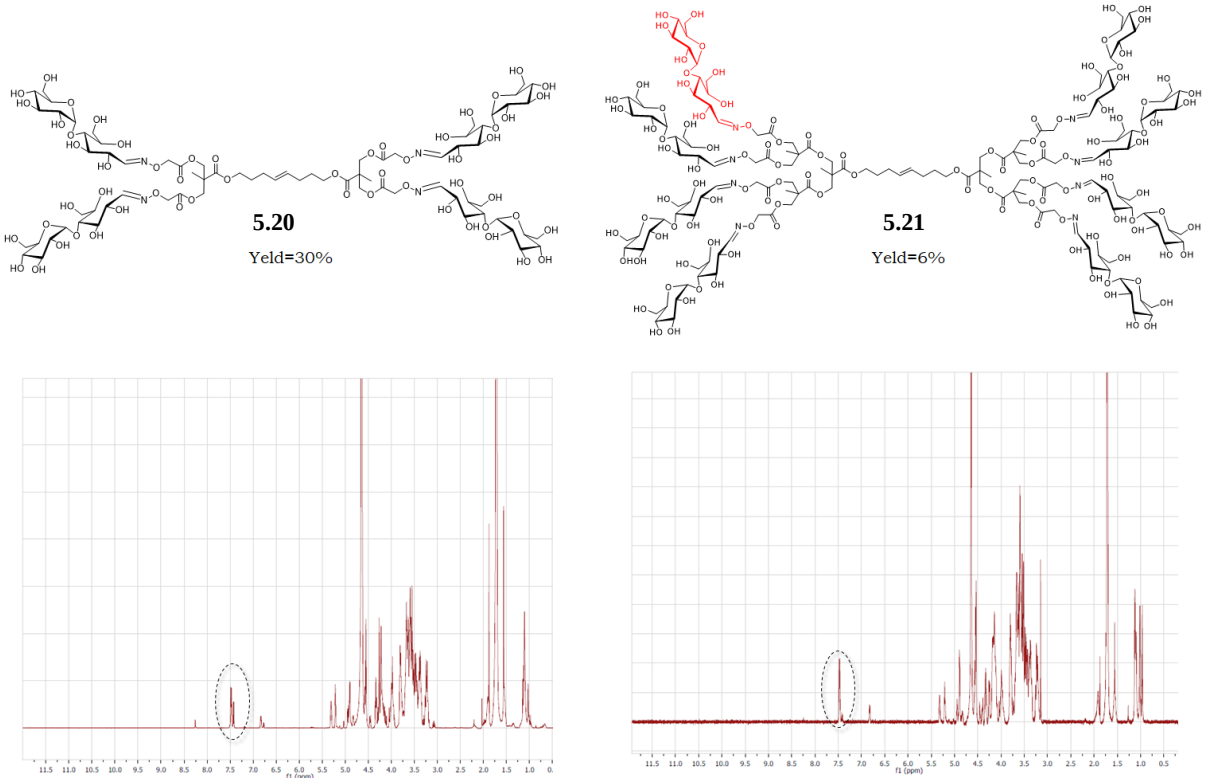

Figure 5.7. Proposed product and respectively NMR spectra, in the circle signals arising from oxime bond. The red glycofunctionality in structure **5.21** represents the lack of last glycoepitope

All data were confirmed by MS analysis. Moreover, in the case of dendrimer **5.21**, MS analysis show a partial degradation deriving from the loss of one, two, or three terminal aminoxyacetic groups.

Considering hexadeca dendrimer **5.19** (**figure 5.8**), NMR spectra are much more complicated than the others, due to the high complexity of its structure; however, ^{1}H-NMR spectrum displays the expected double bond signals and a peak corresponding to the doubly sodiated molecule (m/z = 2292) has been detected in the MS spectrum, thus confirming the presence of the product.

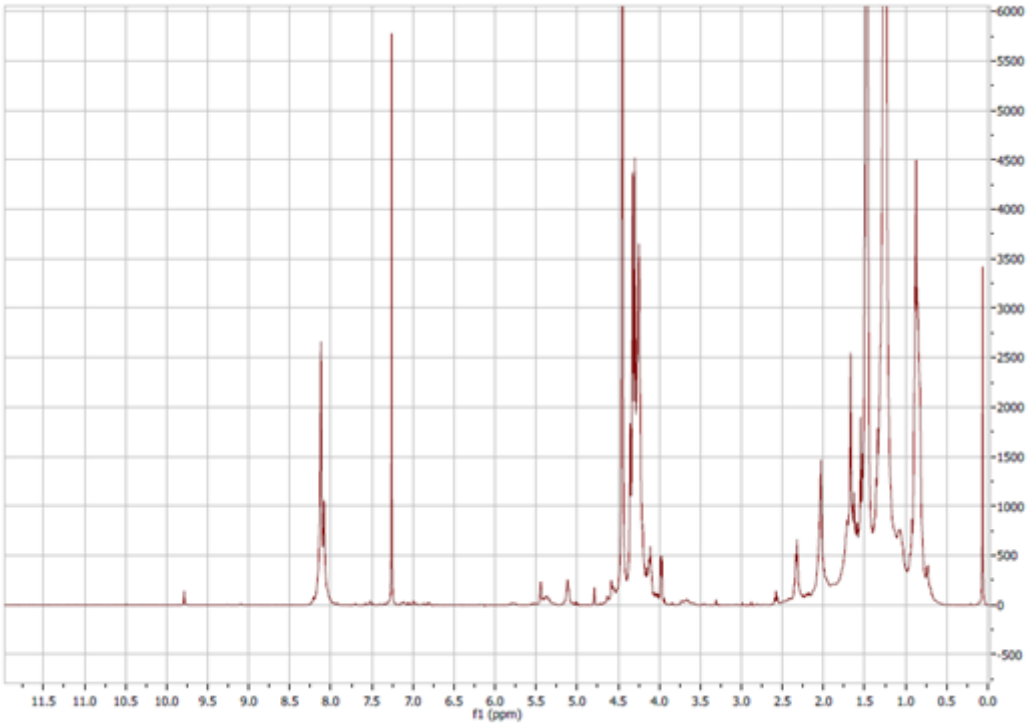

Scheme 5.8. NMR spectra of compound **5.19**

5.5. Materials and Methods

Reactions were monitored by thin-layer chromatography (TLC) on silica gel 60-F254 coated glass plates (Merck). The spots were visualized by charring with a concentrated H_2SO_4(18 M)/EtOH/H_2O solution (10/45/45 v/v/v) or with a solution of $(NH_4)_6Mo_7O_{24}$ (21 g), $Ce(SO_4)_2$ (1 g), concentrated H_2SO_4 (18 M, 31 mL) in water (500 mL) and then by heating to 110 °C for 5 min. Flash column chromatography was performed on silica gel 230–400 mesh (Merck). Routine ^{1}H and ^{13}C NMR spectra were recorded on a Varian Mercury instrument at 400 MHz (1H NMR) or 100.57 MHz (13C NMR). Chemical shifts are reported in parts per million downfield from TMS as an internal

standard; *J* values are given in Hertz. Mass spectra were recorded on a QSTAR Elite instrument (AB Sciex) equipped with a nano-electrospray ion source. The samples were directly injected at room temperature by borosilicate capillaries (Thermo Scientific) employing a spray voltage of 1.1 kV and a declustering potential of 80 V.

*General procedure for Synthesis of **5.6**, **5.19**, **5.12**.*

To obtain several progressive families of protected dendrons figure **5.1**, sequential condensation reactions were performed following modified literature procedures starting from 2,2,5-trimethyl-1,3-dioxane-5- carboxylic acid as a building block through sequential condensation steps (DCC, PPT 0.04 equiv., dry DCM 0.1 mol/L, room temperature) and deprotection. Products were purified by flash chromatography column and obtained in 20%–40% yields using a mixture of petroleum ether and EtOAc as eluent. All reagents were purchased from Sigma-Aldrich and used without any further purification.

*Pent-4-en-1-yl 3-hydroxy-2-(hydroxymethyl)-2-methylpropanoate (**5.5**)*

Bis-MPA 1 (2.0 g, 14.9 mmol) and Cs_2CO_3 (5.54 g, 17.0 mmol) were dissolved in anhydrous DMF (11.2 mL) and heated at 100 °C in oil bath for 2 h. 5-Bromo-1-pentene 3 (2.2 mL, 17.9 mmol) was added; after 15 h at 100 °C, the solvent was evaporated to dryness. The residue was dissolved in 40 mL of EtOAc and washed twice with water. The organic layer was dried over anhydrous Na_2SO_4 and concentrated. The crude product was purified by flash column chromatography (petroleum ether/EtOAc, 25:75) affording pure **5.5** (1.266 g, 6.26 mmol, 42 % yield). 1H NMR (400 MHz, $CDCl_3$): δ = 5.80 (ddt, J = 13.4, 10.1, 6.7 Hz, 1H, $CH=CH_2$), 5.09 – 4.94 (m, 2H, $CH=CH_2$), 4.18 (t, J = 6.5 Hz, 2H, CH_2-O-C=O), 3.90 (d, J = 11.2 Hz, 2H, CH_2-OH), 3.71 (d, J = 11.2 Hz, 2H, CH_2-OH), 2.65 (bs, 2H, -OH), 2.14 (dd, J = 14.1, 7.0 Hz, 2H, CH2-$CH=CH_2$), 1.83 – 1.72 (m, 2H, O-CH_2-CH_2), 1.06 (s, 3H, CH_3). ^{13}C NMR (100.57 MHz, $CDCl_3$): δ =

175.95 (C=O), 137.26 ($CH=CH_2$), 115.49 ($CH=CH_2$), 68.01(CH_2OH), 64.41(CH_2-O-C=O), 49.12 (C-CH_2OH), 29.97 (CH_2-$CH=CH_2$), 27.63 (O-CH_2-CH_2), 17.14 (CH_3). MS (TOF, m/z): [M + Na]+ calcd for $C_{10}H_{18}O_4$, 225.1; found 225.2. $C_{10}H_{18}O_4$ (202.25): calcd. C 59.39, H 8.97; found C 59.45, H 8.99.

*2-Methyl-2-((pent-4-en-1-yloxy)carbonyl)propane-1,3-diyl bis(2-(((tert-butoxycarbonyl)amino)oxy)acetate) (**5.6**)*

(Boc-aminooxy)acetic acid **5.4** (340 mg, 1.78 mmol), **5.5** (150 mg, 0.74 mmol),DMAP (36 mg, 0.30 mmol) and p-toluenesulfonic acid (56 mg, 0.30 mmol) were dissolved in dry CH_2Cl_2 (6.9 mL). DCC (382 mg, 1.85 mmol) was added and the solution was stirred for 48 h at r.t.. The formed precipitate were filtered off and washed with CH_2Cl_2, then the solvent was evaporated, and the residue was purified by flash column chromatography (petroleum ether/EtOAc, 72.5:27.5) to afford pure **5.6** (393 mg, 0.72 mmol, 97 % yield). ^{1}H NMR (400 MHz, $CDCl_3$): δ = 7.92 (s, 2H, NH), 5.74 (ddt, J = 16.9, 10.2, 6.6 Hz, 1H, $CH=CH_2$), 5.04 – 4.92 (m, 2H, $CH=CH_2$), 4.40 (s, 4H, O-CH_2-C=O), 4.34 (d, J = 11.1 Hz, 2H, CH_2O-CO-CH_2), 4.28 (d, J = 11.1 Hz, 2H, CH_2O-CO-CH_2), 4.12 (t, J = 6.5 Hz, 2H, CH_2-CH_2-O- C=O), 2.07 (dd, J = 14.4, 6.9 Hz, 2H, CH_2-$CH=CH_2$), 1.76 – 1.66 (m, 2H, O-CH_2-CH_2), 1.44 (s, 18H, CH_3 Boc), 1.24 (s, 3H, CH_3). 13C NMR (100.57 MHz, $CDCl_3$): δ = 172.33, 169.13, 156.21 (C=O), 136.96 ($CH=CH_2$), 115.63 ($CH=CH_2$), 82.17 (C Boc), 72.32 (O-CH_2-C=O), 65.45 (CH_2O-CO-CH_2), 64.86 (CH_2-CH_2-O-C=O), 46.29 (C-CH_2O-C=O), 29.83 (CH_2-$CH=CH_2$), 28.11 (CH_3 Boc), 27.52 (O-CH_2-CH_2), 17.88 (CH_3). MS (TOF, m/z): [M + Na]+ calcd for $C_{24}H_{40}N_2O_{12}$, 571.3; found 571.4. $C_{24}H_{40}N_2O_{12}$ (548.58): calcd. C 52.55, H 7.35, N 5.11; found C 52.63, H 7.37, N 5.10.

*(E/Z)-((oct-4-ene-1,8-diylbis(oxy))bis(carbonyl))bis(2-methylpropane-3,2,1-triyl) tetrakis(2-(((tert-butoxycarbonyl)amino)oxy)acetate) (Boc-protected tetravalent dendrimer **5.13**.)*

425 mg of compound 5.6 (0.775 mmol), 22 mg of Hoveyda–Grubbs second generation catalyst (4% mol in respect to 1), were dissolved in anhydrous octafluorotoluene (0.1 mol/L). The solution was stirred at room temperature, in the dark, and under argon atmosphere. After 48 h, the solvent was evaporated under vacuum, and then, the crude product was purified by flash chromatography (petroleum ether/EtOAc, 6/4), affording compound 2 (152 mg, 37% yield). ^{1}H NMR (400 MHz, CDCl3) : 7.92 (bs, 4H, NH–O), 5.40 (bs, 2H, CH=CH), 4.43 (s, 8H, NH–O–CH_2), 4.34 (ABq, J = 11.1 Hz, 8H, CO–CH_2), 4.13 (t, J = 6.4 Hz, 4H, CO–CH_2–CH_2), 2.07–1.97 (bs, 4H, CH_2–CH=), 1.74–1.64 (m, 4H, CH_2–CH_2–CH), 1.47 (s, 36H, CH_3(Boc)), 1.27 (s, 6H, CH_3). ^{13}C NMR (101 MHz, $CDCl_3$) : 172.34 (2s, 2COO), 169.15 (4s, 4COO), 156.22 (4s, 4CONH), 129.52 (2d, 2CH=CH), 82.23 (4s, 4C(Boc)), 72.34 (4t, 4NH–O–CH_2), 65.42 (4t, 4COOCH_2C), 64.92 (2t, 2COOCH_2CH_2), 46.30 (2t, 2C($CH_2OCO)_2$), 28.65 (2t, 2CH_2–CH=), 28.33 (2t, 2CH_2–CH_2–CH=), 28.14 (12q, 12CH_3(Boc)), 17.93 (2q, 2CH_3). NanoESI–MS: $C_{46}H_{76}O_{24}N_4$ calcd mass 1068.48, observed m/z = 1069.10 (H+ adduct) and m/z = 1091.10 (Na+ adduct), experimental mass 1068.00.

*(E/Z)-((oct-4-ene-1,8-diylbis(oxy))bis(carbonyl))bis(2-methylpropane-3,2,1-triyl) tetrakis(2-(aminooxy)acetate) (Deprotected tetravalent dendrimer **5.14**)*.

A solution of compound **5.13** (108 mg, 0.101 mmol) in anhydrous dichloromethane (DCM, 0.1 mol/L) was cooled to 0 °C; then, trifluoroacetic acid (TFA) was added dropwise and stirred for 2 h. The reaction was quenched with saturated aq. Na_2CO_3 to neutrality, extracted twice with DCM, and the organic layers were collected and dried over anhydrous Na2SO4. The solvent was evaporated affording product 3 quantitatively (66 mg). The product was used for the subsequent reaction without any further purification. ^{1}H NMR (400 MHz, CDCl3) : 5.81 (bs, 8H, NH2–O), 5.39 (bs, 2H, CH=CH), 4.33 (ABq, J = 11.1 Hz, 8H, CO–CH_2), 4.22 (s, 8H, NH–O–CH_2), 4.11 (t, J = 6.5 Hz, 4H, CO–CH_2–CH_2), 2.11–1.98 (bs, 4H, CH_2–C =), 1.75–1.58 (m, 4H, CH_2–CH_2–CH), 1.24 (s, 6H, CH_3). ^{13}C NMR (101 MHz, CDCl3) : 172.46 (2s, 2COO), 170.30 (4s, 4COO), 129.79 (2d, 2CH=CH), 72.27 (4t, 4NH–O–CH_2), 65.45 (4t, 4COOCH_2C), 64.77 (2t, 2COOCH_2CH_2), 46.31 (2s, 2C(CH2OCO)$_2$), 28.65 (2t, 2CH2–

CH=), 28.17 (2t, $2CH_2$–CH_2–CH=), 17.88 (2q, $2CH_3$). NanoESI–MS: $C_{26}H_{44}O_{16}N_4$ calcd mass 668.27, observed m/z = 669.00 (H+ adduct), experimental mass 668.00.

Tetravalent glycosylated dendrimer ***(5.20)***.

To obtain multifunctional glycosylated dendrimer **5.20**, 25 mg of compound 5.14 (0.037 mmol) were dissolved in 2.5 mL acetate buffer (pH 4.5), and then, maltose (101 mg, 0.296 mmol) and aniline (41 mg, 0.444 mmol) were added. After 72 h, the product was recovered by washing with a small amount of DCM. The aqueous phase was concentrated to dryness and the crude product purified by flash chromatography (gradient eluent from 100% EtOH to EtOH/H20 9/1), affording compound **5.20** (22 mg, 30% yield). ^{1}H NMR (400 MHz, D2O) : 7.48 (d, J = 6.0 Hz, 3H, CH=N), 7.42 (d, J = 6.3 Hz, 1H, CH=N), 5.31 (bs, 2H, CH=CH), 2.11–1.98 (bs, 4H, CH_2-CH). Nano- ESI–MS: $C_{74}H_{124}O_{56}N_4$ calcd mass 1964.70, observed m/z = 1005.35 (2Na+ adduct), experimental mass 1964.70.

2-Methyl-2-((pent-4-en-1-yloxy)carbonyl)propane-1,3-diyl bis(2,2,5-trimethyl-1,3-dioxane-5-carboxylate) ***(5.7)***

5.2 (845 mg, 4.85 mmol), **5.5** (408 mg, 2.02 mmol), DMAP (99 mg, 0.81 mmol) and p-TSOH (154 mg, 0.81 mmol) were dissolved in dry CH_2Cl_2 (19 mL). DCC (1.042 g, 5.05 mmol) was added and the solution was stirred for 24 h at room temperature. The solids were filtered off and washed with a small volume of CH_2Cl_2. The solvent was evaporated, and the residue was purified by flash column chromatography (petroleum ether/EtOAc, 80:20) to afford compound **5.7** (795 mg, 1.54 mmol, 76 % yield). ^{1}H NMR (400 MHz, $CDCl_3$): δ = 5.74 (ddt, J = 16.9, 10.2, 6.6 Hz, 1H, $CH=CH_2$), 5.01 – 4.94 (m, 2H, $CH=CH_2$), 4.29 (s, 4H, CH_2O), 4.12 – 4.09 (m, 6H, CH_2O), 3.58 (d, J = 12.1 Hz, 4H, CH_2O), 2.08 (dd, J = 14.2, 7.0 Hz, 2H, CH_2-$CH=CH_2$), 1.74 – 1.67 (m, 2H, O-CH_2-CH_2), 1.37 (s, 6H, CH_3), 1.32 (s, 6H, CH_3), 1.25 (s, 3H, CH_3), 1.11 (s, 6H, CH_3). ^{13}C NMR (100.57 MHz, $CDCl_3$): δ = 173.53, 172.54 (C=O), 137.12 ($CH=CH_2$), 115.51 ($CH=CH_2$), 98.08 ($C(CH_3)_2$), 65.94, 65.31 (CH_2O), 64.69 (CH_2-CH_2-O-C=O),

46.70, 42.01 (C-CH_2O), 29.94 (CH_2-CH=CH_2), 27.62 (O-CH_2-CH_2), 24.99, 22.19, 18.52, 17.75 (CH_3). MS (TOF, m/z): [M + H]+ calcd for $C_{26}H_{42}O_{10}$, 515.3; found 515.6. $C_{26}H_{42}O_{10}$, (514.61): calcd. C 60.68, H 8.23; found C 60.74, H 8.21.

2-Methyl-2-((pent-4-en-1-yloxy)carbonyl)propane-1,3-diyl bis(3-hydroxy-2-(hydroxymethyl)-2-methylpropanoate) (**5.8**)

Compound **5.7** (772 mg, 1.48 mmol) was dissolved in 10 mL of methanol. Amberlite IR-120 H+ resin (772 mg) was added, and the reaction mixture was stirred for 15 h at room temperature. After completion of the reaction, the resin was filtered off and thoroughly washed with methanol. The methanol was evaporated to give **5.8** (652 mg, 1.48 mmol, quant. yield). ^{1}H NMR (400 MHz, $CDCl_3$): δ = 5.78 (ddt, J =16.9, 10.2, 6.6 Hz, 1H, CH=CH_2), 5.07 – 4.94 (m, 2H, CH=CH2), 4.43 (d, J = 11.1Hz, 2H, CH_2OC=O), 4.25 (d, J = 11.1 Hz, 2H, CH_2OC=O), 4.15 (t, J = 6.6 Hz, 2H,CH_2-CH_2-O-C=O), 3.82 (dd, J = 11.3, 3.0 Hz, 4H, CH_2OH), 3.73 – 3.65 (m, 4H, CH_2OH), 3.24 (bs, 4H, OH), 2.11 (dd, J = 14.5, 6.9 Hz, 2H, CH_2-CH=CH_2), 1.80 – 1.69 (m, 2H, O-CH_2-CH_2), 1.29 (s, 3H, CH_3), 1.04 (s, 6H, CH_3). ^{13}C NMR (100.57 MHz, $CDCl_3$): δ = 174.97, 173.02 (C=O), 137.04 (CH=CH_2), 115.56 (CH=CH_2), 66.41, 64.76 (CH_2O), 49.79, 46.22 (C-CH_2O), 29.87 (CH_2-CH=CH_2), 27.54 (O- CH_2-CH_2), 18.11, 17.07 (CH_3). MS (TOF, m/z): [M + H]+ calcd for $C_{20}H_{34}O_{10}$, 435.2; found 435.4. $C_{20}H_{34}O_{10}$ (434.48): calcd. C 55.29, H 7.89; found C 55.37, H 7.88.

*(((2-Methyl-2-((pent-4-en-1-yloxy)carbonyl)propane-1,3-diyl)bis(oxy))bis(carbonyl))bis(2-methylpropane-2,1,3-triyl) tetrakis(2-(((tert-butoxycarbonyl)amino)oxy)acetate) (**5.9**)*

(Boc-aminooxy)acetic acid **5.4** (450 mg, 2.35 mmol), **5.8** (213 mg, 0.49 mmol), DMAP (48 mg, 0.39 mmol) and p-toluenesulfonic acid (74 mg, 0.39 mmol) were dissolved in dry CH_2Cl_2 (4.5 mL). DCC (505 mg, 2.45 mmol) was added and the solution was stirred

for 24 h at room temperature. The solids were filtered off and washed with a small volume of CH_2Cl_2. The solvent was evaporated, and the residue was purified by flash column chromatography (petroleum ether/EtOAc 10:0→1:9) to give 10 (371 mg, 0.33 mmol, 67 % yield). ^{1}H NMR (400 MHz, $CDCl_3$): δ = 8.00 (s, 4H, NH), 5.76 (ddt, J = 16.8, 10.2, 6.6 Hz, 1H, CH=CH_2), 5.05 – 4.93 (m, 2H, CH=CH_2), 4.41 (s, 8H, O-CH_2-C=O), 4.33 – 4.19 (m, 12H, CH_2OC=O), 4.13 – 4.06 (m, 2H, CH_2-CH_2-O-C=O), 2.08 (dd, J = 14.2, 7.1 Hz, 2H, CH_2-CH=CH_2), 1.76 – 1.66 (m, 2H, O-CH_2-CH_2), 1.44 (s, 36H, CH_3 Boc), 1.22 (s, 9H, CH_3). ^{13}C NMR (100.57 MHz, $CDCl_3$): δ = 171.65, 169.14, 156.30 (C=O), 137.01 (CH=CH_2), 115.61 (CH=CH_2), 82.13 (C Boc), 72.31 (O-CH_2-C=O), 65.62, 65.24, 64.96 (CH_2O), 46.49, 46.40 (C-CH_2O), 29.88 (CH_2-CH=CH_2), 28.12 (CH_3 Boc), 27.55 (O-CH_2-CH_2), 17.81, 17.60 (CH_3). MS (TOF, m/z): [M + Na]+ calcd for $C_{48}H_{78}N_4O_{26}$, 1149.5; found 1149.5. $C_{48}H_{78}N_4O_{26}$ (1127.14): calcd. C 51.15, H 6.98, N 4.97; found C 51.26, H 6.97, N 4.98.

(E/Z)-(4,17-bis((formyloxy)methyl)-4,17-dimethyl-5,16-dioxo-2,6,15,19-tetraoxaicos-10-ene-1,20-dioyl)tetrakis(2-methylpropane-3,2,1-triyl) octakis(2-(((tert-butoxycarbonyl)amino)oxy)acetate) (Boc-protected octavalent dendrimer ***5.16).***

A solution of compound **5.9** (834 mg, 0.740 mmol) and 18 mg Hoveyda–Grubbs second generation catalyst (4% in mol in respect to 5) was prepared in anhydrous octafluorotoluene (0.2 mol/L) and reacted as described for compound **5.13**. After 24 h, the solvent was evaporated by rotary evaporator, and the crude product was purified by flash chromatography (petroleum ether/EtOAc 5/5), affording pure product **5.16** (143 mg, 30% yield calculated on reacted 5) and 350 mg of unreacted **5.5**. ^{1}H NMR (400 MHz, $CDCl_3$) : 8.02 (bs, 8H, NH–O), 5.42 (bs, 2H, CH=CH), 4.44 (s, 16H, NH–O–CH_2), 4.35–4.23 (ABq, J = 11.2 Hz, 24H, CO–CH_2), 4.10 (t, J = 6.4 Hz, 4H, CO–CH_2–CH_2), 2.11–2.00 (bs, 4H, CH_2–CH=), 1.69 (bs, 4H, CH_2–CH_2–CH), 1.47 (s, 72H, CH_3(Boc)), 1.24 (s, 18H, CH_3). ^{13}C NMR (101 MHz, $CDCl_3$) : 171.67 (2s, 2COO), 169.16 (4s, 4COO), 161.63 (8s, 8COO), 156.31(8s, 8CONH), 129.78 (2d, 2CH=CH), 82.17 (8s, 8C(Boc)), 72.34 (8t, 8NH–O–CH_2), 65.60, (4t, 4COOCH_2C), 65.25 (8t,

8CO–CH_2), 65.06 (2t, 2COOCH_2CH_2), 46.51 (2s, 2C(CH_2OCO)2), 46.43 (4s, 4C(CH_2OCO)$_2$), 28.67 (2t, 2CH_2–CH), 28.15 (24q, 24CH_3(Boc), 27.92 (2t, 2CH_2–CH_2–CH), 17.84 (6q, 6CH_3). NanoESI–MS: $C_{94}H_{152}O_{52}N_8$ calcd mass 2224.95, observed m/z = 2247.30 (Na+ adduct), experimental mass 2224.27.

*(E/Z)-(4,17-bis((formyloxy)methyl)-4,17-dimethyl-5,16-dioxo-2,6,15,19-tetraoxaicos-10-ene-1,20-dioyl)tetrakis(2-methylpropane-3,2,1-triyl) octakis(2-(aminooxy)acetate) (Deprotected octavalent dendrimer **5.17**)*.

A solution of 5.16 (210 mg, 0.094 mmol) in dry DCM (0.1 mol/L) was cooled to 0 °C and then TFA was added dropwise and stirred for 2 h at 0 °C. The reaction was quenched with saturated aq. Na_2CO_3 to neutrality, the crude product was extracted twice with DCM, and the organic layers were dried over anhydrous Na_2SO_4. The solvent was evaporated to give compound **5.17** (114 mg, 85% yield) that was used for the subsequent reaction without any further purification. ^{1}H NMR (400 MHz, $CDCl_3$) : 6.22–5.50 (bs, 16H, NH_2–O), 5.42 (bs, 2H, CH=CH), 4.35–4.23 (bs, 32H, NH–O–CH_2, CO–CH_2), 4.17 (8H, CO–CH_2), 4.11 (t, J = 6.5 Hz, 4H, CO–CH_2–CH_2), 2.14–1.98 (bs, 4H, CH_2–CH), 1.75–1.64 (bs, 4H, CH_2–CH_2–CH), 1.25 (s, 18H, CH_3). ^{13}C NMR (101 MHz, $CDCl_3$) : 172.10 (2s, 2COO), 171.84 (4s, 4COO), 170.31 (8s, 8COO), 129.78 (2d, 2CH=CH), 72.25 (8t, 8CO–CH_2), 65.65 (4t, 4CO–CH_2), 65.34 (8t, 8NH–O–CH_2), 64.97 (2t, 2 COOCH_2CH_2), 46.54, 46.46 (6s, 6C(CH_3)$_3$), 28.51 (2t, 2t, 2CH_2–CH=), 28.22 (2t, 2CH_2-CH_2-CH=), 17.79 (6q, 6CH_3). NanoESI–MS: $C_{54}H_{88}O_{36}N_8$ calcd mass 1424.53, observed m/z = 713.50 (2H+ adduct), experimental mass 1425.00.

*Octavalent glycosylated dendrimer (**5.21**).*

First, 81 mg of compound **5.17** (0.057 mmol) were dissolved in 2.5 mL acetate buffer (pH = 4.5); subsequently, 312 mg of maltose and 126 mg aniline (0.912 mmol and 1.36 mmol, respectively) were added and the mixture was allowed to stir. After 72 h, the

reaction was stopped and washed twice with DCM. Finally, crude product was purified through flash chromatography (EtOH + 0.2% AcOH), affording compound **5.21** (13 mg, 6% yield). ^{1}H NMR (400 MHz, D_2O) : 7.47 (d, J = 6.1 Hz, 5H, CH=N), 7.41 (d, J = 6.6 Hz, 1H, CH=N), 5.31 (bs, 2H, CH=CH), 2.11–1.98 (bs, 4H, CH_2–CH). NanoESI–MS: $C_{150}H_{248}O_{116}N_8$ calcd mass 4017.37, observed m/z = 1832.50 (2Na+ adduct, minus one aminoxyacetic moiety, $C_{14}H_{24}O_{12}N$), m/z = 1634.00 (2Na+ adduct, minus two aminoxyacetic moieties) and m/z = 1435.50 (2Na+ adduct, minus three aminoxyacetic moieties), experimental mass 4017.13.

*(((2-methyl-2-((pent-4-en-1-yloxy)carbonyl)propane-1,3-diyl)bis(oxy))bis(carbonyl))bis(2-methylpropane-3,2,1-triyl) tetrakis(2,2,5-trimethyl-1,3-dioxane-5-carboxylate) (**5.10**)*

A solution of **5.8** (400 mg, 2.29 mmol), **5.2** (193 mg, 0.95 mmol), DMAP (47 mg, 0.38 mmol) and p-TSOH (72 mg, 0.38 mmol) were prepared in dry CH_2Cl_2 (9 mL), then DCC (493 g, 2.39 mmol) was added and the solution was stirred for 24 h at room temperature. The solids were filtered off and washed with a small volume of CH_2Cl_2. The solvent was evaporated, and the residue was purified by flash column chromatography (petroleum ether/EtOAc, 80:20) to afford compound **5.10** (376 mg, 0.72 mmol, 76 % yield). ^{1}H NMR (400 MHz, $CDCl_3$): δ = 5.74 (ddt, J = 16.9, 10.2, 6.6 Hz, 1H, $CH=CH_2$), 5.01 – 4.94 (m, 2H, $CH=CH_2$), 4.30 (s, 8H, CH_2O), 4.14 (d, 12H, CH_2O), 3.61 (d, J = 12.1 Hz, 8H, CH_2O), 2.11 (dd, J = 14.2, 7.0 Hz, 2H, CH_2-$CH=CH_2$), 1.75 (dt, 2H, O-CH_2-CH_2), 1.41 (s, 12H, CH_3), 1.32 (s, 12H, CH_3), 1.26 (s, 9H, CH_3), 1.14 (s, 12H, CH_3). ^{13}C NMR (101 MHz, $CDCl_3$) δ 173.92 (s), 172.29 (C=O), 137.56 ($CH=CH_2$), 116.00 ($CH=CH_2$), (m), 66.41, 66.36, (CH_2O),65.35 (CH_2O), 47.29 (s), 47.04 (C-CH_2-O), 42.48 (C-CH_2-O), 34.11 (s), 25.62 (CH_3), 22.48 (CH_3), 18.94 (CH_3), 18.13 (CH_3).

*(((2-methyl-2-((pent-4-en-1-yloxy)carbonyl)propane-1,3-diyl)bis(oxy))bis(carbonyl))bis(2-methylpropane-3,2,1-triyl) tetrakis(3-hydroxy-2-(hydroxymethyl)-2-methylpropanoate) (**5.11**)*

Compound **5.10** (300 mg, 0.57 mmol) was dissolved in 4 mL of methanol. Amberlite IR-120 H+ resin (300 mg) was added, and the reaction mixture was stirred for 15 h at room temperature. After completion of the reaction, the resin was filtered off and thoroughly washed with methanol. The methanol was evaporated to give **5.11**(259 mg, 0.57 mmol, quant. yield). ^{1}H NMR (400 MHz, $CDCl_3$): δ = 5.84 (ddt, J =16.9, 9.9, 6.5 Hz, 1H, $CH=CH_2$), 5.07 – 4.94 (m, 2H, $CH=CH_2$), 4.43 (d, J = 11.1Hz, 12H, $CH_2OC=O$), 4.25-4.20 (d, J = 11.1 Hz, 12H, $CH_2OC=O$), 4.15 (t, J = 6.6 Hz, 2H,CH_2-CH_2-O-C=O), 3.82 (dd, J = 11.3, 3.0 Hz, 4H, CH_2OH), 3.73 – 3.65 (m, 8H, CH_2OH), 3.24 (bs, 8H, OH), 2.11 (dd, J = 14.5, 6.9 Hz, 2H, CH_2-$CH=CH_2$), 1.80 – 1.69 (m, 2H, O-CH_2-CH_2), 1.29 (s, 9H, CH_3), 1.04 (s, 12H, CH_3). ^{13}C NMR (101 MHz, cd_3od) δ 174.44, 172.30 C=O), 137.29 (*C*H=CH_2), 114.44 (CH=*C*H_2), 64.72 (*C*H_2O), 64.63 (CH_2-*C*H_2-C-O-C=O), 64.36 (CH_2OH), 29.75 (*C*H_2-$CH=CH_2$), 27.46 (O-CH_2-*C*H_2), 16.83 (CH_3), 15.88 (CH_3).

*(((2-Methyl-2-((pent-4-en-1-yloxy)carbonyl)propane-1,3-diyl)bis(oxy))bis(carbonyl))bis(2-methylpropane-2,1,3-triyl) tetrakis(2-(((tert-butoxycarbonyl)amino)oxy)acetate) (**5.12**)*

(Boc-aminooxy)acetic acid **5.4** (450 mg, 2.35 mmol), 12 (213 mg, 0.49 mmol), DMAP (48 mg, 0.39 mmol) and p-toluenesulfonic acid (74 mg, 0.39 mmol) were dissolved in dry CH_2Cl_2 (4.5 mL). DCC (505 mg, 2.45 mmol) was added and the solution was stirred for 24 h at room temperature. The solids were filtered off and washed with a small volume of CH_2Cl_2. The solvent was evaporated, and the residue was purified by flash column chromatography (petroleum ether/EtOAc 10:0→1:9) to give 5.12 (371 mg, 0.33 mmol, 67 % yield). ^{1}H NMR (400 MHz, $CDCl_3$): δ = 8.10 (s, 8H, NH), 5.79 (ddt, J = 16.8, 10.2, 6.6 Hz, 1H, $CH=CH_2$), 5.06 – 4.96 (m, 2H, $CH=CH_2$), 4.44 (s, 16H, O-CH_2-

C=O), 4.36 – 4.18 (m, 28H, $CH_2OC=O$), 4.13 – 4.06 (m, 2H, CH_2-CH_2-O-C=O), 2.08 (dd, J = 14.2, 7.1 Hz, 2H, CH_2-CH=CH_2), 1.76 – 1.66 (m, 2H, O-CH_2-CH_2), 1.46 (s, 72H, CH_3 Boc), 1.24 (s, 21H, CH_3). ^{13}C NMR (101 MHz, $CDCl_3$) δ 171.69, 169.20, 156.37 (C=O), 137.09 (*C*H=CH_2), 82.14 (C-Boc), 72.34 (O-CH_2=O),65.25, 65.00 (CH_2O), 46.67, 46.44 (*C*-CH_2O), 29.68 (*C*H_2-CH=CH_2), 28.15 (CH_3-Boc), 17.78, 17.51 (CH_3).

*Boc-protected hexadeca dendrimer **5.18**.*

Compound **5.12** (110 mg, 0.048 mmol) and 2 mg (7% mol in respect to **5.9**) Hoveyda–Grubbs second generation dissolved in anhydrous octafluorotoluene (0.2 mol/L) were reacted as described for compound **5.16**. After 72 h, the solvent was evaporated under vacuum, and then, the crude product was purified by flash chromatography (petroleum ether/EtOAc 4/6) to afford pure **5.18** (34 mg, 31% yield). ^{1}H NMR (400 MHz, $CDCl_3$) : 8.10 (s, 16H, NH–O), 5.44 (bs, 1H, CH=CH), 5.12 (bs, 1H, CH=CH), 4.45 (s, 32H, NH–O–CH_2), 4.31-4.20 (ABq, J = 11.6 Hz, 56H, CO–CH_2), 4.11 (t, J = 6.6 Hz, 4H, CO–CH_2–CH_2), 2.02 (bs, 4H, CH_2–CH), 1.66 (bs, 4H, CH_2–CH_2–CH), 1.47 (s, 144H, CH_3(Boc)), 1.26 (bs, 42H, CH_3). ^{13}C NMR (101 MHz, $CDCl_3$) : 173.54 (2s, 2COO), 171.69 (4s, 4COO), 171.43 (8s, 8COO), 169.22 (16s, 16COO), 156.40, (16s, 16CONH), 82.11 (16s, 16C(Boc)), 72.34 (16t, 16NH–O–CH_2), 65.84, (16t, 16CO–CH_2), 65.26 (12t, 12CO–CH_2), 65.06 (2t, 2COOCH_2CH_2) 46.64, 46.43(14s, 14C($CH_2OCO)_2$), 34.01 (2CH_2–CH), 31.83 (2t, 2CH_2–CH_2–CH), 28.16 (48q, 48CH_3(Boc)), 17.79 (14q, 14CH_3). NanoESI–MS: $C_{190}H_{304}O_{108}N_{16}$ calcd mass 4537.88, observed m/z = 2291.90 (2Na+ adduct), experimental mass 4537.80.

5.6. Conclusion

As discussed above, cell–cell and cell–environment interactions are mediated by protein–carbohydrate recognition processes at the cell surface during the first step of cellular sensing, triggering a wide variety of biological events. In this context carbohydrate represent key elements. This is the reason why, highly branched glycosylated structures, are considered promising tools to enhance these events and further, help us to understand the biological role behind this biomolecule class as signalling molecules or as agonist/antagonists of relevant recognition events (i.e. involving viruses or bacteria). Here, it was presented a novel method for the synthesis of dendrimers, starting from dendrons precursor and, through olefin-metathesis reaction, were synthesized hyperbranched dendrimers structures with central double bond as focal point. During the synthesis of precursor, dendron arms have been equipped with aminooxy functionalities, which were exploited to glycosylations to generate highly branched structures displaying multiple carbohydrate moieties. One of the most interesting features of these structures regard internal double bond, which might be further reduced to the corresponding saturated structure, thus allowing an increase in conformational flexibility, broadening possibilities of fruitful interactions with biological targets. In addition, the length of the hydrocarbon chain can be varied at will (i.e., alkeneterminated linear polymers can be used as the dendron core), allowing an additional degree of structural variation. Moreover, aniline has been used as a stabilizer of glycosyl intermediate for improving dendron glycoconjugation. It should be noted, however, that as the complexity of the structure increases, side reactions may occur, affording partially degraded products, as already reported for this kind of hyperbranched structures.[353]

Final conclusions and general remarks

During my PhD, several biomaterials were developed, analyzed from chemical and physical point of view and tested with biological assay. Several biomaterials were developed, starting from 2D collagen based scaffold toward more complex gelatin based 3D-scaffold with the focus to mimic mechanotransduction stimuli arising from complex networks like ECM s. Regarding 2D scaffolds, signalling peptides, due to their biological relevance, have been considered as excellent candidates for the decoration of these biomaterials, with the aim to study their potential effects on different biological systems. The functionalization with peptides has been achieved using the well-known Thiol-Michael reaction. Bioactivated-collagen patches have been successfully obtained, as demonstrated by their physico-chemical characterizations. Collagen matrices, decorated with HVP and Tβ4 have been employed in different biological assays with several cell-lines. In all cases, collagen matrices have not caused any detrimental effect on cell growth and proliferation. Moreover, based on the peptide conjugated, collagen matrices have been able to modulate adhesion, proliferation or growth factor expression. Functional analysis have highlighted that collagen matrices, decorated with HVP, promote osteoblast in adhesion processes, meanwhile Tβ4 promote human dermal lymphatic epithelial cells to VEGF (vascular growth factor) overexpression, highlighting the key role of this motif in vasculogenesis processes during wound healing. These results reinforce the idea that short signalling peptides represent an important tool of enlightenment for cellular and molecular medicine for tissue repair processes. The same time, another important key feature for tissue engineering and VEGF expression is represented by oxygen perfusion at molecular surface of bio-engineered scaffolds. For these reasons, exploiting scientific knowledge regarding perfluorocarbon (PFC), as oxygen storage systems, and their role in physiological gases perfusion, we projected new, in this way inspired, scaffolds. We functionalized 2D collagen scaffold with fluorinated oxiadiazoles. An important study about best reaction conditions were performed giving desired product. Physical test to evaluate oxygen

concentration on scaffold surface is in due course. At the same time biological assay were programmed.

Subsequently, gelatin-based hydrogels have been synthesized using different synthetic strategies, based on crosslinking agents. On one side tyrosine chemistry has been explored through new synthesized triazolinedions. Hydrogels obtained by this strategy possess mechanical and physical properties hardly applicable in biological world, especially for their poor stability and necessity to work in non aqueous solvent, due to sensibility of triazolinediones toward protic conditions.

Alternatively, hydrogels obtained by lysine crosslinking with 3,4-Diethoxy-3-cyclobutene-1,2-dione, shows interesting mechanical and physical properties. In addition, the reaction occurs in aqueous solvent making them suitable for further biological test. An overall view of mechanical and physical properties such as enzymatic stability, viscosity and swelling ability have provided a good analysis of this 3D scaffoldPreliminary biological tests on two cell lines show average pores diameters represent a fundamental requirement to allow cell growth into network, through cells adhesion on pores wall. Here it has been reinforced the idea that a porous structure with small diameters doesn't allow cell diffusion, contrasting to adhesion processes. Finally, preliminary drug release tests have also been carried on studying rhodamine uptake and release properties, affording preliminary data on the release kinetics of the system.

Finally, new "glyconjugated dendrimers" were synthesized exploiting carbohydrate chemistry and optimizing current chemical strategies regarding carbohydrates conjugation. In particular, exploiting aldehydic groups of reducing-end carbohydrates it was possible develop new dendrimeric like structure presenting alpha anomer glucoses. In literature these structures are well known to interact with protein and other supramolecular structure providing a plethora of hypothetical applications.

References

[1] Zadpoor, A. A.; *Mater. Today* **2013**, 11.16, 408-409.
[2] Cohendet, P.; Ledoux, M.J.; Zuscovitch, E.; *New. Adv. Mater*, Springer, Hidelberg, **1988**; 320-328.
[3] Mao, A.S.; Mooney, D.J.; *PNAS* **2015**, *112*, 14452–14459.
[4] Bianco, P.; Gehron Robey, P.; *Nat.* **2001**, *414*, 118-121.
[5] Heath, C. A.; *Trends Biotechnol*. **2000**, *18*, 17-19.
[6] Ingber, D.E.; *Ann. Biomed. Eng*. **2010**, *38*, 1148–1161.
[7] McMurray, R. J.; Dalby, M. J.; Tsimbouri, P. M. *J.; Tissue Eng. Regen. Med*. **2015**, *9*, 528–539.
[8] Kim, H.N.; Jiao, A.; Hwang, N.S.; Kim, M.S.; Kang, D.H.; Kim, D.H.; Suha, K.Y.; *Adv. Drug Deliver. Rev.* **2013**, *65*, 536–558.
[9] Tibbitt, M.W.; Anseth, K.S.; *Biotechnol. Bioeng*. **2009,** *103*, 655–663.
[10] Kyburz, K.A.; Anseth, K.S.; *Ann. Biomed. Eng*. **2015**, *43*, 489–500.
[11] Hinderer, S; Layland, S.L.; Schenke-Layland, K.; *Adv.Drug Deliv. Rev*. **2016**, *97*, 260-269.
[12] Frantz, C.; Stewart, K.M.; Weaver, V.M. *J. Cell. Sci.* **2010;** *123*; 4195–4200.
[13] Clause, K.C.; Barker, T.H.; *Curr. Opin. Biotech.* **2013**; 24 (2013) 830–833.
[14] Theocharis, A.D.; Gialeli, C.; Hascall, V.C.; Karamanos, N.K.; *Walter de Gruyter GmbH & Co. KG, Berlin/Boston* **2012**, pp. 3–20.
[15] LeBleu, V.S.; Macdonald, B.; Kalluri, R.; *Exp. Biol. Med.* **2007**; *232*; 1121–1129.
[16] Halfter, W.; Oertle, P.; Monnier, C.A.; Camenzind, L.; Reyes-Lua, M.; Hu, H.; Candiello, J.; Labilloy, A.; Balasubramani, M.; Henrich, P.B.; Plodinec, M.; *Febs J.* **2015**, *282.23*, 4466-4479.
[17] Werz, D. B.; Ranzinger, R.; Herget, S.; Adibekian, A.; von der Lieth, C.-W.; Seeberger, P. H. *ACS Chem. Biol.* **2007**, *2*, 685–691.
[18] Ohtsubo, K.; Marth, J. D.; *Cell.* **2006**, *126*, 855–867.
[19] Grayson, W. L.; Martens, T. P.; Eng, G. M.; Radisic, M.; Vunjak-Novakovic, G.; *Seminar in Cell and Development Biology* **2009**, *20*, 665–673.
[20]Yurchenco, PD.; In Yurchenco, P. D.; Birk, D. E.; Mecham, R. P. Extracellular Matrix Assembly and Structure (Yurchenko PD, Birk DE, Mecham RP, eds) **1994**, 281–314.
[21]Mullin, N. P.; Hall, K. T.; Taylor, M. E.; *j. Bio. Chem.* **1994**, *269(45)*, 28405-28413.
[22]Shin, H.; Jo, S.; Mikos, A. G.; *Biomat.* **2003**, *24(24)*, 4353-4364.
[23]Russo, L.; Sgambato, A.; Bini, D.; Calloni, I.; Origgi, D.; Cetin Telli, F.; Cipolla, L.; *Imperial College Press* **2015**, 395-418,ISBN: 978-1-78326-721-7.
[24]Behonick, D. J.; Werb, Z.; *Mech Dev* **2003**, *120*, 1327-1336.
[25]Stevens, M. M.; George, J. H.; *Sci* **2005**, *310*, 1135-1138.
[26] Furth, M.E.; Atala, A.; Van Dyke, M.E.; *Biomat.* **2007**, *28*, 5068-5073.
[27] Engel, E.; Michiardi, A.; Navarro, M.; Lacroix, D.; Planell, J.A.; *Trends Biotechnol* **2007**, *26*, 39-47.
[28]Yang, C.; Hillas, P.J.; Báez, J.A.; Nokelainen, M.; Balan, J.; Tang, J.; Spiro, R.; Polarek, J.W.; *BioDrugs* **2004**, *18*, 103–119.
[29]Londono, R.; Badylak, S.F.; *Ann. Biomed. Eng* **2015**; *43*; 577-592.
[30]Lutolf, M. P.; Hubbell, J. A.; *Nat. Biotechnol.* **2005**; 23; 47–55.
[31]Goddard, J.M.; Hotchkiss, J.H.; *Prog. Polym. Sci.* **2007**; *32*; 698–725.
[32]Amass, W.; Amass, A.; Tighe, B.; *Polym. Int* **1998**; *47*; 89–144.
[33]Vert, M.; Maudit, J.; Ll, S.; *Biomat.* **1994**; *15*; 1209–1213.
[34]Chevalier, J.; Gremillard, L.; *J Eur. Ceram. Soc.* **2009**; *29*; 1245-1255.
[35]Hench, L.L.; *Sci. Mater. Med.* **2006**; *17*; 967–978.
[36]Russo, L.; Landi, E.; Tampieri, A.; Natalello, A.; Doglia, S. M.; Gabrielli, L.; Cipolla, L.; Nicotra, F.; *Carbohyd. Res.* **2011**; *346*; 1564–1568.
[37]Sandri, M.; Natalello, A.; Bini, D.; Gabrielli, L.; Cipolla, L.; Nicotra, F.; *Synlett.* **2011**, *13*, 1845-1848.

[38]Russo, L.; Zanini, S.; Giannoni, P.; Landi, E.; Villa, A.; Sandri, M.; Riccardi, C.; Quarto, R.; Doglia, S.M.; Nicotra, F.; Cipolla, L.; *J. Material Sc.i: Mater. Med.* **2012**, *23*, 2727-2738.
[39]Russo, L.; Taraballi, F.; Lupo, C.; Jiménez-Barbero, J.; Sandri, M.; Tampieri, A.; Nicotra, F.; Cipolla, L.; *RSC Interface Focus* **2014**; *4*; 20130040.
[40]Jones, J.R.; *Acta Biomater.* **2013**; *9*; 4457–4486.
[41]Connell, L. S.; Gabrielli, L.; Mahony, O.; Russo, L.; Cipolla, L.; Jones, J.R.; *Polym. Chem*. **2017**; *8*; 1095-1103.
[42]Gabrielli, L.; Russo, L.; Poveda, A.; Jones, J.R.; Nicotra, F.; Jiménez-Barbero, J.; Cipolla, L.; *Eur. J.* **2013**; *19*; 7856-7864.
[43]Russo, L.; Gabrielli, L.; Valliant, E.M.; Nicotra, F.; Jiménez-Barbero, J.; Cipolla, L.; Jones, J.R.; *J. Mater. Chem. Phys.* **2013**; *140*; 168-175.
[44] Gabrielli, G.; Connell, L.; Russo, L.; Jimenez-Barbero, J.; Nicotra, F.; Jones, J.R.; Cipolla, L.; *RSC Adv.* **2014**; *4*; 1988-1995.
[45] DeForest, C.A.; Polizzotti, B.D.; Anseth, K.S.; *Nat. Mater.* **2009**; *8*; 659–664.
[46] Azagarsamy, M.A.; Anseth, K.S.; *ACS Macro Lett.* **2013**; *2*; 5–9.
[47] Place, E.S.; Evans, N.D.; Stevens, M.M.; *Nat. Mater.* **2009**, *8*, 457-470.
[48]Zhang, Y. H. P.; Myung, S.; You, C.; Zhu, Z.; Rollin, J. A.; *J. Mater. Chem.* **2011**; *21(47)*, 18877-18886.
[49]Langer, K.; Coester, C.; Weber, C.; Von Briesen, H.; Kreuter, J. Eur. J. Pharm. *Biopharm.* **2000**; *49;* 303–307.
[50] Goddard, J. M.; Hotchkiss, J. H.; *Prog. Polym. Sci.* **2007**; *32;* 698-725.
[51] Lutolf, M. P.; *Adv. Mater.* **2003**; *15;* 888-892.
[52] Xu, T.; Zhang, N.; Nichols, H. L.; Shi, D.; Wen, X.; *Mater. Sci. Eng. C.* **2007**, 27, 578.
[53] Zhang, Y.; Moheban, D. B.; Conway, B. R.; Bhattacharyya, A.; Segal, R. A; J. *Neurosci.* **2000**; *20*; 5671–78.
[54] Seliktar, D.; Zisch, A. H.; Lutolf, M. P.; Wrana, J. L.; Hubbel, J. A.; *J. Biomed. Mater. Res. A*. **2004**, *68*, 704–716
[55] Dinbergs, I. D.; Brown, L.; Edelman, E. R.; *J. Biol. Chem.* **1996**, *271*, 29822–29829.
[56] Favia, P.; d'Agostino, R.; *Surf. coat Tech.* **1998**; *98(1-3)*, 1102-1106.
[57] Hersel, U.; Dahmen, C.; Kessler, H. *Biomat.* 2003, 24, 4385-415.
[58]La Ferla B.; Zona, C.; Nicotra, *F; Synlett.* **2009;** *14;* 2325−2327.
[59]Dubruel, P.; Vanderleyden, E.; Bergadà, M.; De Paepe, I.; Chen, H.; Kuypers, S.; Luyten, J.; Schrooten, J.; Van Hoorebeke, L.; Schacht, E.; *Surf. Sci***. 2006;** *600;*2562-2571.
[60] Huh, D.; Hamilton, G.A.; *Trends Cell. Biol. **2011**; 21*l; 745–754.
[61] Choi, S.W.; Yeh, Y.C.; Zhang, Y.; Sung, H.W.;, Xia, Y.; *Small **2010**; 6*; 1492–1498.
[62] Hartgerink, J.D.; Beniash, E.; *Natl. Acad. Sci.* **2002**; *99;* 5133–5138.
[63] Hartgerink. J.D.; Beniash, E.; *Science* **2001***,* 294:1684 –1688.
[64] Marks, Jr S.C.; Odgren, P.R.; *Academic Press* **2002;** p. 3–15.
[65] Ratner, B. D.; Hoffman, A. S.; Schoen, J. F.; Lemons, J. E.; *Biomat. Sci. Int.* **1996**, pp1-8.
[66] van Hest, J. C. M.; Tirrell, D. A.; *Chem. Commun.* **2001**, *19*, 1897–1904.
[67] Lee, C. H.; Singla, A.; Lee, Y.; *Int. J. Pharm.* **2001**; *221,* 1–22.
[68] Suhr, J.; Victor, P.; Ci, L.; Sreekala, S.; Zhang, X.; Nalamasu, O.; Ajayan, P. M.; *Nat. nanotech.* **2007**; *2*(7), 417.
[69] Wang, S. F.; Shen, L.; Zhang, W. D.; & Tong, Y. J.; *Biomacromol.* **2005***; 6*(6), 3067-3072.
[70] Mattson; M. P.; Haddon; R. C.; Rao; A. M.; *J. Mol. Neuro.* **2000**; 14, 175–182
[71] Lovat, V.; Pantarotto, D.; Lagostena, L.; Cacciari, B.; Grandolfo, M.; Righi, M., ... & Ballerini, L.; *Nano letters*, **2005**; *5*(6), 1107-1110.
[72] Mazzatenta, A.; Giugliano, M.; Campidelli, S.; Gambazzi, L.; Businaro, L.; Markram, H.; ... & Ballerini, L.; *J. Neurosci*, **2007**; *27*(26), 6931-6936.
[73] Bianco, A.; Del Gaudio, C.; Baiguera, S.; Armentano, I.; Bertarelli, C.; Dottori, M.; ... & Folin, M.; *IJAO;* **2010**; *33*(5), 271-282.

[74] Heo, S. J.; Kim, S. E.; Wei, J.; Kim, D. H.; Hyun, Y. T.; Yun, H. S.; Shin, J. W.; *Tissue Eng PT A*, **2008**; *15*(5), 977-989.
[75] Alsberg, E.; Feinstein, E.; Joy, M. P.; Prentiss, M.; Ingber, D. E.; *Tissue eng.* **2006**; *12*(11), 3247-3256.
[76] Souza, G. R.; Molina, J. R.; Raphael, R. M.; Ozawa, M. G.; Stark, D. J.; Levin, C. S.; Bankson, J. A.; *Nat. nanotechol.* **2010**; *5*(4), 291.
[77] Dvir, T.; Timko, B. P.; Kohane, D.S.; Langer, R.; *Nat. Nanotechol.* **2011;** *6*(1), 13.
[78]Philp, D.; Huff, T.; Gho, Y.S.; Hannappel, E.; Kleinman, H.K.; *Faseb j.* **2003**; *17(14)*; 2103-5.
[79]Palumbo, F. S.; Di Stefano, M.; Palumbo Piccionello, A.; Fiorica, C.; Pitarresi, G.; Pibiri, I.; Buscemi, S.; Giammona, G.; *RSC Adv.* **2014**; *4 (44)*; 22894.
[80] Ruoslahti, *Annu. Rev. Cell Dev. Biol.* **1996**; *12*, 697–715.
[81] Hersel, U.; Dahmen, C.; Kessler, H.; Biomat. **2003**; *24*, 4385–4415.
[82] Shin, H.; Jo, S.; Mikos, A.G.; Biomat. **2003**; *24*, 4353–4364.
[83] Massia, S.P.; & Hubbell, J.A.; *J. Cell Biol.* **1991**; *114*, 1089–1100 (1991).
[84] Löwik, D. W.; Leunissen, E. H. P.; van den Heuvel, M.; Hansen, M. B.; van Hest, J. C.; *Chem. Soc. Rev.* **2010**; *39*(9), 3394-3412.
[85] Altunbas, A.; Pochan, D. J.; *Peptide-Based Materials* **2011**; (pp. 135-167). Springer, Berlin, Heidelberg.
[86] Woolfson, D. N.; Mahmoud, Z. N.; *Chem. Soc. Rev.* **2010**; *39*(9), 3464-3479.
[87] Aili, D.; Stevens, M.M.; *Chem. Soc. Rev*. **2010**; *39*(9), 3358-3370..
[88] Ruoslahti E.; *Annu. Rev. Cell Dev. Biol.* **1996**, *12*, 697.
[89]Maude, S.; Tai, L. R.; Davies, R.P.W.; Liu, B.; Harris, S. A.; Kocienski, P. J.; Aggeli,A.; *Peptide Bas. Mat.* **2012**, *310*, 27.
[90] Gallant, N. D.; Lavery, K. A.; Amis, E. J.; Becker, M. L.; *Adv. Mater.* **2007**; *19*; 965.
[91] Hansen, T. S.; Lind, J. U.; Daugaard, A. E.; Hvilsted, S.; Andresen, T. L.; Larsen, N. B.; *Langmuir*, **2010**; *26*, 16171.
[92]Philip, D.; Huff, T.; Gho, Y. S.; Hannappel, E.; Kleinman, H. K.; *The FASEB J.* **2003**; *17*(14), 2103-2105.
[93]Neufeld, G.; Cohen, T.; Gengrinovitch, S.; Poltorak, Z.; *The FASEB J.* **1999**; *13*(1); 9-22.
[94]Huff, T.; Müller, C. S.; Otto, A. M.; Netzker, R.; Hannappel, E.; *Int. J. Biochem. Cell boil.* **2001**; *33*(3); 205-220.
[95]Dedova, I. V.; Nikolaeva, O. P.; Safer, D.; Enrique, M.; Remedios, C. G.; *Biophysical J.* **2006**; *90*(3); 985-992.
[96]Huff, T.; Rosorius, O.; Otto, A. M.; Müller, C. S.; Ballweber, E.; Hannappel, E.; Mannherz, H. G.; *J. Cell Sci.* **2004**; *117*(22); 5333-5341.
[97] Vancompernolle, K.; Goethals, M.; Huet, C.; Louvard, D.; Vandekerckhove, J.; *EMBO J.* **1994**; *11*(13); 4739-4746.
[98] Van Troys, M.; Dewitte, D.; Goethals, M.; Carlier, M. F.; Vandekerckhove, J.; Ampe, C.; *EMBO J.* **1996**; *15*(2); 201-210.
[99]Grant, D. S.; Kinsella, J. L.; Kibbey, M. C.; LaFlamme, S.; Burbelo, P. D.; Goldstein, A. L.; & Kleinman, H. K.; *J. Cell Sci.* **2008**; *108*(12); 3685-3694.
[100]Fujio, Y.; Nguyen, T.; Wencker, D.; Kitsis, R. N.; Walsh, K.; *Circulation* **2000**; *101*(6); 660-667.
[101]Misra, A.; Haudek, S. B.; Knuefermann, P.; Vallejo, J. G.; Chen, Z. J.; Michael, L. H.; ... & Mann, D. L.; *Circulation* **2003**; *108*(25)**,** 3075-3078.
[102]Aoki, S.; Nakagomi, A.; Asai, K.; Takano, H.; Yasutake, M.; Seino, Y.; Mizuno, K.; *J. Cardiol.* **2011**; *57*(2); 202-207.
[103]Smart, N.; Rossdeutsch, A.; Riley, P. R.; *Angiogenesis*, **2007**; *10*(4); 229-241.
[104]Sosne, G.; Xu, L.; Prach, L.; Mrock, L. K.; Kleinman, H. K.; Letterio, J. J.; ... & Kurpakus-Wheater, M.; *EXP. Cell Res.* **2004**; *293*(1), 175-183.
[105]Pilcher, B. K.; Dumin, J. A.; Sudbeck, B. D.; Krane, S. M.; Welgus, H. G.; Parks, W. C. *J. Cell Biol.* **1997**; *137*(6); 1445-1457.
[106]Dee, K. C.; Andersen, T. T.; Bizios, R.; *J. Biomed. Mat. Research* **1998**; *40*(3), 371-377.
[107]Pierschbacher, M. D.; Ruoslahti, E.; *Nature* **1984**; *309*(5963); 30-33.

[108]Dettin, M.; Conconi, M. T.; Gambaretto, R.; Bagno, A.; Di Bello, C.; Menti, A. M.; ... & Parnigotto, P. P. *Biomat.* **2005**; *26(22)*; 4507-4515.
[109] Conlan, J. W.; Clarke, I. N.; Ward, M. E.; *Mol. Microbiol.* ***1988****; 2.5*; 673-679.
[110] Boyd, N. A.; Bradwell, A. R.; Thompson, R. A.; *J. Clin. Pathol.* **1993**; *46.11;* 1042-1045.
[111] Maimone, M. M.; Tollefsen, D.M.; *J. Biochem. Chem.* **1990**; *265.30*; 18263-18271.
[112]Schwartz, S. H.; *Appl. Psychol.* **1999**; *48*(1); 23-47.
[113]Jin, H.; Varner, J.; *British J. Cancer* **2004**; *90(3)*, 561.
[114]Klaus T.; *Annual Rev. Cell Biol.* **1991**; *7.1*; 275-310.
[115]Pan, Y. X.; Zhang, Z. Z.; Guo, Z. M.; Feng, G. Y.; Huang, Z. D.; He, L.; *J. Prot. Chem* **2003**; *22(4)*; 395-402.
[116]Hubbell, J. A.; Massia, S. P.; Desai, N. P.; Drumheller, P. D. *Nat. Biotech.***1998**; *9(6)*, 568.
[117]Ranieri, J. P.; Bellamkonda, R.; Bekos, E. J.; Vargo, T. G.; Gardella Jr, J. A.; Aebischer, P.; *J. Biomed. Mat. Res.* **1998**; *29(6)*, 779-785.
[118]Dee, K. C.; Andersen, T. T.; Bizios, R.; *J. Biomed. Mat. Res.* **1998***; 40(3)*; 371-377.
[119]Dee, K. C.; Andersen, T. T.; Bizios, R.; *Biomat.* **1998**; *20(3)*, 221-227.
[120]Rezania, A.; Johnson, R.; Lefkow, A. R.; Healy, K. E.; *Langmuir* **1999**; *15(20)*, 6931-6939.
[121]Xiao, S. J.; Textor, M.; Spencer, N. D.; Sigrist, H.; *Langmuir* **1998**; *14(19)*, 5507-5516.
[122]Massia, S. P.; Hubbell, J. A.; *Ann. N. Y. Acad. Sci.* **1990**; *589(1)*, 261-270.
[123] Smethurst, P. A.; Onley, D. J.; Jarvis, G. E.; O'Connor, M. N.; Knight, C. G.; Herr, A. B.; Ouwehand, W. H.; Farndale, R. W.; J. *Biol. Chem.* **2007**; *282*; 1296–1304.
[124] Pierschbacher, M. D.; Ruoslahti, E.; *Nat.* **1984**; *309*; 30–33.
[125]Cacchioli, A.; Ravanetti, F.; Bagno, A.; Dettin, M.; Gabbi, C.; *Tissue Eng. PT. A* **2009**; *15(10)*, 2917-2926.
[126]Dugdale, B.; Kato, M.; Deo, P.; Plan, M.; Harrison, M.; Lloyd, R., ... & Dale, J.; *Plant Biotechnol. J.* **2018**; *16(2)*, 394-403.
[127]Nair, D. P.; Podgorski, M.; Chatani, S.; Gong, T.; Xi, W.; Fenoli, C. R.; Bowman, C. N.; *Chem. Mater.* **2013**, *26*, 724.
[128] Tang, W.; Becker, M. L.; *Chem. Soc. Rev.* **2014**; *43(20),* 7013-7039.
[129]Chan, J. W.; Hoyle, C. E.; Lowe, A. B.; Bowman, M.; *Macromol.* **2010**; *43*, 6381.
[130]Lutolf, M. P.; Tirelli, N.; Cerritelli, S.; Cavalli, L.; Hubbell, J. A.; *Bioconjugate Chem.* **2001**; *12*; 1051.
[131]Lutolf,M. P.; Raeber, G. P.; Zisch, A. H.; Tirelli, N.; Hubbell J. A.; *Adv. Mater.* **2003**; *15*; 888
[132]Nair, D.P.; Podgorski, M.; Chatani, S.; Gong, T.; Xi, W.; Fenoli, C.R.; Bowman, C.N.; *Chem. Mater.* **2013**, 26, 724.
[133]Barth, A.; *BBA-Bioenerg.* **2007**; *1767.9*; 1073-1101.
[134]Taraballi, F.; Zanini, S.; Lupo, C.; Panseri, S.; Cunha, C.; Riccardi, C.; Marcacci, M.; Campione, M.; Cipolla, L.; *J. Colloid Interface Sci.* **2013**; *394*; 590−597.
[135]Jain; P., Au; J., Tam; D.G., Duda; D., Fukumura; *Nat. Biotechnol.* **2005**; *23;* 821–823.
[136] Brookes, M; Richards, D.J.; Singh, M.; *Angiology* ***1970****; 21*; 355–367.
[137] Laurnen, E.L.; Kelly, P.J.; *J. Bone Joint. Surg. Am*. **1969**; *51*; 298–308, 1969.
[138] Rhinelander, F.W.; *J. Bone Joint. Surg. Am.* **1968**; *50*; 784–800.
[139] Rhinelander, F.W.; Phillips, R.S.; Steel, W.M.; Beer, J.C.; *J. Bone Joint Surg. Am.* **1968**; *50;* 643–662.
[140] Brighton, C.T.; Krebs, A.G.; *Surg. Gynecol. Obstet.* **1972**; *135*; 379–385.
[141] Friedman, R.B.; *NCI. Monogr.* **1990**; *9*: 145–149.
[142] Gordon, L.; Chiu, E.J.; *Bone Joint. Surg. Am.* **1988**; *70*; 377–386.
[143] Goad, D.L.; Rubin, J.; Wang, H.; Tashjian, A.H.; Jr, and Patterson C.; *Endocrinology*; **1996**; *137*; 2262–2268.
[144] Harada, S.; Nagy, J.A.; Sullivan, K.A.; Thomas, K.A.; Endo, N.; Rodan,G.A.; Rodan, S.B.; *J. Clin. Invest.* **1994**; *93*; 2490–2496.
[145] Saadeh, P.B.; Mehrara, B.J.; Steinbrech, D.S.; Dudziak, M.E.; Greenwald, J.A.; Luchs, J.S.; Spector, J.A.; Ueno, H.; Gittes, G.K.; *Am. J. Physiol. Cell. Physiol.* **1999**; *277*; C628–C637.
[146] Saadeh, P.B.; Mehrara, B.J.; Steinbrech, D.S.; Spector, J.A.; Greenwald, J.A.; Chin, G.S.; *Endocrinology*; **2000**; *141*; 2075–2083.

[147] Schlaeppi, J.M.; Gutzwiller, S.; Finkenzeller, G.; Fournier, B.; *Endocr. Res.* **1997**; *23*; 213–229.
[148] Steinbrech, Douglas. S; et al. *Am. J. Phys. Cell Phys.* **2000**; *278.4*; C853-C860.
[149] Go, A.S.; Mozaffarian, D.; Roger, V.L.; Benjamin, E.J.; Berry, J.D.; Borden, W.B.; *Heart disease and stroke statistics*; **2013**;*127.*
[150] Annex, B. H.; *Nat. Rev. Cardiol.* **2013;** *10*; 387–396.
[151] Fraisl, P.; Mazzone, M.; Schmidt, T.; Carmeliet, P; *Dev. Cell* **2009**; *16*(2), 167-179.
[152] Phng, L. K.; Gerhardt, H.; *Dev. Cell* **2009**; *16*(2), 196-208.
[153] Rouwkema, J.; & Khademhosseini, A.; *Trends in biotechnol.* **2016**; *34*(9), 733-745.
[154] Folkman, J.; Hochberg, M.; *J. Exp. Med.* **1973**;*138*; 745–53.
[155] Khademhosseini, A.; Langer, R.; Borenstein, J.; Vacanti, J.P.; *Proce. Nat. Ac. Sci. USA* **2006**; *103*; 2480–7.
[156] Ahrendt, G.; Chickering, D.E.; Pranieri, J.P.; *Tissue Eng.*; **1998**; *4*; 117–30.
[157] Smith, M.K.; Peters, M.C.; Richardson, T.P.; Garbern, J.C.; Mooney, D.J.; *Tissue Eng.* **2004**;*10*; 63–71.
[158] Harrison, B.S; Eberli, D.; Lee, S.J; Atala, A.; Yoo, J.J., *Biomat.* **2007***; 28*; 4628–34.
[159] Stump, D.G.; Holson, J.F.; Harris, C.; Pearce, L.B.; Watson, R.E.; DeSesso, J.M.; *Reprod. Toxicol*. **2015**; *52*; 108-117.
[160] Khattak, S.F.; Chin, K.S.; Bhatia, S.R.; Roberts, S.C.; *Biotehnol. Bioeng.* **2007**; *96*; 156–66.
[161] Gordon, J.E.; Dare, M.R.; Palmer, A.F.; *Biotechnol. Prog.* **2005**, *21*; 1700–7.
[162] Ward, C.; Corona, B. T.; Yoo, J. J.; Harrison, B. S.; Christ, G.J.; *PLoS One*, **2013**, *8*, e72485.
[163] Wijekoon, A.; Fountas-Davis, N.; Leipzig, N. D.; *Acta Biomater.* **2013**; *9*; 5653.
[164] Oh, S. H.; Ward, C. L.; Atala, A.; Yoo, J. J.; Harrison, B. S. *Biomat.* **2009**; *30*; 757.
[165] Harrison, B.S. Eberli, D.; Lee, S. J.; Atala A.; Yoo, J. J. *Biomat.* **2007**; *28*, 4628.
[166] Abdi, S. I.; Ng, S. M.; Lim, J. O.; *Int. J. Pharm.* **2011**; *409*; 203.
[167] Li, Z.; Guo, X.; Guan, J.; *Biomat.* **2012**; *33*, 5914.
[168] Kra, M. P.; *Adv. Drug Delivery Rev.* **2001**; *47*; 209.
[169] Li, Z.; Guo, X.; Guan, J.; *Biomat.* **2012**; *33*, 5914.
[170] Riess, Jean G.; *Artif. Cells Blood Sub.* **2006**; 34.6; 567-580.
[171] 2. Riess, J.G.; *Tetrahedron*; **2002**; *58*; 4113–4131.
[172] Zhou, Y.; Wang, Z.; Chen, Y.; Shen, H.; Luo, Z.; Li, A.; ... & Yang, Z. *Adv. Mater.* **2013**; *25*(30), 4123-4130.
[173] Schutt, E. G.; Klein, D. H.; Mattrey, R. M.; & Riess, J. G. *Angew. Chem. Int. Ed.* **2003**; *42*(28), 3218-3235.
[174] Song, X.; Feng, L.; Liang, C.; Yang, K.; & Liu, Z. *Nano Lett.* **2016**; *16*(10), 6145-6153.
[175] Riess, J. G.; *Biotechnol.* **2006**; *34*; 567.
[176] Buscemi, S.; Pace, A.; Palumbo Piccionello, A.; Pibiri, I.; Vivona, N.; *Heterocycles,* **2004**; *63*; 1619.
[177] Buscemi, S.; Pace, A.; Palumbo Piccionello, A.; Vivona, N.; *J. Fluorine Chem.* **2006**, *127*, 1601.
[178] Buscemi, S.; Pace, A.; Palumbo Piccionello, A.; Vivona, N.; *Heterocycles* **2004**, *63*, 1619.
[179] Alvarez-Paino, M.; *Polym. Chem.* **2012**; *3.12*; 3282-3288.
[180] Rimal, S.; Koskey, S.; Mukherjee, T.; Goswami, A.; Abdelghani, J.; Ross, N.; & Chyan, O.; SEMICON korea 2013, SEMI technology symposium (STS), *conference paper,* **2013.**
[181] Henderson, T.J.; *Anal. Chem.* **2002**; *74.1*; 191-198.
[182] Jhon, M. S.; Andrade, J. D. J. *Biomed. Mater. Res.* **1973**; *7*; 509.
[183] Jen, A. C.; Wake, M. C.; Mikos, A. G.; *Biotech. Bioeng.* **1996**; *50*; 357.
[184] Drury, J. L.; Mooney, D. J.; *Biomat.* **2003**; *24*, 4337–4351.
[185] Drury, J. L.; Mooney, D. J.; *Biomat.* **2003**; *24*, 4337–4351.
[186] Jonker, A. M.; Löwik, D. W.; van Hest, J. C.; *Chem. Mat.* **2012**; *24(5)*; 759-773.
[187] Hoare, T. R.; Kohane, D. S.; *Polym.* **2008**; *49(8)*; 1993-2007.
[188] Dahlmann, J.; Krause, A.; Möller, L.; Kensah, G.; Möwes, M.; Diekmann, A.; Martin, U.; Kirschning, A.; Gruh, I.; Dräger, G.; *Biomat.* **2013**, *34(4)*, 940–951.

[189] Liu, Y.; Wang, R.; Zarembinski, T. I.; Doty, N.; Jiang, C.; Regatieri, C.; Zhang, X.; Young, M. J. *Tissue Eng. Pt A* **2013**; *19(1-2)*; 135-142.
[190] Aroguz, A. Z.; Baysal, K.; Adiguzel, Z.; Baysal, B. M.; *Appl. Biochem. Biotech.* ***2014***; *173(2)*, 433-448.
[191] Delmar, K.; Bianco-Peled, H.; *Carbohyd. Polym*. **2015**, 127, 28–37.
[192] Li, B.; Wang, L; Xu, F.; Gang, X.; Demirci, U.; Wei, D.; Li, Y.; Feng, Y.; Jia, D.; Zhou, Y. Acta *Biomat.* **2015**, *22*, 59–69.
[193] Assaad, E.; Maire, M.; Lerouge, S.; *Carbohyd. Polym*. **2015**, *130*, 87-96.
[194] Qiu, Y.; Park, K. Adv. *Drug Deliver. Rev***. 2012**, *64S*, 49–60.
[195] Klouda, L. Eur. J. Pharm. *Biopharm***. 2015**, *97B*, 338–349.
[196] Orienti, I.; Treré, R.; Zecchi, V. *Drug Dev. Ind. Pharm*. **2001**, *27*, 877–84.
[197] El-Sherbiny; Yacoub. *Global Card Sci Pract*. **2013**; *3*: 38.
[198] Rosiak, Janusz M.; Fumio Y.; *Nuclear Instruments and Methods in Physics Research Section B: Beam Interactions with Materials and Atoms* **1999**; *151.1-4*; 56-64.
[199] De Jong, S. J.; et al. *J. App. Pol. Sci* **2002**; *86.2*; 289-293.
[200] Rosiak, Janusz M.; Fumio Y.; *Nuclear Instruments and Methods in Physics Research Section B: Beam Interactions with Materials and Atoms* **1999**; *151*.1-4; 56-64.
[201] Rosiak, Janusz M.; Fumio Y.; *Nuclear Instruments and Methods in Physics Research Section B: Beam Interactions with Materials and Atoms* **1999**; *151*.1-4; 56-64.
[202] Shantha, K. L.; Harding, D. R. K.; *J. Appl. Polym*. *Sci*. **2002**, *84*, 2597–2604.
[203] Shantha, K. L.; Harding, D. R. K.; *Eur. Polym. J.* **2003**, *39*, 63–68.
[204] El-Sherbiny, I. M.; Abdel-Bary, E. M.; Harding, D. R. K. *Int. J. Polym. Mater*. **2006**, *55*, 789–802.
[205] Jabbari, E.; Nozari, S*. Eur. Polym. J.* **2000**, *36*, 2685–2692.
[206] Akin, H.; Hasirci, N.; *Polym. Preprint.* **1995**, *36*, 384–385.
[207] C Echave, M.S.; Burgo, L.L. Pedraz, J.; Orive, G.; *Curr. Pharm. design* **2017***; 23(24)*; 3567-3584.
[208] Aldana, A. A.; Abraham, G. A.; *Int. J. Pharm*, **2017**; 523(2), 441-453.
[209] Li, X.; Zhang, J.; Kawazoe, N.; Chen, G.; *Polym.* **2017,** *9(8)*, 309.
[210] Dash, R., Foston, M. & Ragauskas, A. J.; *Polym.* **2013**; *91*; 638–645.
[211] Xing, Q.; Yates, K.; Vogt, C.; Qian, Z.; Frost, M. C.; Zhao, F.; *Sci. Rep.* **2014**; 4; 4706.
[212] Oryan, A.; Kamali, A.; Moshiri, A.; Baharvand, H.; Daemi, H.; *Int. J. Biol. Macromol*. **2018**; *107*, 678-688.
[213] Sgambato, A.; Cipolla, L.; Russo, L.; *Gels* **2016**; *2(4)*, 28.
[214] Shankar, K.G.; Gostynska, N.; Montesi, M.; Panseri, S.; Sprio, S.; Kon, E.; ... & Sandri, M.; *Intern. J. boil. Macromol.* **2017***; 95*, 1199-1209.
[215]Reddy, N.; Reddy, R.; Jiang, Q.; *Trends in biotechnol.* **2015**; 33(6); 362-369.
[216] Basle, E.; Joubert, N.; Pucheault, M.; *Chem. Bio.* **2010**; 17(3), 213-227.
[217] Spicer, C. D.; Davis, B. G.; *Nat. Com.* **2014**; 5; 4740.
[218] Sletten, E. M.; Bertozzi, C. R.; *Angew. Chem.* **2009**; *48*; 6974–6998.
[219]Lallana, E.; Fernandez-Trillo, F.; Sousa-Herves, A.; Riguera, R.; Fernandez-Megia, E.; *Pharm. Res.* **2012**; *29(4)*, 902-921.
[220] Jiang, Y., Chen, J.; Deng, C.; Suuronen, E. J.; Zhong, Z.; *Biomat.* **2014**; 35(18), 4969-4985.
[221] Hoyle, C. E.; Bowman, C. N.; *Ang. Chem. Int. Ed.* **2010**; 49(9); 1540-1573.
[222] Dondoni, A.; *Ang. Chem. Int. Ed.* **2008**; 47(47), 8995-8997.
[223] Lutz, J. F.; & Zarafshani, Z.; *Adv. Drug Del. Rev.* **2008**; *60(9)*, 958-970.
[224] Murabayashi, H.; Mitamura, S., Taguchi, T.; *J. Mat. Sci. Mat. Med*. **2008**;*19*(3), 1297-1305.
[225] Duan, X.; and Sheardown, H.; *J. Biomed. Mater. Res. Part A* **2005**; *75A*, 510–518
[226] Orban, J.M.; et al. *J. Biomed. Mater. Res.;* **2004**; *68A*, 756–762
[227] Madhurakkat Perikamana, S. K.; Lee, J.; Lee, Y. B.; Shin, Y. M.; Lee, E. J.; Mikos, A. G.; *Biomat.* **2015**; *16*(9), 2541-2555.
[228] Partlow, B. P.; Applegate, M. B.; Omenetto, F. G.; Kaplan, D. L.; *ACS Biomat. Sci. Eng.* **2016**, *2(12)*, 2108-2121.

[229] Kodadek, T., Duroux-Richard, I., & Bonnafous, J. C.; *Trends Pharmacol. Sci.* **2005**; *26*(4), 210-217.
[230] Hoare, T. R., & Kohane, D. S; *Polym.* **2008**; *49*(8), 1993-2007.
[231] Tessmar, J. K., & Göpferich, A. M; *Adv. Drug Deliv. Rev.* **2007**; *59*(4-5), 274-291.
[232] Lin, C. C., & Anseth, K. S.; *Pharm. Res.* **2009**; *26*(3), 631-643.
[233] Lin, C. C., & Metters, A. T.; *Adv. Drug Deliver. Rev.* **2006**; *58*(12-13), 1379-1408.
[234] Siepmann, J., & Göpferich, A.; *Adv. Drug Deliver. Rev.* **2001**; *48*(2-3), 229-247.
[235] Siepmann, J., & Siepmann, F.; *Int. J. Pharm.* **2008**; *364*(2), 328-343.
[236] Rao, K. R., & Devi, K. P.; *Int. J. Pharm.* **1998**; *48*(1-3), 1-13.
[237] Bouwstra, J.A. and Junginger, H.E. *In Encyclopaedia of Pharmaceutical Technology* (Swarbrick, J. and Boylan, J.C., eds), **1993**; pp. 441–465, Marcel Dekker
[238] Gulrez, S. K., Al-Assaf, S., & Phillips, G. O. *Progress in molecular and environmental bioengineering-from analysis and modeling to technology applications*. InTech. **2011.**
[239] Hoffman, A. S. .; *Adv. Drug Deliver. Rev.* **2012**; *64*, 18-23.
[240] Begam, T.; Nagpal, A. K.; Singhal, R.; *J. App. Polim. Sci.* **2003**; *89*(3), 779-786.
[241] Davis, B.K.; *P.N.A.S.* **1974**; *71*(8), 3120-3123.
[242] Langer, R.; Vacanti, J. P.; Vacanti, C. A.; Atala, A.; Freed, L. E.; Vunjak-Novakovic, G.; *Tissue Eng.* **1995**;*1*(2), 151-161.
[243] West, J. L.; Hubbell, J. A.; *P.N.A.S.* **1996**; *93*(23), 13188-13193.
[244] Hill-West, J. L.; Dunn, R. C.; Hubbell, J. A.; *J. Surg. Res.* **1995**; *59*(6), 759-763.
[245] An, Y.; Hubbell; J. A.; *J. Contr. Rel.* **2000**; *64*(1-3), 205-215.
[246] Bergmann, N. M.; Peppas, N. A.; *Prog. Polym. Sci.* **2008**; *33*(3), 271-288.
[247] Vashist, A.; Vashist, A.; Gupta, Y. K.; Ahmad, S.; *J. Mat. Chem. B.* **2014**; *2*(2), 147-166.
[248] Vashist, A.; Vashist, A.; Gupta, Y. K.; Ahmad, S.; *J. Mat. Chem. B.* **2014**; *2*(2), 147-166.
[249] Cruise, G. M.; Hegre, O. D.; Lamberti, F. V.; Hager, S. R.; Hill, R.; Scharp, D. S.; Hubbell, J. A.; *Cell Transp.* **1999**; *8*(3), 293-306.
[250] C Echave, M.; S Burgo, L.; L Pedraz, J.; Orive, G.; *Current Pharm. Des.* **2017**; *23*(24), 3567-3584.
[251] Aldana, A. A.; Abraham, G. A.; *Int. J. Pharm.* **2017**; *523*(2), 441-453.
[252] Foox, M.; Zilberman, M.; *Expert Opin. Drug Del.* **2015**; *12*(9), 1547-1563.
[253] Li, X.; Zhang, J.; Kawazoe, N.; Chen, G.; *Polym* **2017**; *9*(8), 309.
[254] Dash, R.; Foston, M.; Ragauskas, A. J.; *Carbohyd. Polym.* **2013**; *91*(2), 638-645.
[255] Xing, Q.; Yates, K.; Vogt, C.; Qian, Z.; Frost, M. C.; Zhao, F.; *Sci. Rep*, **2014**; *4*, 4706.
[256] Oryan, A.; Kamali, A.; Moshiri, A.; Baharvand, H.; Daemi, H.; *Int. J. biol. Macromol.* **2018**; *107*, 678-688.
[257] Sgambato, A.; Cipolla, L.; Russo, L.; *Gels*, **2016**; *2*(4), 28.
[258] Shankar, K. G.; Gostynska, N.; Montesi, M.; Panseri, S.; Sprio, S.; Kon, E.; Sandri, M.; *Int. J. Biol. Macromol.* **2017**; *95*, 1199-1209.
[259] Reddy, N.; Reddy, R.; Jiang, Q.; *Trends in Biotech.* **2015**; *33*(6), 362-369.
[260] Lallana, E.; Fernandez-Trillo, F.; Sousa-Herves, A.; Riguera, R.; Fernandez-Megia, E.; *Pharm. Res.* **2012**; *29*(4), 902-921.
[261] Jiang, Y.; Chen, J.; Deng, C.; Suuronen, E. J.; Zhong, Z.; *Biomat.*, **2014**; *35*(18), 4969-4985.
[262] Sletten, E.M.; Bertozzi, C.R.; *Angew. Chem. Int. Ed. Engl.* **2009**, *48(38)*, 6974-98.
[263] Occhetta, P.; Visone, R.; Russo, L.; Cipolla, L.; Moretti, M.; Rasponi, M. *J. Biomed. Mater. Res. A.* **2015**, *103(6)*.
[264] Russo, L.; Sgambato, A.; Visone, R.; Occhetta, P.; Moretti, M.; Rasponi, M.; Nicotra, F.; Cipolla L. *Monatsh. Chem*. **2016**, *147*, 587–592.
[265] García-Astrain, C.; Gandini, A.; Peña, C.; Algar, I.; Eceiza, A.; Corcuera, M.; Gabilondo, N.; *RSC Adv.* **2014**; *4*(67), 35578-35587.
[266] Tamura, M.; Yanagawa, F.; Sugiura, S.; Takagi, T.; Sumaru, K.; Kanamori, T.; *Sci. Rep.* **2015**; *5*, 15060.
[267] EPiluso, S.; Vukićevića, R.; Nöchel, U.; Braun, S.; Lendlein, A.; Neffe, A.T.; *Eur. Polym. J.* **2018**, *100*, 77-85.

[268] Basle, E.; Joubert, N.; Pucheault, M.; *Chem. Biol.* **2010**; *17*(3), 213-227.
[269] Ban, H.; Gavrilyuk, J.; Barbas III, C. F.; *J. Am. Chem. Soc.* **2010**; *132*(5), 1523-1525.
[270] Ban, H.; Nagano, M.; Gavrilyuk, J.; Hakamata, W.; Inokuma, T.; & Barbas III, C. F.; *Bioconju. Chem.* **2013**; *24*(4), 520-532.
[271] Vandewalle, S.; De Coen, R.; De Geest, B. G.; Du Prez, F. E.; *ACS Macro Let.* **2017**; *6*(12), 1368-1372.
[272] Al-Momani, E.; Israel, I.; Buck, A. K.; Samnick, S.; *App. Radiat. Isot.* **2015**; *104*, 136-142.
[273] Bauer, D. M.; Ahmed, I.; Vigovskaya, A.; Fruk, L.; *Bioconj. Chem*. **2013**; *24*(6), 1094-1101.
[274] Hanay, S. B.; Ritzen, B.; Brougham, D.; Dias, A. A.; Heise, A.; *Macromol. Biosci.* **2017**; *17*(7), 1700016.
[275] Culbertson, B.M.; McGrath, J.E.; *Polym. Sci.* **1985**, 31, pp. 8-11, ISBN:13:978-1-4612-9254-8.
[276] Zolfigol, M. A.; Mallakpour, S. E.; Madrakian, E.; Ghaemi, E. *Indian J. Chem., Sect. B: Org. Chem. Incl. Med. Chem.* **2000**, *39*, 308.
[277] Eastoe, J. E.; *Biochem. J.* **1995**; *61*(4), 589.
[278] Begam, T.; Nagpal, A. K.; Singhal, R.; *J. Appl. Polym. Sci.* **2003**; *89*(3), 779-786.
[279] Ryall, J. P.; Dines, T. J.; Chowdhry, B. Z.; Leharne, S. A.; Withnall, R.; *S.A.A. : Molecular and Biomolecular Spectroscopy*, **2011**; *78*(3), 918-925.
[280] Larkin, P.J.; *Infrared and Raman Spectroscopy:* Principles and Spectral Interpretation, 2nd ed, Elsevier, Amsterdam, **2018**, 286, ISBN: 9780128041628
[281] Barth, A.; *Prog. Biophys. Mol. Biol.* **2000**;*74*(3-5), 141-173.
[282] Raspanti, M.; Caravà, E.; Sgambato, A.; Natalello, A.; Russo, L.; Cipolla, L.; *Int. J. Biol. Macromol.* **2016**; *86*, 65-70.
[283] Hanay, S. B., Brougham, D. F., Dias, A. A., & Heise, A. *Polymer Chemistry*, **2017**; *8*(43), 6594-6597.
[284] Van Tomme, S. R.; Storm, G.; Hennink, W. E.; *Int J. Pharm.* **2008**; *355*(1-2), 1-18.
[285] Karim, R.; Palazzo, C.; Evrard, B.; Piel, G.; *J. Control. Rel.* **2016**; *227*, 23-37.
[286] Bastiancich, C.; Danhier, P.; Préat, V.; Danhier, F.; *J. Control. Rel.* **2016**; *243*, 29-42.
[287] Zeeman, R.; Dijkstra, P.J.; Van Wachem, P.B.; Van Luyn, M. J. A.; Hendriks, M.; Cahalan, P. T.; Feijen, J. *Biomed. Mat. Res.* **1999**; *46*(3), 424-433.
[288] Begam, T.; Nagpal, A. K.; Singhal, R.; *J. App. Polim. Sci.* **2003**; *89*(3), 779-786.
[289] Pieper, J.S.; Oosterhof, A.; Dijkstra, P. J.; Veerkamp, J. H.; & Van Kuppevelt, T. H.; *Biomat.* **1999**; *20*(9), 847-858.
[290] Lundquist J.J.; Toone E.J.; *Chem. Rev*. **2002**; 102; 555–78.
[291] Deniaud, D.; Julienne, K.; Gouin, S.G.; *Org. Biomol. Chem.* **2011**; *9*, 966–79.
[292] Gabius, H.J.; André, S.; Kaltner, H.; Siebert, H.C.; *B.B.A.* **2002**; *1572*(2-3), 165-177.
[293] Cummings, R.D.; McEver, R.P.; *Essentials of Glycobiology. 2nd edition*. Cold Spring Harbor Laboratory Press **2009**.
[294] Cummings, R. D.; McEver, R.P.; In *Essentials of Glycobiology. 2nd edition*. Cold Spring Harbor Laboratory Press **2009.**
[295] Sanchez-Navarro, M.; Rojo, J.; *Drug news & perspectives* **2010**, *23*(9), 557-572.
[296] van Die, I., & Cummings, R. D. In *Parasites and allergy* **2006**, Karger Publishers. Vol. 90, pp. 91-112.
[297] Bertozzi, C. R.; Kiessling, L. L.; *Sci.* **2001**; *291*(5512), 2357-2364.
[298] Heldin, C. H.; *Cell* **1995**; *80*(2), 213-223.
[299] Gestwicki, J. E.; Kiessling, L. L.; *Nat*. **2002**; *415*(6867), 81.
[300] Kiessling, L. L.; Gestwicki, J. E.; Strong, L.E.; *Ange. Chem. Int. Ed.* **2006**; *45*(15), 2348-2368.
[301] Dam, T. K.; Gerken, T. A.; Brewer, C. F.; *Biochem.* **2009**; *48*(18), 3822-3827.
[302] Grayson, S. M.; Frechet, J. M.; *Chem. Rev.* **2001**; *101*(12), 3819-3868.
[303] Newkome, G.R.; Shreiner, C.D.; *Polym.* **2008**; *49*(1), 1-173.
[304] Wu, L. P.; Ficker, M.; Christensen, J. B.; Trohopoulos, P. N.; Moghimi, S. M.; *Bioconj. Chem.* **2015**; *26*(7), 1198-1211.
[305] Röglin, L.; Lempens, E. H.; & Meijer, E. W.; *Angew. Chem. Int. Ed.* **2011**; *50*(1), 102-112.

[306] Janaszewska, A.; Mączyńska, K.; Matuszko, G.; Appelhans, D.; Voit, B.; Klajnert, B.; Bryszewska, M.; *New J. Chem.*, **2012**; *36*(2), 428-437.
[307] Janaszewska, A.; Ziemba, B.; Ciepluch, K.; Appelhans, D.; Voit, B.; Klajnert, B.; Bryszewska, M.; *New J. Chem.* **2012**; *36*(2), 350-353.
[308] Ciolkowski, M.; Pałecz, B.; Appelhans, D.; Voit, B.; Klajnert, B.; Bryszewska, M.; *Colloids Surface B.* **2012**; *95*, 103-108.
[309] Hakomori, S.; *P. Ntl. A. Sci. B.* **2002**; *99*(16), 10231-10233.
[310] Dai, Z.; Kawde, A. N.; Xiang, Y.; La Belle, J.T.; Gerlach, J.; Bhavanandan, V. P.; Wang, J.; *J. Am. Chem. Soc.* **2006**;*128*(31), 10018-10019.
[311] Manning, J. C.; Romero, A.; Habermann, F. A.; Caballero, G. G.; Kaltner, H.; Gabius, H.; J. *Histochem. Cell Biol.* **2017**; *147*(2), 199-222.
[312] Mayer, S.; Raulf, M. K.; Lepenies, B.; *Histochem. and Cell Biol.* **2017**; *147*(2), 223-237.
[313] Gabius, H. J.; Manning, J. C.; Kopitz, J.; André, S.; Kaltner, H.; *Cel. Mol life Sci.* **2016**; *73*(10), 1989-2016.
[314] Appelhans, D.; Klajnert-Maculewicz, B.; Janaszewska, A.; Lazniewska, J.; Voit, B.; *Chem. Soc. Rev.* **2015**; *44*(12), 3968-3996.
[315] Tomalia, D. A.; *Prog. Polym. Sci.* **2005**; *30*(3-4), 294-324.
[316] Esfand, R.; Tomalia, D. A.; *Drug Discov. today*, **2001**; *6*(8), 427-436.
[317] Tomalia, D. A.; Huang, B.; Swanson, D. R.; Brothers II, H. M.; Klimash, J. W.; *Tetrahedron*, **2003**; *59*(22), 3799-3813.
[318] Gabellieri, E.; Strambini, G. B.; Shcharbin, D.; Klajnert, B.; Bryszewska, M.; *B.B.A-Proteins and Proteomics*, **2006**; *1764*(11), 1750-1756.
[319] Klajnert, B.; Stanisławska, L.; Bryszewska, M.; Pałecz, B.; *B.B.A.-Proteins and Proteomics*, **2003**; *1648*(1-2), 115-126.
[320] Turnbull, W. B.; Stoddart, J. F.; *Rev. Mol. Biotech.* **2002**; *90*(3-4), 231-255.
[321] Das, R.; Mukhopadhyay, B.; *ChemistryOpen* **2016**; *5*(5), 401-433.
[322] Mulani, S. K.; Hung, W. C.; Ingle, A. B.; Shiau, K. S.; Mong, K. K. T.; *Org Biomol. Chem.* **2014**; *12*(8), 1184-1197.
[323] Sadalapure, K.; Lindhorst, T. K.; *Angew. Chemie Int. ed.* **2000**; *39*(11), 2010-2013.
[324] Fulton, D.A.; Stoddart, J.F.; *Org. Lett.*, **2000**, 1113-1116
[325] Turnbull, W.B.; Pease, A.R.; Stoddart, J.F.; *ChemBioChem,* **2000**, 70-74.
[326] Turnbull, W.B.; Kalovidouris, S.A.; Stoddart, J.F; *Chem. Eur. J.,* **2002**, 2988-3000.
[327] Mintzer, M. A.; Grinstaff, M. W.; *Chem. Soc. Rev.* **2011**; *40*(1), 173-190.
[328] Wu, L. P.; Ficker, M.; Christensen, J. B.; Trohopoulos, P. N.; Moghimi, S. M.; *Bioconj. Chem.* **2015**; *26*(7), 1198-1211.
[329] Röglin, L.; Lempens, E. H. M.; Meijer, E. W.; *Angew. Chem. Int. Ed.* **2011**, 50, 102.
[330] Abbasi, E.; Aval, S. F.; Akbarzadeh, A.; Milani, M.; Nasrabadi, H. T.; Joo, S. W.; Hanifehpour, Y.; Nejati-Koshk, K.; Pashaei-Asl, R.; *Nanoscale Res. Lett.* **2014**, *9*, 247.
[331] Balzani, V.; Ceroni, P.; Maestri, M.; Vicinelli, V.; *Curr. Opin. Chem. Biol.* **2003**; *7*(6), 657-665.
[332] Zeng, Y.; Li, Y. Y.; Chen, J.; Yang, G.; Li, Y.; *Chem. A. J.* **2010**; *5*(5), 992-1005.
[333] Guizzardi, R.; Vacchini, M.; Santambrogio, C.; Cipolla, L.; *Can. J. Chem.* **2017**; *95*(9), 1008-1012.
[334] Feliu, N.; Walter, M. V.; Montañez, M. I.; Kunzmann, A.; Hult, A.; Nyström, A.; Fadeel, B.; *Biomat.* **2012**; *33*(7), 1970-1981.
[335] Lee, C. C.; Gillies, E. R.; Fox, M. E.; Guillaudeu, S. J.; Fréchet, J. M.; Dy, E. E.; Szoka, F. C.; *P. Natl. A Sci.* **2006**; *103*(45), 16649-16654.
[336] Gillies, E. R.; Dy, E.; Fréchet, J. M.; Szoka, F. C.; *Mol. Pharm.* **2005**; *2*(2), 129-138.
[337] Kalomiraki, M.; Thermos, K.; Chaniotakis, N. A.; *Int. J. Nanomed.* **2016**; *11*, 1.
[338] Vida, Y.; Collado, D.; Najera, F.; Claros, S.; Becerra, J.; Andrades, J. A.; Perez-Inestrosa, E.; *R.S.C. Adv.* **2016**; *6*(55), 49839-49844.
[339] Chabre, Y. M.; Roy, R.; *Chem. Soc. Rev.* **2013**; *42*(11), 4657-4708.

[340] Bini, D.; Marchetti, R.; Russo, L.; Molinaro, A.; Silipo, A.; Cipolla, L.; *Carbohyd. Res.* **2016**; *429*, 23-28.
[341] Ambrosi, M.; Cameron, N. R.; Davis, B. G.; *Org. Biomol. Chem.* **2005**; *3*(9), 1593-1608.
[342] Sharon, N.; Lis, H.; *Sci.* **1972**; *177*(4053), 949-959.
[343] Bini, D.; Nicotra, F.; Cipolla, L.; *Beilstein J. Org. Chem.* **2014**; *10*, 1686.
[344] Bini, D.; Russo, L.; Battocchio, C.; Natalello, A.; Polzonetti, G.; Doglia, S. M.; Cipolla, L.; *Org. Lett.* **2014**; *16*(5), 1298-1301.
[345] Samojłowicz, C.; Bieniek, M.; Pazio, A.; Makal, A.; Woź niak, K.; Poater, A.; Cavallo, L.; Wójcik, J.; Zdanowski, K.; Grela, K.; *Chem. Eur. J.* **2011**, 17.
[346] Thygesen, M. B.; Munch, H.; Sauer, J.; Cló, E.; Jørgensen, M. R.; Hindsgaul, O.; Jensen, K. J.; *J. Org. Chem.* **2010**; *75*(5), 1752-1755.
[347] Cordes, E. H.; Jencks, W. P.; *J. Am. Chem. Soc.* **1962**; *84*(5), 826-831.
[348] Dirksen, A.; Dawson, P. E.; *Bioconj. Chem.* **2008**; *19*(12), 2543-2548.
[349] Haas, J. W.; Kadunce, R. E.; *J. Am. Chem. Soc.* **1962**;*84*(24), 4910-4913.
[350] Jencks, W. P.; In Catalysis in Chemistry and Enzymology, 1st ed.; McGraw-Hill: New York**, 1969**; pp 72-74
[351] Thygesen, M. B.; Munch, H.; Sauer, J.; Cló, E.; Jørgensen, M. R.; Hindsgaul, O.; Jensen, K. J.; *J. Org. Chem.* **2010**; *75*(5), 1752-1755.
[352] Ribeiro, J. P.; Diercks, T.; Jiménez-Barbero, J.; André, S.; Gabius, H. J.Biomol. **2015**; *5*(4), 3177-3192.
[353] Žagar, E.; Žigon, M.; *Prog. Polym. Sci.* **2011**, 36, 53.